Ministry of Higher Education and Scientific Research
University of Babylon
College of Science for Women
Department of Laser Physics

Magneto-Optics Properties of Metamaterials with different Nanostructures

A Thesis
Submitted to Council of the College of Sciences for Women
University of Babylon in partial Fulfillment of the Requirement for the Degree of
Doctor of Philosophy in Laser Physics and Its Applications
By

Noora Aziz Alewy

B.Sc. in Physics 2013
M.Sc. Laser Physics and its Application 2017
Supervised by:

Prof.Dr Jinan Ali Abd

University of Babylon
College of Sciences for Women
Laser Physics Department

Asst.Prof. Nizar Salim Shnan

University of Babylon
College of Sciences for Women
Laser Physics Department

2023 A.D **1444 H.D**

بسم الله الرحمن الرحيم

(يَرْفَعِ اللَّهُ الَّذِينَ آمَنُوا مِنْكُمْ وَالَّذِينَ أُوتُوا الْعِلْمَ دَرَجَاتٍ وَاللَّهُ بِمَا تَعْمَلُونَ خَبِيرٌ).

صدق الله العظيم

سورة المجادلة آية(11)

Dedication

To the one who stood by me and taught me patience to reach where I am, my mother, may God keep her as an asset for me

To those who supported and encouraged me, my father, may God protect him

To my companion and life partner who stood by me to achieve my dream, my husband, may God protect him

To the light of my eyes and the seed of my heart, my son, may God protect him

To my beloved brothers, may God grant them success

Noora

Acknowledgements

Praise is to Allah, mercy and peace are to the Prophet Mohammed and his relatives and companions. I would like to sincerely thank my supervisors, **Prof. Dr. Jinan Ali Abd** and. **Asst. Prof. Dr Nizar Salim Shnan**, For their research suggestion and their direction, assistance, guidance, and their recommendations and suggestions for this work. I am deeply indebted to the Head of the Laser Physics Department, the staff and the dean of the College of Science for Women for the support that provided.

Abstract

This work includes four groups of different samples with different compositions were prepared. Tests were conducted for all the prepared samples, and the groups were: Group one (Sample1: One-side 2D grating (PDMS/TiO_2(50nm)), Sample 2: Two-sides 2D grating (etalon) (TiO2 (50nm) /PDMS/ TiO2 (50nm)),Group two (Sample 1: 2D (PDMS/MgF2) different periodic), Group Three(Sample 1: 1D PDMS/MgF_2(10nm), Sample 2: 1D PDMS /MgF_2/ Au (34n), Sample 3: 1D PDMS/MgF_2/ Au/Ni (30), Sample 3: 1D PDMS/MgF_2/ Au/Ni (30nm)), Group four Sample 1: 2D PDMS/TiO_2 (34nm), Sample 2: 2D PDMS /TiO_2/ Au (34nm), Sample 3: 2D PDMS /Tio_2/ Au /Ni (34nm)).

Where XRD tests were conducted for the materials involved in preparing the aggregate structures to confirm the identity of the prepared material, and identical results were obtained by comparing them with the values stated in the international labels for each material. An SEM examination was conducted for the same materials to determine the nanoscopicity of the material, and the results proved this. Tests were conducted. The CCD camera g for groups (1, 2, and 3) was found through it that the intensity for G1 is high in the first sample and for the second sample, the intensity is lower ,As for diffraction, It is noticed that the beam width is greater in the second sample, while the intensity is high at Q1, Q2, while the intensity is lower at Q3, Q4 that in the G2.

Reflection tests were also performed for G1 It is noticed through the results, the increase in the angle due to the increase the separation in the peak its notice that the gradient of the increase in the angle begins to appear and become more clear, as it is noticed its appearance at the angle (52) and the increase at (58) and the most obvious at the angle (60), its noticed the convergence at the wavelength (700)nm and there are the

difference is large at the wavelength (650)nm, where the single is higher and therefore the linear applications of the double are more because it has a greater refractive index and thus decreases speed As for the imaginary refractive index, we note the increase in the single within the wavelengths from (550)nm to the end of the visible spectrumits that noted from the tested refractive index for the G1.

In the second part of the work, the properties magneto-optics of samples in groups 3,4 were studied to determine the change occurring using the setup which was aligned and in the presence of a magnetic field and its noted the effect of the plasmon(localizes surface Plasmon resonance)on the reason of the S_1,S_2 inG3 it is noticed the S_1high rotating that begins to descend to sub-zero (Negative)and then gradually increases to the wavelength at 550nm, becomes the positive peak and then rises at the wavelength of 600nm and it is noticed the high rotation in the behavior, as we notice the increase that occurs between the 500nm and 550nm from negative to positive and the Plasmon appears on the nickel at S_3 the rotation process is very high between the 450nm and 500nm, and we notice at the 525nm the effect of the Plasmon appears on the nickel,while that result for G4 noted that the introduction of Ni may have filled the gaps responsible for Plasmon generation, consequently preventing the formation of the metasurface.

List of Abbreviations

(STFs)	Sculptured Thin Films
(SNR)	Signal-to-noise ratio
CVD	Chemical Vapor Deposition
(OAD)	Oblique Angle Deposition
(SPs)	Surface Plasmons
(SPPs)	Surface Plasmon Polaritons
(SPP)	Surface Plasmon Polariton
(LSP)	Localized Surface Plasmon
(EBG)	Electromagnetic-Bandgap
(GLAD)	Glancing Angle Deposition
(PVD)	physical Vapor Deposition
(e-beam)	Electron Beam
(MS)	Magnetron Sputtering
(SRR)	Split-Ring Resonant
(DPS)	Double Positive
(DNG)	Double Negative
(Ms)	Saturation Magnetization
(Tc)	Curie Temperature
(NIM)	Negative Index Metamaterials
(LHM)	Left-Handed Metamaterials
(MEMS)	Micro Electro Mechanical Systems
(RDRs)	Rectangular Dielectric Resonators
(MO)	Magneto-Optical
(FR)	Faraday Rotation
(TiO2)	Titanium Dioxide

(MgF2)	Magnesium Fluoride
(Ni)	Nickel
(CTAB)	Cationic Surfactant, and Hexadecy Tri-Methyl Ammonium Bromide
(PDMS)	Poly Dimethyl Siloxane
(XRD)	X-Ray Diffraction
(SEM)	Scanning Electron Microscopy
(EPMA)	Electron Probe Microanalysis
(CCD)	Charge-Coupled-Device
(MOS)	Metal Oxide Semiconductor
(E.D)	Electric Dipole
(M.D)	Magnetic Dipole

Chapter One

General Introduction

1-1 Introduction

Thin films can be defined as “thin material layers ranging from fractions of a nanometer to several micrometers in thickness" . A proper distinction between thin film deposition and thick film deposition should be based in mind. Thin film deposition involves deposition of individual atoms, while the latter deals with the deposition of particles, as an example, painting is thick film technique **[1,2].** Usually thick film deposition doesn’t give much control over the quality of films and is relatively inexpensive than thin film deposition. Thin films behave differently from bulk materials of the same chemical composition in several ways. For instance, thin films are sensitive to surface properties while bulk materials generally aren't. Thin films are also relatively more sensitive to thermomechanical stresses. Today thin film technology itself is a separate branch of material science and has evolved into a set of techniques used to fabricate many products **[3].**

Applications include very large scale production of electronic packaging, sensors, integrated circuits, optical film and devices and also protective and decorative coatings. At present, the enormous opportunities and rapidly changing needs for thin films and thin film devices are opening new frontiers for the development of new processes, materials and technologies **[4-5].** Sculptured thin films (STFs) **[6]** exemplify metamaterials. An STF is an assembly of nanowires typically grown by physical vapor deposition, whose bent and twisted forms reengineered via the growth process. As a result of the flexibility in controlling the evolv-ing nanostructure of the films during fabrication, their performance characteristics can be engineered. The emergence of metamaterials at the end of the 20th century heralded a major motivational shift in research on materials and coincided with the

ramping up of nanotechnology **[7] .**Materials researchers began to consider the design of composite materials, called metamaterials, to perform more than role each in specific environments. Among optics researchers today, the term metamaterial is often taken to mean a material with negative refractive index **[8],** but there is much more to metamaterials than that **[9]** coined this term for certain types of artificial materials, and later formally defined metamaterials as "macroscopic composites having a manmade, three-dimensional, periodiccellular architecture designed to produce an optimized combination, not available in nature,of two or more responses [emphasis in the original] to specific excitation. We can relax the requirements of peri odicity today, though not ofcellularity .Indeed, cellularity in morphology yengenders multifunctional performance. The principle of operation of metasurfaces is based on the phenomenon of diffraction. Any flat periodic array can be viewed as a diffraction lattice, which splits the incident light into a few rays. The number and direction of the rays depends on geometrical parameters: the angle of incidence, wavelength and the period of the lattice. The structure of the sub wavelength unit cell, in turn, determines how the energy of the incident light is distributed between the rays. For a negative refractive index it is necessary that all but one of the diffraction rays are suppressed, then all of the incident light will be directed in the required direction **[10].** Plasmonic nanostructures have been proposed as a new efficient heat source when illuminated by their correspondence resonance light source **[11, 12]** regarding the Nano scale control of temperature distribution **[13],** drug delivery **[14, 15],** photo-thermal imaging **[16],** and various other useful applications. Nowadays, different evidence is available concerning the metal nanoparticle-based structure for satisfying the abovementioned SNR in the temperature distribution, resulting in introducing novel development in chemistry and biology

while not in the physics **[17].** All these evaluations aim to establish a better understanding about the physical phenomenon such as the thermo-plasmonic effect in nanoparticle-based structures **[18]** It has been proposed that electromagnetic metamaterials—composite structured materials, formed from either periodic or random arrays of scattering elements—should respond to electromagnetic radiation as continuous materials, at least in the long wavelength limit **[19,20].** In recent experiments and simulations **[21,22],** it has been demonstrated that certain metamaterial configurations exhibit scattering behavior consistent with the assumption of approximate frequency dependent forms for permittivity(ε) and permeability (μ). However, the techniques applied in those studies probed the materials indirectly, and did not provide an explicit measurement that would assign values for ε and μ **[22].**Magneto-optical effects are at the core of polarization-control, telecommunications, sensing, and the emerging field of nonreciprocal photonics**[23,24]** where axial symmetry of the magnetic field is the enabling mechanism for the violation of parity-time symmetry of the optical response. Unfortunately, homogeneous materials available in nature exhibit relatively weak magneto optical activity. Artificial magneto-optical behavior has been recently demonstrated in photonic-crystal-inspired structures and in waveguide geometries**,[25,26]** configurations known for their sensitivity to long-range order and, therefore, highly susceptible to fabrication imperfections

1-2 Literature Review

Shridhar E. Mendhe et.al. in 2011 have been discussed fundamental properties of metamaterials. It also discuss the recent research activities on metamaterials in various areas such as antenna design, design of high frequency components & devices, microwave

engineering etc. The metamaterials are engineered media whose electromagnetic responses are different from those of their constituent components **[27].**

Ivan D. Rukhlenko et.al. in 2012 have been studied the concept of metamaterials and how it radically changed the way we think about light matter interactions and significant enrichment in the classical domains and Quantum electrodynamics. Where this new understanding revolutionized the optical device design prototype and product quickly in an experimental demonstration of several axioms Effects with far reaching penetration applications. **[28].**

Filiberto Bilotti et.al. in 2012 have been studied definition, origin, terminology, fundamental properties design concepts and procedures, basic applications, modeling, and numerical simulation of metamaterials**[29].**

Myung-Geun Jeong ,et.al. in 2012 they was coated TiO_2 by PDMS using the CVD note that the bare TiO_2 exhibits a phase transition from anatase to rutile at approximately 700 °C. When the heating temperature was increased to 800°, The enhanced photocatalytic activity of 800 °C-annealed PDMS-coated TiO_2 could be also sustainable under UV illumination**[30].**

R. Yahiaoui et.al. in 2012 have been reported a strong magnetic activity using an all-dielectric metamaterial, A good agreement was achieved between numerical simulations and experiment in the case of one meta-layer based on TiO_2-disks, manufactured using a simple bottom-up approach. They also demonstrate through numerical simulations a negative refractive index within the same investigated metamaterial made of high dielectric permittivity single-size pellets.

This is a promising step towards innovative and complex electromagnetic functions, involving cheap and easy made metamaterials for millimeter wave applications**[31].**

H. Neˇmec et.al in 2012 have been prepared single layers of microspheresand characterized by time-domain terahertz spectroscopy. They developed an experimental approach allowing simultaneous measurement of complex transmittance and reflectance of a thin layerwhich in turn enables evaluation of its effective dielectric permittivity and effective magnetic permeability. Numerical finite-element-method calculations of the electromagnetic response show that the prepared microparticles are suitable for preparing a metamaterial with negative effective magnetic permeability**[32].**

Filiberto Bilotti et.al. in 2012 have been reviewed definition, origin, terminology, fundamental properties, design concepts and procedures, basic applications, modeling, and numerical simulation of metamaterials. It is shown that metamaterial origin can be easily understood by placing metamaterials in the more general context of artificial electromagnetic materials and of the efforts performed by the scientific community working in complex materials to mimic and overcome the properties of natural materials**[33].**

S.M. Hamidi et.al. in 2012 have been presented the study of the optical and magneto-optical properties of crystalline Ce:YIG thin films with Au nanoparticles deposited with the PLD technique at cubic quartz and GGG substrate the results show that large enhancement of the FR was obtained in samples with Au nanoparticles on quartz substrates due to the SPR and an increase in the refractive index of the sample**[34].**

Anand Kumar Tripath et.al. in 2013 have been prepared Pure and mixed phase TiO_2 by sol–gel method at four different

temperaturesat four different temperatures results indicatestrain at 400, 500 and 600 _C while compressive strain at 700 _C. Scanning electron microscopy (SEM) shows that the particles are non-uniform, X-ray diffraction (XRD) showed that prepared nanocrystals have pure anatase and anatase-rutile mixed structures **[35].**

Yizhuo He et.al. in 2013 have been demonstrated that Oblique angle deposition (OAD) as a powerful technique for various plasmonic applications due to its advantages in controlling the size, shape, and composition of metallic nanostructure and they reviewedfocus on the fabrication of metallic nanostructures by OAD and their applications in plasmonics **[36].**

M.T.S. Tavares et.al. In 2014, studied polydimethylsiloxane (PDMS)/TiO_2 Nano composite was processed by spray methodTiO_2 nanoparticles were synthesized by microwave-assisted hydrothermal method .The results indicated that the addition of TiO_2 nanoparticles to PDMS provided coating with good photo catalytic activity in the decomposition of methylene blue dye. PDMS/TiO_2 Nano composites prepared by spray showed good chemical stability to UV radiation, the FTIR results**[37].**

S. **M. Hamidi et.al. in 2014** have been synthesized Ni NWs by a combined technique of AAO template and electrodeposition method Structural, magnetic, optic and magneto-optical characterizations of the composite were performed by SEM, X-ray diffraction pattern, EDAX analysis, AGFM, SPR and Spectral MO rotation respectively the results show the very sufficient alignment of NWs in the PDMS matrix and the good squareness has been observed in the sample**[38].**

S. M. Hamidi et.al. in 2014 have been studied Surface Plasmon resonance magneto-optical Kerr effect in magneto-plasmonic multilayer as Au /Co/ Au on this new experimental setup, the sample

exposed under external magnetic field at surface Plasmon resonance angle. The results showed sufficient surface Plasmon resonance magneto-optical Kerr effect in visible region, thanks to the resonant excitation of surface Plasmon's which is very suitable for miniaturized and controllable magneto-optical imaging systems, memory, and also magneto-optical isolators**[39].**

Claire M. Watts in 2015 described an implementation of novel imaging applications with electromagnetic metamaterials. Metamaterials have proven to be host to a multitude of interesting physical phenomena and give rich insight electromagnetic theory. There is a strong need for efficient, low cost imaging solutions, specifically in the longer wavelength regime. While this technology has often been at a standstill due to the lack of natural materials that can effectively operate at these wavelengths, metamaterials have revolutionized the creation of devices to fit these needs**[40].**

Chrysikapridaki et.al. in 2015 have been designed two hydrophobic hybrid SiO_2–TiO_2 materials and their application in the field of monument conservation. The Nano composite consolidates were based on the modification of tetraethoxysilane (TEOS) with the incorporation of both TiO2 nanoparticles and hydroxyl-terminated polydimethylsiloxane (PDMS). The physico-chemical properties of the designed hydrophobic Nano crystalline SiO_2–TiO_2–PDMS composites have been extensively studied before their application as consolidates on a limestone. The results was that the TiO_2–SiO_2–PDMS Nano composites functioned as hydrophobic coatings. Furthermore, the results obtained from micro drilling resistance and Fourier Transform Infrared spectroscopy (FTIR)

revealed a penetration depth of the Nano composites within the stone of c. 15 mm**[41].**

Claire M. Watts in 2015 reviewed the implementation of novel imaging applications with electromagnetic metamaterials. Metamaterials have proven to be host to a multitude of interesting physical phenomena and give rich insight electromagnetic theory and explored the many applications of metamaterials**[42].**

Gurwinder Singh et.al. in 2015 have been reviewed of the history of metamaterials, some of salient features, various types, applications and different modeling methods of metamaterials have been discussed. The metamaterials have resulted in surprising improvements in electromagnetic response functions that can offer exciting possibilities of future design of devices, components and salient properties of metamaterials **[43].**

Irina Khromova et.al. in 2016 have been fitting the Fano line shape model to the experimentally obtained spectra of the electric field detected by the sub-wavelength aperture probe, they found that the magnetic dipole resonances in TiO_2 spheres have narrow line widths of only tens of gigahertz. Anisotropic TiO_2 micro-resonators can be used to enhance the interplay of magnetic and electric dipole resonances in the emerging THz all-dielectric metamaterial technology **[44].**

S. M. Hamid et.al. in 2017 have been fabricated sample using the finite difference time domain method. In order to investigate the effect of rotation speed on the anisotropy of the samples and their magneto-plasmonic responses, these patterned structures are fabricated under dissimilar holder rotation speeds for inner cobalt layer deposition the results showed that the transverse magneto-plasmonic Kerr effect measurements can provide unique and useful

information about the structure and quality of the fabricated samples'**[45].**

Fan, B., Nasir et.al. in 2019 have designed and demonstrated magneto-optical response of plasmonic shelled Nano rod metamaterials. Theoretically, they have developed the effective medium technique for understanding the effective magneto-optical response and validated this technique via full-wave solutions of the Maxwell equations. Experimentally. experimental results indicate that the magneto-optical response of nanostructured Ni is significantly stronger than the tabulated response of its bulk counterpart **[46].**

Shan Peng et.al. in 2019 presented a highly efficient, cost-effective, and wide-applicable functionalized SiO2/TiO2-polymer based coating to fabricate a translucent, fluorine free, chemically stable, photo catalytic active, was consisted of two mixed functionalized particles (MFP) and PDMS in a proper ratio. Both SiO2 and TiO2 powders were functionalized with PDMS brushes to achieve super hydrophobicity. In order to maximally optimize properties, This investigation indicated that this PDMS graftedSiO_2/TiO_2@PDMS coating with multiple superior properties is believed to have very promising commercial applications**[47].**

Syed S. Bukhari et.al. in 2019 have been reviewed of metasurfaces, which are planar metamaterials. Metamaterials ofer bespoke electromagnetic applications and novel properties which are not found in naturally occurring materials and they discussed salient features and applications of metasurfaces; wave front shaping; phase jumps; non-linear metasurfaces; and their use as frequency selective surfaces (FSS)**[48].**

N. S. Shnan et.al. in 2020 have been a thin layer of the gold grating was typically deposited on a patterned polydimethylsiloxane

substrate using the Nano imprint lithography method. The surface Plasmon resonance of the fabricated plasmonic structure was excited by the surface Plasmon . the findings, the Fourier image appeared as bright disks relying on the optical axis and the distance from outward to the center of the disk. The applied voltage caused the rapid heating of Nano rods, leading to a quick increase in the temperature dueto the thermo-plasmonic effect**[49].**

Yixin Chen et.al. in 2020 have been reviewed different types of soft and reconfigurable optical metamaterials and their fabrication methods, highlighting their exotic properties. Future directions to employ soft optical metamaterials in next generation metamaterial devices are identified**[50].**

Tian Gu1 et.al. in 2022 reviewed the state-of-the-art of active metasurface technologies and their applications while highlighting key research advances essential to enabling their transition from laboratory curiosity to commercial reality**[51].**

S. V. TOMILIN in 2022 have been founded a giant enhancement of the Faraday effect in magneto plasmonic Nano composite films based on Au nanoparticles and bismuth substituted iron garnet BiIG layer. It is due to the excitation of the single and collective localized Plasmon resonances in the Au nanoparticles **[52].**

N. S. Shnan1,2 et.al. in 2022 have been demonstrated a one-dimensional IMI magneto- plasmonic grating based on patterned MgF_2, gold, and Ce:YIG nanostructure is reported. The grating design was inspired by merging the plasmonic properties of the gold array and the magneto-optical activity of the garnet material Magneto-optical activity of the magneto-plasmonic structure was studied in the LMOKE configuration. ED and MD excited by the light localization

result in the amplification of the LMOKE in the structured sample **[53].**

D. A. Djemmah et.al. in 2022 demonstrated the fabrication and characterization of TiO2 ceramics material with high refractive index and low losses in the 300- 1400 GHz range. The optimized fabrication process allows for the elaboration of high-density materials whose dielectric properties make them good candidates for the design of fully dielectric metamaterials**[54].**

N. S. Shnan et.al in 2023 have been fabricated Magneto plasmonic samples based on two-dimensional and all dielectric CoFeB thin films supported by gold and TiO_2 metasurfaces, respectively. To get the main physical reason for the magneto-optics (MO) enhancement in plasmonic and all-dielectric ones, the results showed the MO response enhancement in district channels based on LSPR (in green region) and electric and magnetic dipole moment(in red area) **[55] .**

1-3 The Aim of Research

The aim of this work is study the magneto- optics properties for different metamaterail by satisfy many goals

1- Study of the optical properties of one-sided and two-sided samples, 4-periodesity samples

2- Study of the magneto-optics properties of(TiO_2+PDMS+Au+Ni) And (MgF_2+PDMS+Au+Ni)

Chapter Two

Theoretical Part

2-1 Introduction

This chapter includes a general description of the theoretical part of this study , physical concepts , scientific clarifications , relationships , and laws used to interpret the study results.

2.2 Plasmonic

Plasmonic is the field of study the optical phenomena that results from interaction of conduction free electrons of noble metal nanoparticles with electromagnetic waves (especially at visible optical frequencies) and collective oscillation called as surface plasmon **[56]**, where the plasmons are collective charge density oscillations and longitudinal waves propagating in a bulk metal, and they cannot couple directly with light. However, at the interface between a metal and dielectric the oscillation mode of the electron wave to couple with light exists under certain matching conditions. **[57]** This mode is called surface Plasmon's (SPs) or surface plasmon polaritons (SPPs) that are localized at a metal surface and propagate along the interface between a metal and dielectric. SPs are represented schematically in Figure (2-1). When SPs are excited, an electric field in the z-direction is enhanced, providing a remarkably high sensitivity for interfacial characterizations. For this reason, new optics utilizing this resonance character has attracted attention in various fields**[58]**. If light is directly incident on a flat metal film, SPs are not excited since the dispersion relation is different of SPs from light propagating in free space. Hence, the optical system to match the condition is needed to excite SPs. Otto **[59]** and Kretschmann **[60]** designed optical systems using total reflection to excite SPs. Fast electrons or gratings can also excite SPs, however, the technique exciting SPs would be restricted to the total-reflective optical systems **[57]**.

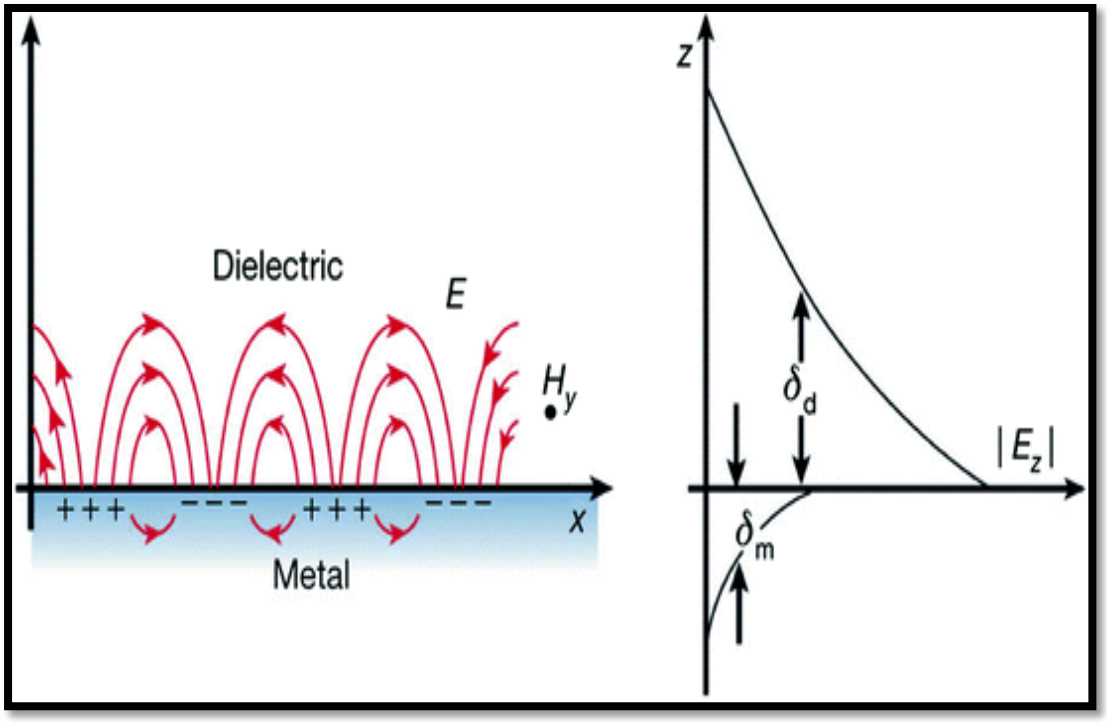

Figure (2-1): Schematics of the electromagnetic field of surface plasmons or SPP propagating along the interface between a metal and dielectric. (δ_d) is a decay length into the dielectric and (δ_m) is a decay length (skin depth) into the metal [57].

Plasmonic is a major part of the nanophotonics which can confine electromagnetic waves smaller than the diffraction limit. The development of nanofabrication techniques helps to increase applications of plasmonic nanostructures **[61]**.

When electromagnetic waves are incident on a metal surface, it will accelerate electrons and lead to induce polarization that creates restoring force which causes an oscillation of the free electron of the metal as shown in Figure (2-2). This oscillation is quantized and free electrons oscillation is quantization of plasma oscillations and it is called a plasmon **[62]**.

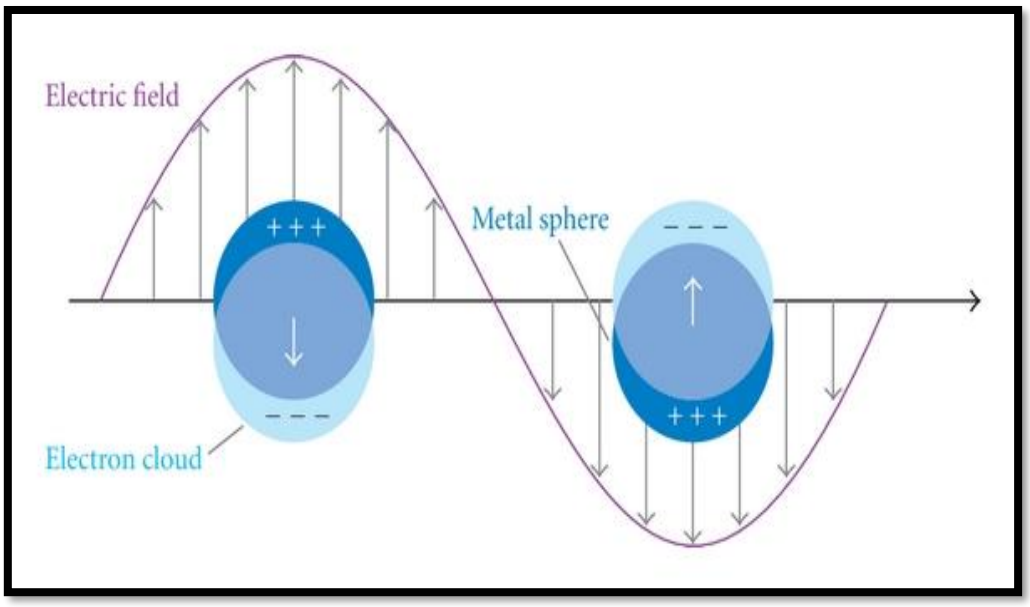

Figure (2-2): Localized Surface Plasmon resonance of metallic nanoparticle [63].

There are two types of surface plasmon according to their interface: Surface Plasmon Polariton (SPP) and localized surface plasmon (LSP).

2-2-1 Surface Plasmon Polariton (SPP): are longitudinal waves, which propagate at the interface between a dielectric and metal. These waves travel parallel to the direction of propagation; so they cannot be excited by a transverse waves. The most effective way to excite a plasmon is to use electrons i.e. when light excites the electrons, electrons will pass through a thin metal layer and lose some energy, this loss in energy use to excite SPP **[64]**.

2-2-2 Localized Surface Plasmon (LSP): are non-propagating waves. In case of a spherical nanoparticle, the curved surface of the nanoparticle creates a restoring force on the electrons to result in a localized resonance. This kind of resonance can be excited by direct light irradiation **[65]**.

The interaction of metallic nanostructures with electromagnetic fields can be described by a classical form of Maxwell's equations. Maxwell's

equations are describe the electromagnetic field for a given system through four vectors strength of the electric field (E), the displacement (D), the strength of magnetic field (H), and the flux density (B) **[66]**.

$$\nabla . \vec{E} = \frac{\rho_e}{\epsilon_\circ} \qquad (2.2)$$

$$\nabla . \vec{B} = 0 \qquad (2.3)$$

$$\nabla \times \vec{E} = -\frac{\partial \vec{B}}{\partial t} \qquad (2.4)$$

$$\nabla \times \vec{B} = \mu_\circ \epsilon_\circ \frac{\partial \vec{E}}{\partial t} + \mu_\circ \vec{J} \qquad (2.5)$$

Where (ϵ_0) ,(μ_0): are the permittivity and the permeability of free space, (ρ_e): is the total charge density and ($\vec{J}$): is the total current density. The incident external electric field excites the free electrons and displaces it from their normal positions in the metal lattice. Movement of oscillating free electron can be described by equation of motion **[67]**:

$$m_e \ddot{x} + m_e \gamma \dot{x} = -q_e E \qquad (2.6)$$

Where (m_e): is the free electron mass, (x): is the electron displacement, $\dot{x}$: First derivative , $\ddot{x}$: second derivative (q_e): is the electron charge and E is the external electric field, (γ): is electron damping factor.

The general solution of oscillating electric field is $E=E_0 e^{-i\omega t}$ so that the solution of equation (2.6) for given amplitude (x_0): is **[67]**:

$$x_\circ = \frac{q_e}{m_e(\omega^2 + i\omega\gamma)} E_\circ \qquad (2.7)$$

Where (ω): is the angular frequency. While in the case of (n) number of electrons a macroscopic polarization is rise $P=-nq_e x$ and given by:

$$P = \frac{n\, q_e^2}{m_e(\omega^2 + i\omega\gamma)} E \qquad (2.8)$$

The electric displacement (D) depends on the dielectric function of the free electron as:

$$D = \epsilon_{\circ} E + P \qquad (2.9)$$

So that equation (2.9) becomes:

$$D = \epsilon_{\circ}\left(1 + \frac{\omega_p^2}{(\omega^2 + i\omega\gamma)}\right)E \qquad (2.10)$$

The plasma frequency of the free electron is **[68]**:

$$\omega_p^2 = \frac{n\, q_e^2}{\epsilon_{\circ} m_e} \qquad (2.11)$$

The dielectric function of the free electron (ϵ_{ω}) is:

$$\epsilon_{\omega} = 1 - \frac{\omega_p^2}{\omega^2 + i\omega\gamma} \qquad (2.12)$$

The equation describes the behavior of plasmonic in a bulk metal using the Drude model.

For very small spherical metallic nanoparticles (compared to the wavelength of incident light), the nanoparticle polarisability (Pa): is **[69]**:

$$Pa = 4\pi R^3 \frac{\epsilon(\omega) - \epsilon_d}{\epsilon(\omega) + 2\epsilon_d} \qquad (2.13)$$

Where (R): is the nanoparticle radius, ϵ (ω): is the metal's dielectric function and (ϵ_d): is the dielectric function of the surrounding.

LSP resonance occurs when the polarisability of the nanoparticle reaches to maximum value i.e. ($\epsilon(\omega)+2\epsilon_d$) is minimized.

The optical cross section of the spherical nanoparticles enhances (strong scattering and absorption properties) under plasmonic conditions and given by **[70]**:

$$\sigma_{scs} = \frac{k^4}{6\pi}|Pa|^2 \qquad (2.14)$$

$$\sigma_{acs} = kIm\,[Pa] \qquad (2.15)$$

Where σ_{scs},σ_{acs} are the scattering and the absorption cross sections, and (k): is the wave vector of incident light **[70]**.

2-3 Metamaterials

Metamaterials certainly represent the most recent achievement of the research in the field of unconventional materials and complex media. The name has been proposed within the scientific community working on complex media **[71, 72].** To identify a class of artificial materials exhibiting surprising and anomalous electromagnetic properties that cannot be found in natural materials. Following this definition and according to the general point of view of that community,the Greek word meta has been used in the sense of emergence of new properties from a special combination of materials exhibiting conventional electromagnetic behaviors**[73].** Nowadays, however, the most common meaning given to the prefix meta in metamaterials is beyond, as in the word metaphysics. Following this signification, metamaterials may be defined as artificial engineered materials exhibiting unique or unusual properties that cannot be found in natural materials at the frequencies of interest and, thus, allow going beyond some of the limitations encountered when using natural materials in microwave and optical components. For the time being, it seems that this is the most common definition of metamaterials adopted worldwide **[74, 75].** This definition is also in agreement with the official one adopted by the first and sole international society metamaterials existing worldwide, the Virtual Institute for Artificial Electromagnetic Materials and Metamaterials (METAMORPHOSE VI) **[76].** Before going in further details concerning the definition of metamaterials, we would like to put them in a proper scientific context, to understand how and from where they come from. The context and the origin of metamaterials we share with the scientific community working on complex media are

schematically represented in Figure(2-3). At first, scientists studied the interaction between electromagnetic waves and natural materials. These studies have been typically developed at optical frequencies. In that frequency range, in fact, electromagnetic waves can effectively interact with the structural constituents (i.e., the molecules) of the natural materials. As a result of these investigations, some interesting properties, due to the symmetry of the molecules, have been found. One interesting example of this scientific research was the observation of the change of the light polarization of an electromagnetic wave travelling through an optically active material sample **[77].** This phenomenon, commonly recognized as optical activity, has been quickly referred to the chiral symmetry of the molecules of some particular materials (i.e., chiral materials). Some other interesting side phenomena were observed in natural chiral materials, such as the decomposition of a linearly polarized light into two right-handed and left-handed circularly polarized waves **[78].** The degrees of freedom available in the frame of complex artificial materials allowed obtaining some unusual combinations of inclusions and host dielectrics, giving rise to new properties, not actually known in optical natural materials. For instance, in 2000, San Diego group managed to fabricate for the first time a material with a negative refractive index **[79]**. This was the beginning of the metamaterial era. Nowadays, two main research directions are the most active in the field of metamaterials. One research line is devoted to exploit metamaterials as loading materials in conventional microwave components (e.g., circuits and antennas) **[80–81].** By properly loading microwave components with metamaterials, in fact, it is possible to obtain interesting operation and anomalous properties that allow beating most of the main limitations of conventional components, opening the door to new revolutionary ultracompact devices with improved performances. Here, the key aspect

is that metamaterials do not represent a new technology at microwaves, but simply a new way of thinking of already existing technologies. Most of the metamaterial samples realized at microwaves, in fact, are based on the well-established printed circuit technology **[82].** Such degrees of freedom permit the design of an artificial material owning some desired electromagnetic properties. However,it is worth remarking that, to describe the behavior of a metamaterial through its macroscopic constitutive parameters, granularity of the inclusions does disappear at the frequencies of interest. Therefore, for a proper definition of the macroscopic effective constitutive parameters (e.g., permittivity, permeability, chirality, etc.) of a metamaterial, inclusion size, and inclusion separation must be both electrically small **[83].** This strong requirement brings us to separate the concepts of metamaterials and other artificial materials, such as the electromagnetic-bandgap (EBG) materials, which are commonly and erroneously mixed up. EBGs, for instance, are also a class of artificial material constituted by inclusions arranged in a host material. However, in this case, although the size of the inclusions may be electrically small, their separation is not (it is typically of the order of the wavelength). EBG materials, in fact, derive their interesting properties (e.g., existence of frequency bands forbidden to the propagation of the electromagnetic field) from the periodicity of the inclusion arrangement, rather than from the effective macroscopic response of the artificial material. Therefore, in the case of an EBG, constitutive parameters, that are commonly used to describe the electromagnetic behavior of a metamaterial, such as permittivity, permeability, index of refraction, cannot be defined at all. The metamaterail may be manufactured by sputtering with the oblique angle technique.

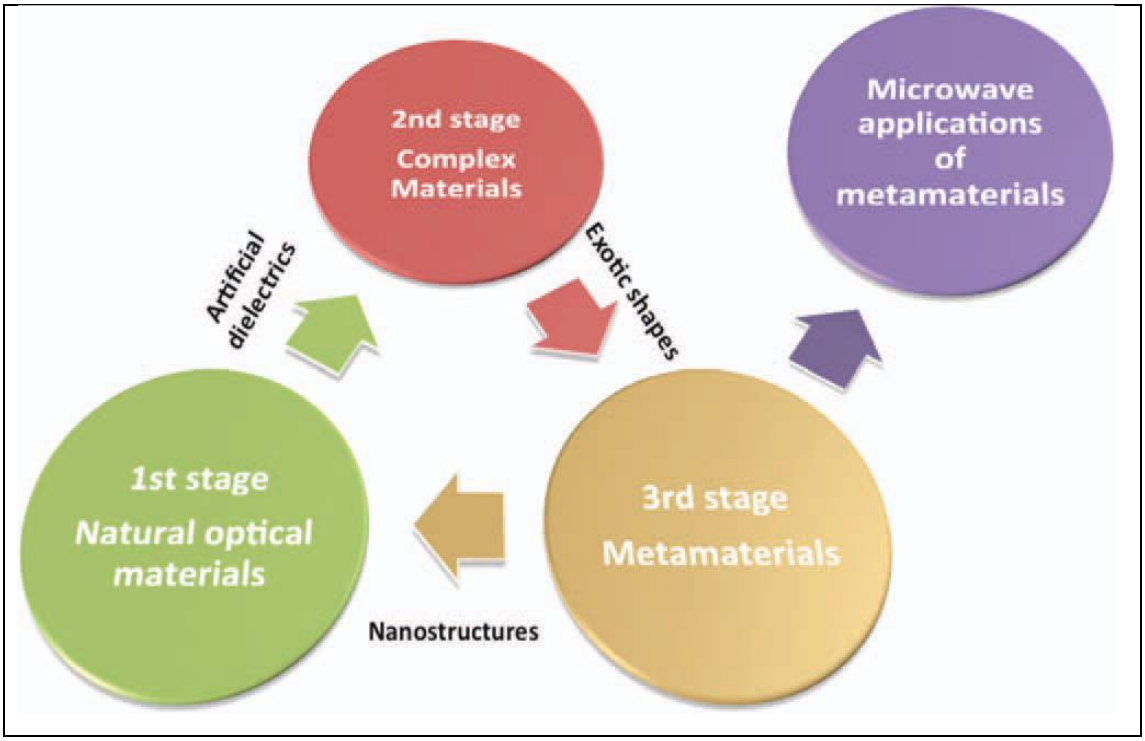

Figure (2-3) Conceptual scheme showing the context and the origin of metamaterials.

2-4 Oblique angle deposition of thin films

Surface engineering is a technological area of high scientific and industrial interest thanks to the wide set of applications benefitting from its contributions. In addition to classical areas such as optics, tribology and corrosion/wear protection, where high compactness and a low porosity are important microstructural requirements, the advent of emerging technologies requiring porous or highly structured layers has fostered the development of thin film deposition procedures aimed at enhancing these morphological characteristics. A typical experimental approach in this regard is the use of an oblique angle geometrical configuration during deposition. Evidence of highly porous, optically anisotropic thin films grown using this technique were first reported more than a hundred years ago **[84],** but it was not focus was given to the tilted columnar microstructure of these films and the factors controlling its

development **[85].**Following these initial steps, the last 20–25 years have witnessed the systematic application of oblique angle deposition (OAD) procedures for the development of a large variety of devices in fields such as sensor technology, photovoltaic cells, magnetism, optical devices, electrochemistry and catalysis; all of which require strict control over porosity, anisotropy and/or crystallographic texture of the film**[86–87].**

In general, the term OAD or other widely used alternatives such as ‘‘glancing angle deposition” (GLAD), and ‘‘ballistic deposition”, are all associated in the literature with the physical vapor deposition (PVD) of thin films prepared by evaporation, which usually entails electron beam (e-beam) bombardment. Since the OAD concept can be more broadly applied whenever the source of deposition particles and the substrate surface are obliquely aligned**[88]**. To discuss the OAD of thin films from a perspective that is not restricted to evaporation, but also considers plasma- and laser-assisted deposition methods such as the magnetron sputtering (MS) technique, in which the presence of gas molecules may induce the scattering of particles and alter their otherwise rectilinear trajectory. the mechanisms controlling the morphological development of OAD thin films its porosity, the tilt orientation of the nanostructures and any preferential texture. Although different geometrical models and empirical rules have been proposed in the last few decades to roughly account for these features in films prepared by e-beam evaporation, and to a lesser extent by MS, preferably knowing accuracy the atomic mechanistic effects controlling the development of morphology and crystallography of OAD thin films.

Overall, the increasing interest shown by the scientific community in these films has been a direct consequence of their unique morphology,

which has fostered the development of new applications and devices with specific functionalities.**[89].**

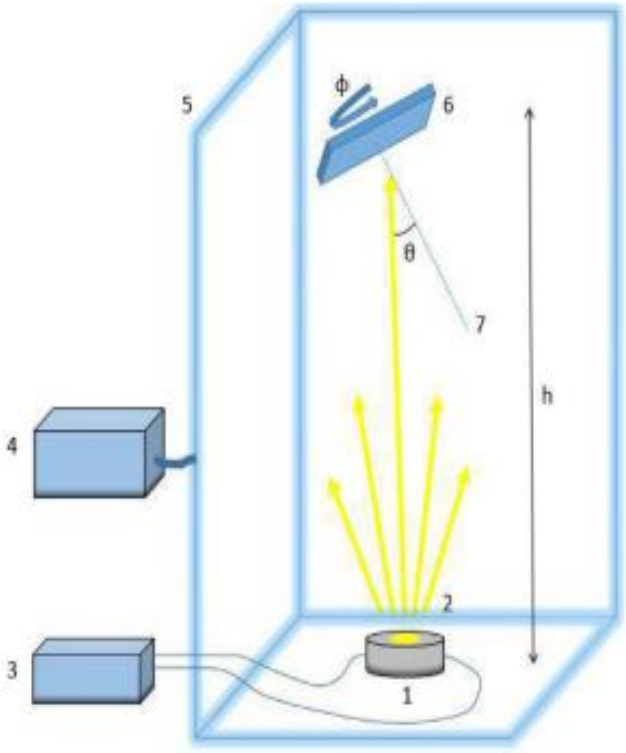

Figure (2-4) shows the mechanism of preparing samples (thin films) by the (OAD. Oblique angle deposition) method [90].

2-5 Applications of Metamaterials

2-5-1 Metamaterial as Antenna

Metamaterial coatings have been used to enhance the radiation and matching properties of electrically small electric and magnetic dipole antennas. Metamaterial step up the radiated power. The newest Metamaterial antenna radiate 95% of input radio signal at 350 MHz Experimental metamaterial antenna are as small as one fifth of a wavelength. Patch antenna with metamaterial cover have increased directivity. Flat horn antenna with flat aperture constructed of zero index metamaterial has advantage of improved directivity. Zero-index metamaterials can be used to achieve high directivity antennas. Because a

signal Propagating in a zero-index metamaterial will stimulate a spatially static field structure that varies in time; the phase at any point in a zero-index metamaterial will have the same constant value once steady state is reached. Metamaterial can enhance the gain and reduce the return loss of a patch antenna **[91]** .

2-5-2 Metamaterial as Absorber

A metamaterial absorber manipulates the loss components of metamaterials' permittivity and magnetic permeability, to absorb large amounts of electromagnetic radiation. This is a useful feature for photodetection **[92]** and solar photovoltaic applications.**[93]** Loss components are also relevant in applications of negative refractive index (photonic metamaterials, antenna systems) or transformation optics (metamaterial cloaking, celestial mechanics), but often are not utilized in these applications.

2-5-3 Metamaterial as Superlens

Super lens uses metamaterials to go beyond the diffraction limit, it has resolution capabilities that go beyond ordinary microscopes. Conventional optical materials suffer a diffraction limit because only the propagating components are transmitted from a light source. The non-propagating components, the evanescent waves, are not transmitted. One way to improve the resolution is to increase the refractive index but it is limited by the availability of high-index materials. the super lens is distinguished its aptitude to significantly enhance and recover the evanescent waves that carry information at very small scales. No lens is yet able to completely reconstitute all the evanescent waves emitted by an object. So the future challenge is to design a super lens which can constitute all evanescent waves to get perfect image.

2-5-4 Metamaterial as Cloaks

Cloaking can be achieved by cancellation of the electric and magnetic field generated by an object or by guiding the electromagnet wave around the object. Guiding the wave means transforming the coordinate system in such a way that inside the hollow cloak electromagnetic field will be zero this makes the region inside the shell disappear**[94]** .

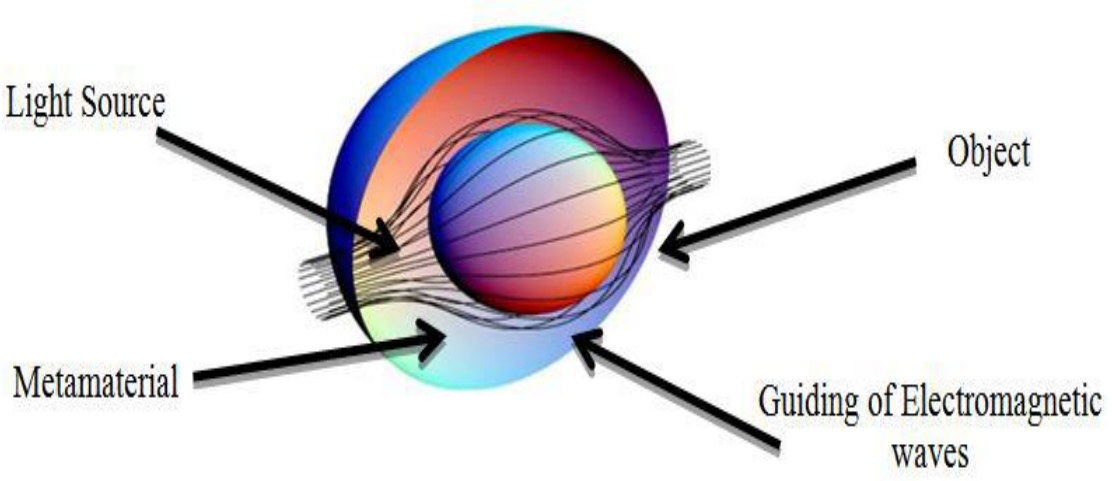

Figure (2-5) Cloaking[94].

2-5-5 Metamaterial as Sensor

Metamaterial opens a door for designing sensor with specified sensitivity. Metamaterials provide tools to significantly enhance the sensitivity and resolution of sensors. Metamaterial sensors are used in agriculture, biomedical etc. In agriculture the sensors are based on resonant material and employ SRR to gain better sensitivity, In bio medical wireless strain sensors are widely used, nested SRR based strain sensors have been developed to enhance the sensitivity**[95]**.

2-5-6 Metamaterial as Phase Compensator

Metamaterial act as a phase compensator, when wave passes through a (double positive) DPS slab having positive phase shift while DNG slab

has opposite phase shift so when wave exit from a DNG slab the total phase difference is equal to zero**[96].**

2-5-7 Seismic Protection

A seismic metamaterial, is a metamaterial that is designed to counteract the adverse effects of seismic waves on artificial structures, which exist on or near the surface of the earth **[97]** Current designs of seismic metamaterials utilize configurations of boreholesor proposed underground resonators to act as a large scale material. Experiments have observed both reflections and bandgap attenuation from artificially induced seismic waves. These are the first experiments to verify that seismic metamaterials can be measured for frequencies below 100 Hz, where damage from Rayleigh waves is the most harmful to artificial structures**[98]**.

2-5-8 Sound Filtering

Metamaterials textured with nanoscale wrinkles could control sound or light signals, such as changing a material's color or improving ultrasound resolution. Uses include nondestructive material testing, medical diagnostics and sound suppression. The materials can be made through a high-precision, multi-layer deposition process. The thickness of each layer can be controlled within a fraction of a wavelength. The material is then compressed, creating precise wrinkles whose spacing can cause scattering of selected frequencies**[99].**

2-5-9 Guided Mode Manipulations

Metamaterials can be integrated with optical waveguides to tailor guided electromagnetic waves (meta-waveguide).**[100]** Subwavelength structures like metamaterials can be integrated with for instance silicon waveguides to develop and polarization beam splitters and optical

couplers, **[101][102]** adding new degrees of freedom of controlling light propagation at nanoscale for integrated photonic devices.**[103]** Other applications such as integrated mode convertors,**[104]** polarization (de)multiplexers,**[105]** structured light generation, and on-chip bio-sensors can be developed**[106][107].**

2-6 Magnetic Properties

In discussing the magnetic properties of thin films, it is helpful to have a familiarity with the basic terminology of ferromagnetism. The term ‘particle’ is used in its general sense to indicate a localized magnetic entity and includes particulate systems, lithographically defined structures and grains. The fundamental properties of magnetic materials are the saturation magnetization MS(T), the anisotropy K(T), the exchange constant A(T), and the Curie temperature (Tc). In thin films the saturation magnetization is normally expressed as magnetic moment per unit volume. In cgs units this is emu/cm3 and in SI kA/m, where 1 emu/cm3 is equivalent to 1 kA/m**[108–109].**

1-Saturation magnetization (Ms): The saturation magnetization (at a particular temperature) describes the strength of the sum of the ordered magnetic moments from each atomic site when all the moments are pointing in the same direction, usually achieved by applying a sufficiently strong magnetic field in the direction along which the measurement is taken.

2-Anisotropy constant (K): The anisotropy (at a particular temperature) is a measure of the preference of the magnetization to lie in a particular direction or directions.

3-Curie temperature (Tc): The Curie temperature is the temperature at which spontaneous ordering of the atomic magnetic moments is lost due

to thermal excitation. Here thermal energy is comparable to the energy gain associated with ordering. The Curie temperatures have a large span, ranging from close to 0 K to 1,400 K in the case of Co. Thin film materials used in applications are typically required to have Tc significantly above room temperature and values in the range 500–700 K are common. As examples, the Curie temperature of a Co/Pd multilayer for possible application as a magnetic recording medium is reported to be 600 K **[110],**

4-Exchange constant (A): The exchange constant quantifies preference of atomic magnetic moments to align parallel to each other (or antiparallel in the case of an antiferromagnetic material) in an equilibrium direction. When the moments are not perfectly aligned, the total energy of the system (material) is increased. This alignment of atomic magnetic moments is often referred to as the exchange stiffness**[109].**

Three ordered magnetic states are known: ferromagnetism, ferrimagnetism and antiferromagnetism, and all three states are found in thin films. The strength of the exchange interaction is described by the exchange integral which represents this overlap of charge distributions between neighboring atoms **[111].** In the simplest case the saturation magnetization is determined by the number of unpaired electrons that are available for alignment. As the temperature increases, thermal energy acts to disorder this alignment, reducing M.S monotonically, and at a sufficiently high temperatures alignment is lost, this being the Curie temperature (Tc)**[109, 112].** In a ferrimagnet there are two ferromagnetic sublattices with opposite orientation which sum to give the total moment of the material. Ferrimagnetic thin films are important in magneto-optic recording and very recently have been shown to switch using only optical excitation,

The magnetic properties of thin films differ from those of bulk materials in several important particulars:

magnetostatic interactions are typically dominated by the effectively infinite ratio between lateral dimensions and thickness,

the ability to grow templated structures where specific seedlayers can be employed to create artificial crystallographic structures not thermodynamically isolatable in the bulk .

atomic control of interfacial structure allowing magnetic phenomena to be tailored, e.g. exchange bias, exchange springs, perpendicular anisotropy.

2-7 Magneto-Plasmonics

Surface plasmons are waves that propagate along a metal-dielectric interface **[113–114].** A localised surface plasmon is the result of the confinement of a surface plasmon in a metallic nanoparticle of size comparable to or smaller than the wavelength of light used to excite the plasmon. Metallic nanoparticles at or near their plasmonic resonance generate highly localised electric field intensities. Varieties of nanoparticles and their constellations (e.g., nanoantennas **[115]**) were shown to enhance the local field and thus improve light-matter interaction. Since all metals absorb light in the visible and infrared spectral ranges, maximum efficiency of a plasmonic device can be achieved by using metals with the lowest absorption cross-section. Therefore, most of the plasmonic devices are made of gold or silver because these two metals exhibit the lowest absorption losses at optical frequencies. However, in many practical cases, these metals must be combined with optically active materials in order to provide active control of plasmons **[116].** In particular, plasmons can be controlled by a

magnetic field applied to a hybrid device consisting of a plasmonic metal nanostructure combined with a ferromagnetic layer. The research field that combines magnetic and photonic functionalities is called magneto-plasmonics **[117][118]**.

2-8 Permittivity and Permeability of Metamaterail

Metamaterials have become a remarkable research area in recent years and have received burgeoning interest due to their unprecedented properties that are unattainable from ordinary materials. Veselago pointed out that a material exhibiting negative values of dielectric permittivity (ε) and magnetic permeability (μ) would have a negative refractive index **[119] [120].** Generally speaking, dielectric permittivity (ε) and magnetic permeability (μ) are both positive for natural materials. In fact, it is possible to obtain negative values for ε and μ by utilizing appropriate designs of metamaterials. To be specific, negative permittivity values at microwave frequencies are accessed by making use of thin metallic wire meshes **[121] [122].** It is rather difficult to obtain negative permeability due to the absence of magnetic charges. design consisting of two concentric rings with a split on each ring. This structure is called the split-ring resonator (SRR), since it exhibits a certain magnetic resonance at a certain frequency. An array of SRRs is then demonstrated to have

negative permeability close to the resonance frequency**[123].** The first steps to realizing these novel types of materials were taken by Smith *et al*, where they were able to observe a lefthanded propagation band at frequencies where the dielectric permittivity and magnetic permeability of the composite metamaterial are negative Soon after, left-handed**[124–125].**

metamaterials with an effective negative index of refraction were successfully demonstrated by various groups **.**Negative refraction is also

achieved by using periodically modulated two-dimensional photonic crystals One of the most exciting applications of negative-index metamaterials (NIM) is a perfect lens **[126-127].** Stimulated by J B Pendry's seminal work, superlenses that are capable of imaging subwavelength-size objects have attracted a great dealof interest **[128–129].** Sub-diffraction free imaging has been demonstrated experimentally for photonic crystals **,**lefthanded transmission lines **[130],** and left-handed metamaterials (LHM) **[131–132].** In the near-field regime, the electrostatic and magnetostatic limits apply and thus the electric and magnetic responses of materials can be treated as being decoupled. This, in turn, brings forth the possibility of constructing superlenses from materials with negative permittivity **[133–134]** or negative permeability **[135].** Metamaterials offer a wide range of exciting physical phenomena that are not attainable with ubiquitous materials. To be specific, it has recently been shown that one can achieve cloaking by using metamaterial coatings **[136, 137].** Metamaterial structures have recently been used to obtain novel mechanisms in nonlinear optics and to increase the performance of active devices **[138-139].** Metamaterials are geometrically scalable, and therefore they offer a wide range of operating frequencies including radio ,microwave **[140- 141].**millimetre-wave farinfrared (IR) **,**mid-IR **,**near-IR frequencies, and even visible wavelengths **.**Recently, an acoustic analogue to electromagnetic metamaterials, the socalled ultrasonic metamaterials, was demonstrated **[142], [143].**

2-9 Negative refractive index metamaterials

The refractive index is a basic parameter of materials which it is essential to know for the manipulation of electromagnetic waves. However, there are no naturally occurring materials with negative

refractive indices, and high-performance materials with negative refractive indices and low losses are demanded in the terahertz waveband.

Terahertz metamaterials **[144]** are artificial materials with subwavelength structures and can manipulate terahertz waves such as absorber [**145**], antireflection coating and polarization conversion [**146-147].** Metamaterials have evolved into metadevices **[148**] for active control of terahertz waves with various external modulations such as optical pump **[149–150**], electric field temperature and Micro Electro Mechanical Systems (MEMS) **[151,152] .**Metamaterials can provide unprecedented refractive indices such as negative refractive indices due to the direct control of the relative permittivity and permeability**[153-154].** A material with a negative refractive index would make possible a perfect lens and superlenses with resolutions beyond the diffraction limit in imaging**[155] [156]**. The work in was the first to report a negative refractive index utilizing the meta-atoms of split ring resonators and metal wires in the microwave band. A steric structure consisting of metal rings and wires has demonstrated near perfect imaging beyond the diffraction limit in the microwave band **[157,158] .**A low-loss metamaterial with a negative refractive index would be essential, especially for high resolutions even though conductor and dielectric losses are in principle unavoidable. However, it is not straightforward to demonstrate an ideal metamaterial in the terahertz waveband because the dimensions of the meta-atoms are of the order of ten to a hundred microns, and this considerably limits the design flexibility of steric structures**[159] [160].** Further, substrates are commonly required to be able to fabricate metamaterials, but there are few materials with low losses in the terahertz waveband. Two-dimensional metamaterials, meta-surfaces, have a high potential utility in the terahertz waveband as the application of a lamination structure would

make bulky metamaterials with a three-dimensional structure possible. Some papers have reported measurements and simulations of meta-surfaces with a negative refractive index in the terahertz wave band which were composed of several meta-atoms, such as an I-shaped structure a cross-shaped structure **[161-162].**

2-10 Metasurfaces

Metasurfaces are two-dimensional or surface counterparts of metamaterials. Just like metamaterials, it is possible to characterise their response through their electric and magnetic polarizabilities. They are also referred to in the literature as metafilms **[163].** Metamaterials control the propagation of light due to their bespoke permittivity and permeability values; however, they still use the propagation effect to manipulate the electromagnetic waves. This can result in a complicated relatively bulky structure whereas metasurfaces try to manipulate the wave over a single extremely thin layer **[164,165**]. The two-dimensional nature of metasurfaces, therefore makes them less bulky and offers the possibility of lower loss structures **[166].** Due to their 3D nature, it is also difficult to fabricate metamaterials. Metasurfaces offer an extremely promising alternative. Due to their planar structure, metasurfaces can be easily fabricated using planar fabrication tools **[167,168].** The planar fabrication process is also very cost-effective in comparison to the manufacturing of the complex 3D metamaterials **[169].** Metasurfaces, being two-dimensional materials, can, therefore, be easily integrated into other devices which can make them a salient feature for nanophotonic circuits; this property will also allow them to be a part of “lab on chip” photonics **[170].**The negative index of the metamaterials is due to the resonance of the individual meta-atoms. This property makes the metamaterials inherently dispersive, thus the electromagnetic properties

of such materials are highly sensitive to the changes in the operating frequency, thus making such materials bandwidth limited. It has been shown in **[171]** that by using extremely thin metasurfaces with deep sub-wavelength to make a broadband metasurface filter. The (in-band) transmission and (out of band) rejection was achieved by respectively matching and mismatching the impedance of this metasurface (to the free space)**[171].** Due to the variety of advantages offered by metasurfaces over metamaterials, the scientific community has shown a keen recent interest in this area. This has led to rapid development in the underlying physics which govern the behaviour of metasurfaces and their potential applications.

2-11 Applications of Metasurfaces

The interaction of surface plasmon with the electromagnetic wave leads to a phase discontinuity across the metasurface. Since elements on a metasurface can be spatially varied, this variation can cause the currents on the surface to lead (or lag) depending on the individual resonant element. This localized phenomenon allows us to tailor the wave fronts as they pass through a metasurface and leads to a variety of applications.

2-11-1 Wave front Control/Shaping Using Metasurfaces

In the past, wave front shaping in the microwave regime has been achieved with the help of reflect- and transmit-arrays **[172,173].** Such arrays have used variable element size and rotation (in case of reflect-arrays), and aperture coupled miniaturized delay lines (with a patched ground) for the transmit-array, in order to shape the wave fronts **[174,175].** Such arrays, however, have a periodicity of the order $\lambda/4 - \lambda/2$, therefore, they do not provide sub-wavelength resolution (sub-wavelength resolution can improve the aperture efficiency of such arrays) **[176,177].** Due to large periodicity, the induced electric and magnetic

polarize abilities can no longer completely define their response and they cannot be considered ‘homogenized’, hence they are not classified as metasurfaces. Metasurfacas allow the 360 control of the phase by introducing anisotropy through its individual elements-shaped anisotropic elements have been used to obtain full control of the phase , however, reflection losses reduce the efficiency of the structure to 50% and since anisotropy exploits the cross –polar component to achieve a full 360_ of phase manipulation, the efficiency of the structure is further halved **[178,179].** In order to unlock further potential of metasurface design, multi-layered Huygens surfaces have been proposed **[180].** These surfaces eliminate the reflection losses completely. Huygen’s metasurfaces with an efficiency of 86% at 10 GHz **[181].** This design also showed a wide 3-dB bandwidth of 24%.The local phase manipulation by metasurfaces has also been used to shape the wave fronts of the reflected wave. The variation in the dimensions of square patches on a dielectric layer backed by a ground plane has been shown to tailor the reflected wave front **[182].** By carefully controlling the size and response of each sub-wavelength inclusion in along both perpendicular axes, a birefringent metasurface has been successfully constructed in **[183].** This metasurface showed an efficiency of 92% with the additional advantage of splitting the incoming non-polarized electromagnetic wave into two orthogonal linear polarizations. A similar approach using perpendicular strip dipoles in a triangular lattice in terahertz range has been presented in**[184]** Another technique has been developed to replicate the behavior of arbitrary materials by using heterogeneous layers **[185] [186].**

2-11-2 Metasurface Lenses

Metasurfaces can also be employed to fabricate ultrathin lensesThis profile also alters the shape of the wave front from planar to spherical, a condition necessary for focusing. High numerical aperture efficiency can

be achieved as long as the electromagnetic wave strikes the surface at normal. However, when the angle of incidence is not perpendicular, a phenomenon known as 'coma' occurs, which can cause significant degradation in the numerical aperture efficiency. The effects of 'coma' can be reduced by placing the surface on a curved piece of dielectric **[187].** Metasurface consisting of v-shaped antennas have been shown to focus energy at telecom frequencies**[188].** Another metasurface lens based on reflect-arrays is presented in **[189].** The lens was designed for the near infrared region and was designed on a metal-insulator-metal structure. Gold bricks were deposited on silicon dioxide and the individual elements were optimized in order to engineer the desired reflection response. This lens showed a theoretical efficiency of 78%.

A metasurface lens based on rectangular dielectric resonators (RDRs) has been shown to focus energy at a single focus for three different frequencies. This was made possible by making the sum of the phase transversed by the wave and the phase jump imparted by the metasurface constant at three distinct frequencies. The resulting metasurface ended up being completely aperiodic **[190].**

2-11-3 Non-Linear Metasurfaces

Non-linear metasurfaces have been deployed to protect sensitive electronics and reduce interference on a shared platform. Non-linearity was introduced using diodes and capacitors which were incorporated in the design process and controlled the response of the metasurface. This surface absorbed the high-powered radio frequency signals while causing a minimal distortion to the low powered ones **[191].** In non-linear electrodynamics, metasurfaces and metamaterials can be used to enhance the magnitude of the non-linearity. They also allow targeting of the magnetic non-linear phenomenon and can combine it with the electric non-linearity **[192].** One of the most important aspects of non-linearity is

the second harmonic generation which is the process where two photons combine to form a single photon. This new photon has twice the energy and its frequency are also double in comparison to the original photon(s). This phenomenon happens when two photons interact with a non-linear material **[193,194].** Metasurfaces have been deployed to enhance this process, an enhancement in the resonance of the second harmonic generation spectrum was observed using spectroscopy **[195].** It needs to be noted that if a medium is inversion symmetric, it cannot generate the second harmonic and thus breaking the symmetry is imperative in order to observe the second harmonic generation.

2- 12 Magneto –optics properties for Metamaterials

Magneto-optical (MO) phenomena such as Faraday rotation (FR) provide physical information on spin and electronic structure of magnetized materials. Therefore, it is desirable to achieve a high rotation angle at short wavelengths (UV, visible and near-infrared regions)**[196].**

Magneto-optical effects are at the core of polarization-control, telecommunications, sensing, and the emerging field of non-reciprocal photonics **[197,198]** where axial symmetry of the magnetic field is the enabling mechanism for the violation of Parity-Time symmetry of the optical response. Unfortunately, homogeneous materials available in nature exhibit relatively weak magneto-optical activity. Artificial magneto-optical behavior has been recently demonstrated in photonic-crystal-inspired structures and in wave guided geometries **[199,200],** configurations known for their sensitivity to long-range order and, therefore, highly susceptible to fabrication imperfections. Planar multilayered and more complex geometries have been suggested theoretically **[201].** multicomponent nanostructured metamaterials can be used to significantly enhance magneto optical response of their inclusions by combining field enhancement, enabled by plasmonic nanostructures,

and the strong anisotropy of Nano rod composites**[202,203].** The metamaterial is fabricated using standard electrode position protocols**[204]**. and operates inthe effective medium regime, known for its tolerance to small-scale geometry variations.

Chapter Three

Experimental Work

3-1 Introduction

This chapter deals with an introductory description and a study of all the materials and devices used in this study, as well as the method of preparing the various samples and the devices used in the samples, and a detailed description of the optical systems that were approved in order to obtain the results, as well as the description of these systems and their components, and how to obtain the magneto optics properties , and it includes the lobe of the samples using the samples are XRD, SEM ,CCD Camera, spectrometer .

3-2 Materials that Used in the Experimental Part:

3-2-1 Titanium Dioxide (TiO_2)

Titanium dioxide (TiO2) is a white inorganic compound, an insulator.TiO2 absorbs UV light. This property makes it appear bright white under light, unlike other white materials that can look slightly yellow.Importantly, TiO2 also has a very high refractive index (its ability to scatter light), even higher than diamond. This makes it an incredibly bright substance and an ideal material for aesthetic design use.Another crucial property of TiO2 is that it can show photocatalytic activity under UV light. This makes it effective for environmental purification, for different kinds of protective coatings, sterilisation and anti-fogging surfaces, and even in cancer therapy. Titanium dioxide has a number of unique characteristics that make it ideally suited to many different applications **[205].**

Table (3-1): physical properties of TiO_2[206]

Molecular formula	**TiO_2**
Appearance	**White**
density	**4.23 gm/cm^3 (rutil) ,3.78gm/cm^3 (anataz)**
melting point	**1843 c°**

3-2-2Magnesium Fluoride (MgF_2)

Magnesium fluoride is an inorganic compound with the formula MgF_2. The compound is a white crystalline salt and is transparent over a wide range of wavelengths, with commercial uses in optics that are also used in space telescopes. Windows, lenses, and prisms made of this material can be used over the entire range of wavelengths from 0.120 μm (ultraviolet) to 8.0 μm (infrared).Magnesium fluoride is tough and polishes well but is slightly birefringent and should therefore be cut with the optic axis perpendicular to the plane of the window or lens **[207].** Due to its suitable refractive index of 1.37, magnesium fluoride is commonly applied in thin layers to the surfaces of optical elements as an inexpensive anti-reflectivecoating.Its Verdetconstant is0.00810 arcmin·G^{-1}·cm^{-1} at 632.8 nm. The properties of MgF_2 showing in table.

Table (3-2): The properties of MgF_2 [208]

Chemical formula	MgF2
Molar mass	62.3018 g/mol
Density	3.148 g/cm^3
Appearance	White tetragonal crystals
Refractive index	1.37397
Melting point	1,263 °C (2,305 °F; 1,536)K
Boiling point	2,260 °C (4,100 °F; 2,530 K)

3-2-3 Nickel (Ni)

Nickel is a hard, silvery-white metal whose strength, ductility and resistance to heat and corrosion make it extremely useful for the development of a wide variety of materials from wires to coins to military equipment. This extremely useful metal is No. 28 in the periodic table of the elements, between the elements cobalt and copper. Nickel is a fairly good conductor of electricity and heat and is one of only four elements (cobalt, iron, nickel and gadolinium) that are ferromagnetic (magnetized easily) at room temperature. Nickel is a transition metal, meaning it has valence electrons in two shells instead of one, allowing it to form several different oxidation states. Nickel is the fifth most abundant element on Earth. However, it is 100 times more concentrated below the Earth's crust than in it, according to Chemical. In fact, nickel is

believed to be the second most abundant element in the Earth's inner core, with iron being the first by a large margin. Nickel is typically found in two types of deposits: laterite deposits, which are the result of intensive weathering of surface nickel-rich rocks, and magmatic sulfide deposits. Nickel can also be found in manganese nodules and crusts on the deep sea floor, but currently these are not being mined. Alnico magnets a combination of aluminum (Al), nickel (Ni) and cobalt (Co) are very strong permanent magnets that retain their magnetism even when heated until they glow red, according to Chemical**[209]**

Table (3-3): The properties of Ni[210]

atomic number	28
atomic weight	58.69
melting point	1,453 °C (2,647 °F)
boiling point	2,732 °C (4,950 °F)
Density	8.902 (25 °C)
oxidation states	0, +1, +2, +3
electron configuration	[Ar]3d84s2

3-2-4 Gold (Au)

Gold is one of the densest of all metals. It is a good conductor of heat and electricity. It is also soft and the most malleable and ductile of the elements **[211].** Due to its beautiful appearance and the fact that it is a metal that does not tarnish or corrode, it was one of the first metals that attracted humans. **[212],** Gold is one of the noblest—that is, least chemically reactive—of the transition elements. It is not attacked by

oxygen or sulfur, although it will react readily with halogens or with solutions containing or generating chlorine, such as aqua regia. It also will dissolve in cyanide solutions in the presence of air or hydrogen peroxide. Dissolution in cyanide solutions is attributable to the formation of the very stable dicyanoaurate ion, [Au(CN)2] **[213, 214].** the gold chemical inertness being a bulk metal appeared to provide very few chances to open up chemistries being exciting and new. The new nanotechnology field render it possible to find the matter unique properties if sub-classified to nano scale **[215].** At the point when the size of a gold molecule is dynamically diminished underneath about10nm, such particles, frequently named nanoparticles **[216].** Gold nanoparticles (Au NPs) are especially intriguing a direct result of its simple readiness and high strength. In view of measurements, Au NPs might partition into 3 sections: (a) Au Nps of 0- dimensional: quantum dots, spherical nanoparticales. (b) Au NPs of 1-dimensional: nanowires, nano-rods, nano-belts, nanotubes. (c) Au NPs of 2-dimensional: nano-shell, and nano-plates of gold, and (d) Au NPs of 3-dimensional: nano-tadpoles of gold, nanodumbbells of gold (Au NDs), Au NPs being spread, for example, nano-stars, nano-pods, and nano-dendrites of gold **[217,218].** Au Nano-spheres: The diameter of Au Nano-sphere could range from (1 to 100) nm, and might be produced via reducing solution as aqueous $HAuCl_4$ under specific parameters and conditions with the addition of various reducing agents. Citrate is reducing agent mostly used commonly was that made Au Nano-spheres as mono disperse **[219, 220].** Au Nano-rods: The Au Nano-rod diameter of could be established of template membrane holes. Au Nano-rod length might be measured through dropped Au quantity inside the membrane hole **[221, 222].** In 1997, the basic Au NRs were blended through electro-chemical strategy. Platinum and gold as cathode and anode, respectively were immersed in an 76

electrolytic organization having co-surfactant, cationic surfactant, and hexadecy tri-methyl ammonium bromide (CTAB) **[223].**Au NPs were shaped via rotating the bulk metal of gold being structure of anode into nanoparticles **[224, 225].** Au Nano-shells: Nano-shell denoted as spherical nanoparticle type with core being dielectric that was enclosed via a thin shell being metallic (Au usually) **[226][227].** gold Nano-shells presented of small Nano-spheres of Au to the silica core with (2-4nm) diameter. The silica core diameter control Au Nano-shell diameter. Thickness of shell might be measured via dropped Au quantity on surface of core **[228].**

3-2-5 Polydimethylsiloxane (PDMS)

Polydimethylsiloxane (PDMS) is a polymer belonging to the group of silicone elastomers. It is a hyperplastic material that has a wide application in the biomedical industry, from contact lenses to medical devices, and also in the area of research and behaviors of diseases **[229],** thus attracting the attention of many researchers who see PDMS as a more sophisticated material which can replace previous methods and obtain more accurate data. The synthesis of silicone was first obtained in 1950 by the Wacker Chemiecompany **[230].** One of the first uses of PDMS occurred in the encapsulation of electronic components in order to extend the lifespan of the chips. With the development of technology and of behavioral studies and their characteristics, PDMS has been gaining new applications in micro and nanotechnology, and in the study of the biophysical behavior of blood flow in micro vessels **[231].** PDMS is a material that has good microstructural characteristics, good manufacturing ability and a low cost. In the study of the microfluidics, it has been verified that PDMS presents higher properties than the old

techniques that used materials such as glass and silicon, once the use of PDMS makes the work simpler and cheaper **[232], [233].** In addition, PDMS is thermally stable, optically transparent **[234],** works as a thermal and electrical insulation **[235],** has good chemical stability and degrades quickly in the natural environment when compared to other polymers, and it presents no environmental problem. PDMS, a synthetic polymer whose main axis is made from the repetition of silicon and oxygen bonds and methyl groups **[236]**, PDMS has a unique property and can be altered for different applications one of the advantages of the PDMS is able to chemically modify its structure, consequently opening the way to new applications and showing the need for new studies to understand its behavior and applicability **[237], [238].** Other important properties of PDMS are the permeability and elasticity. Permeability is the product of the solubility of a gas in a polymer and its diffusion. Siloxanes have greater permeability than most elastomers. The permeability of PDMS makes it advantageous for industrial applications in which it is necessary the separation of gases from the material, for example, in the development of artificial skins for burns **[239]**.

3-3 The using Devises:

3-3-1 X-Ray Diffraction (XRD):

The crystal structures of (**PDMS /TiO_2) , (TiO_2/PDMS/TiO_2), (PDMS/MgF_2) ,(AuNps/MgF_2) (AuNps/MgF_2/Ni),(AuNps/Tio_2/Ni)** films were determined using X-ray diffraction equipment. The crystal structure, orientation, and grain size may all be determined using X-ray diffraction, which is a strong non-destructive approach for material characterization. A typical X-ray wavelength that is equivalent to the interatomic distance in a crystal is used for characterization. When the

path difference is an integer multiple of the wavelength, constructive interference occurs. This is the diffraction Bragg condition. In the corresponding directions, the intensity of the reflected beam exhibits distinct peaks. They're known as the Bragg peaks. The Bragg peak can be detected by changing the detector's angle (2θ).

$2d \sin\theta = n\lambda$ ... ... (3−1)

Where n is an integer , d is a distance between the atomic layers, λ is a wavelength of the incident X-ray beam

Scherer's formula measures the grain size (D) in a polycrystalline film:

$$D = \frac{0.9\,\lambda}{\beta\, cos\theta} \quad \ldots\ldots\ldots\ldots\ldots\ldots\ldots (3-2)$$

Where β :is the full width at half maximum (in radians) of the peak (FWHM), (θ) :is the Bragg angle, (λ)=1.5406 A^0 **[240].**Figure (3-1, a and b) illustrates the image and diffraction of a beam of parallel and monochromatic X-rays of wavelength (λ) incident at an angle (θ) on a crystal. if the wavelength in equation (3-1) is less than or equal to twice the distance between two successive planes in the crystal can Bragg diffraction occur.

Figure (3-1): XRD used device to measure the prepared samples.

3-3-2 Scanning Electron Microscopy(SEM)

The scanning electron microscope (SEM) uses a focused beam of high-energy electrons to generate a variety of signals at the surface of solid specimens. The signals that derive from electron and specimen interactions reveal information about the sample including external morphology (texture), chemical composition, and crystalline structure and orientation of materials making up the sample. Areas ranging from approximately 1 cm to 5 microns in width can be imaged in a scanning mode using conventional SEM techniques .The SEM is also capable of performing analyses of selected point locations on the sample; this approach is especially useful in qualitatively or semi-quantitatively determining chemical compositions ,crystalline structure, and crystal orientations .

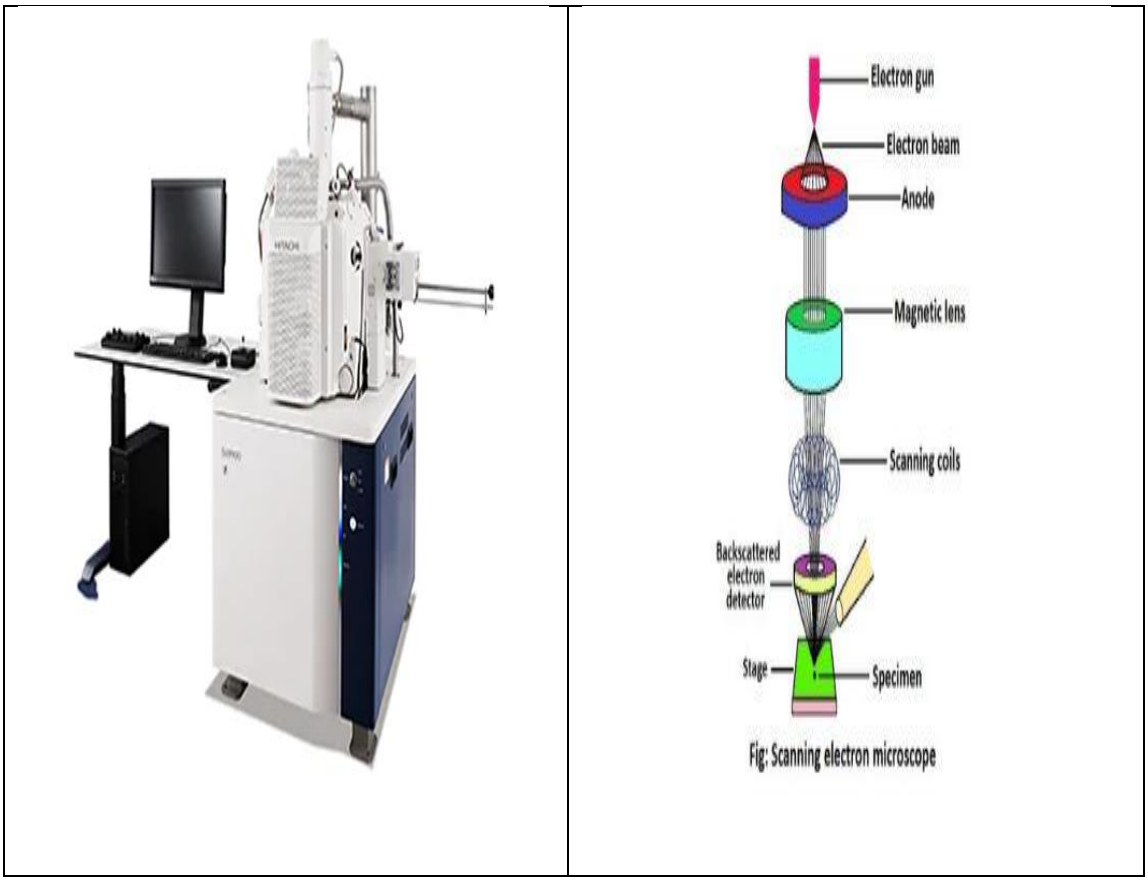

a b

Figure (3-2)(a) Scanning Electron Microscopy(SEM)(b)Structure and description

3-3-3 Charge-Coupled-Device (CCD Camera)

CCD sensor is a multifunction electronic component with high demand in today's industries. This type of sensor is very special in its architecture design where it consists of more than a thousand numbers of very small sensor which sensitive to light sources. In an optical tomography system, high number of sensors will give higher resolution of image reconstruction. For CCD sensor, the size of its optical sensor can be a few microns and this allows the existence of a thousand sensors in one projection. **[241], [242],** CCD was used as a memory storage. After a few years, this electronic component became popular as one of the

optoelectronic sensors for image detection. The basic principle that used by is based on electrical charge moving. The sensor of this component is made by a Metal Oxide Semiconductor (MOS) capacitor. When the light strikes onto the surface of the CCD, photon charges will attract an electron charge to escape from its covalence band. The number of electrons produced depends on the number of photons striking the glass of this detector. Then electrons will be shifted to the next sensor until it reaches the last sensor. Last sensor will send the data to the computer to process and produce an image reconstruction **[243].** The CCD was used in many engineering fields such as astronomy, medical and process industries. Different field has different requirement of CCD. For an example, the high quality of CCD required by astronomy field because it needs a robust component that can deal with the drastic changes of temperature and high capability of capturing outer space image. Meanwhile for process industries, usually it is low cost and consists of two types of sensor; colour CCD and monochromatic CCD. The colour sensor is usually used in video and photographic cameras, while the monochromatic sensor is used in facsimile machines and scanners for medical purposes**[244].**

Figure (3-3)Charge-Coupled-Device (CCD camera)

3-3-4 High Reclusion Spectrometer(HRS)

is a small-footprint, high-resolution spectrometer that is well suited for applications such as wavelength characterization of lasers and LEDs, monitoring of gases and monochromatic light sources, and determination of elemental atomic emission lines, Chemicals absorption, and color analysis, depending on spectrometer configuration, optical resolution as fine as ~0.02 nm(FWHM) is possible. Also, users can add (HRS) accessories such as light sources, probes and optical fibers to configure a variety of application-specific systems. (HRS)A draws power from the both power supply and also host PC, eliminating the need for an external power supply. (HRS)A is perfect for applications where fast reactions need to be monitored and high resolution is necessary, such as chemistry and biochemistry applications. Data programmed into a memory chip on each (HRS) includes wavelength calibration coefficients, linearity coefficients, and the serial number unique to each spectrometer. Our spectrometer operating software simply reads these values from the spectrometer. a feature that enables hot swapping of spectrometers among

PCs. (HRS) Spectrometer connects to a notebook or desktop PC via USB port.

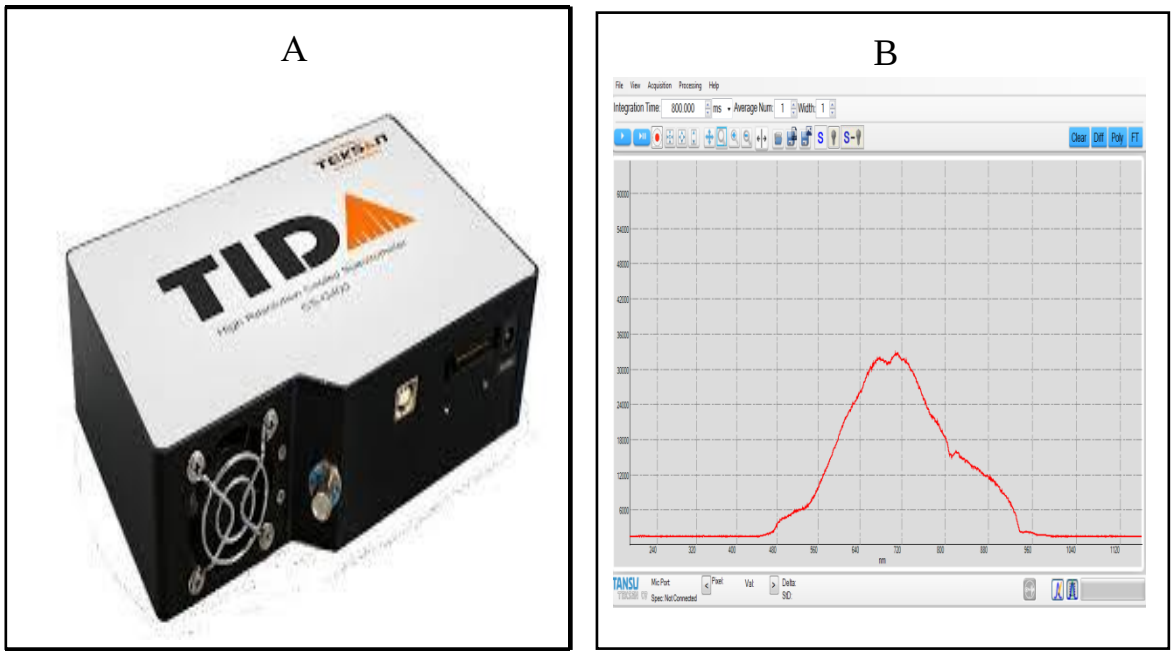

Figure (3-4)(A) high reslusion spectrometer (B) A model of the resulting pulse

3-4 Samples preparation

3-4-1 Sample Fabrication Process

Two-dimensional samples based on polydimethylsiloxane (PDMS) substrate were fabricated using a soft Nano-lithography technique. In this method, the charge-coupled device (CCD) of a camera was used as a stamp, which has a two-dimensional periodic square pattern with a high resolution. Also, PDMS material was chosen as a substrate, which is a flexible and transparent polymer that makes it a good candidate for soft Nano-lithography technique. A schematic layout of the fabrication process of two-dimensional samples by soft Nano-lithography method is shown in Fig. 3-5. First, a CCD was carefully extracted from a camera without damaging its surface. Then, the CCD was placed on a glass and the mold was fixed on it and around it was sealed with thermal glue to

prevent leakage. In parallel, PDMS polymer and curing agent were mixed at a weight ratio of 10:1 with a DC stirrer for 5 minutes to obtain a homogeneous mixture. The mixture of PDMS base and curing agent was injected into the prepared mold on the CCD. For degassing, the sample was placed in the vacuum chamber for 15 minutes. Afterward, the PDMS composite was cured for an hour at the temperatures of 50°C to 100°C using a hot plate. Finally, the sample was kept at room temperature for 24 hours to finalize the pattern transferring on the PDMS substrate. After 24 h, the patterned PDMS film was carefully peeled off from the CCD stamp, and a 2D periodic PDMS-based nanostructure was successfully achieved

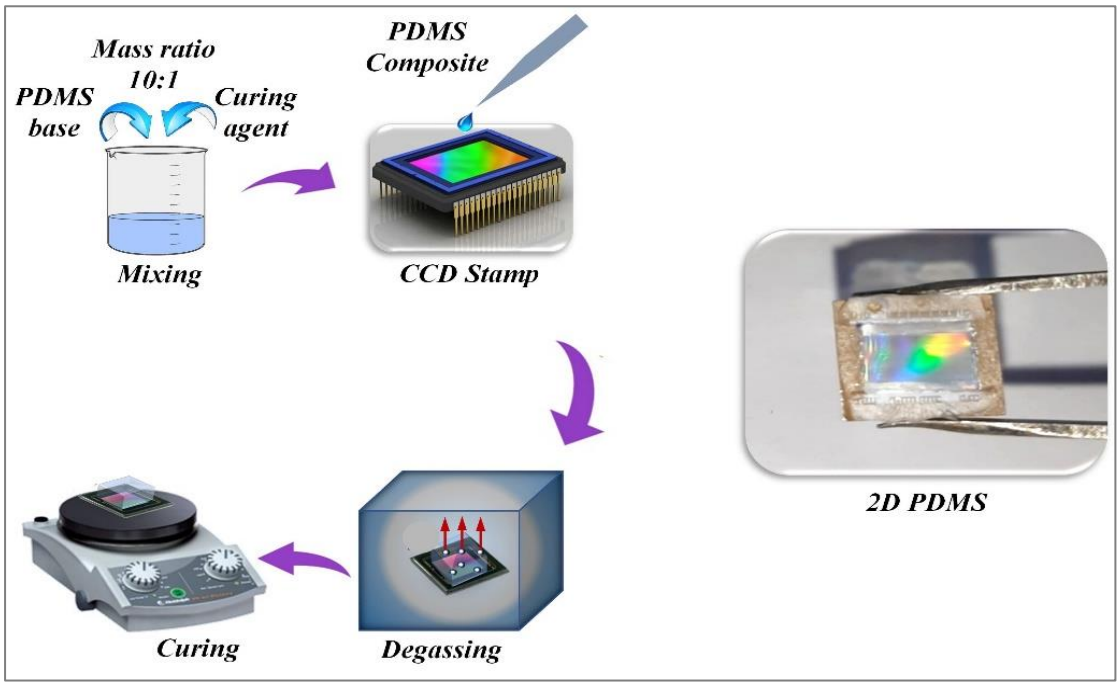

Figure (3-5) Schematic array of the PDMS preparation steps

In this way, two 2D samples based on PDMS substrate were produced, and a thin layer of TiO_2 (34 nm) and MgF_2 (10 nm) was deposited onto the patterned 2D PDMS-based samples using the sputtering technique. Consequently, two-dimensional all-dielectric nanostructures (2D PDMS/TiO_2 and 2D PDMS/MgF_2) were successfully fabricated with a

low-cost, and simple design method based on soft nanolithography .the detail of preparing each sample are mentioned in the paragraph (3-6)

3-5 sputtering system

The system consists of a cathode and an anode where the substrate is placed obliquely between the cathode and an anode, the distance between the cathode and the anode is 20 cm and argon gas is connected to the device and the pressure inside the (champer) is adjusted (5-33)mb ,Parameters are tuned to obtain high specification quality of thin films.this system in in the central laboratory of university alsheed bahasty

Figure (3-6) sputtering system

3-6 The used Samples

In this work, four different groups of samples were used:

Group one

- **Sample1: One-side 2D grating (PDMS/TiO_2(50nm))**

This sample was from a two-dimensional single grating (PDMS/TiO2(50nm)) This sample consists of a periodic two-dimensional square array, basal PDMS, which is a thin layer of TiO_2 laminated with a surface shaped. This sample is a fully dielectric based microstructure which consists of a two- dimensional grating on one sides .as in Figure(3-7)(a)

- **Sample 2: Two-sides 2D grating (etalon) (TiO2 (50nm) /PDMS/ TiO2 (50nm)**

This sample consists of a two-dimensional square periodic matrix, based on PDMS, which is covered by a thin layer of TiO_2 on its surface this sample (etalon-based) both sides of the sample have a 2D periodic microstructure as in Figure (3-7)(b).

Group two

- **Sample 1: 2D (PDMS/MgF2) different periodic(50nm)**

This sample consists of 4 samples of different periodic sizes. This specimen also has a 2D pattern on one side and a thin layer of MgF2 coated on its surface.

Group Three

- **Sample 1: 1D PDMS/MgF_2(10nm)**

This sample was from a one-dimensional single grating (PDMS/MgF2 (10nm)) This sample consists of a periodic one-dimensional square array, basal PDMS, which is a thin layer of MgF_2 prepared by Radio Frequency sputtering laminated with a surface shaped This sample is a fully dielectric based microstructure.

Sample 2: 1D PDMS /MgF_2/ Au (34n)

This sample was from a one-dimensional single grating (PDMS/ MgF2 (10nm))/Au(34) This sample consists of a periodic one-dimensional square array, basal PDMS, which is a thin layer of MgF_2prepared by Radio Frequency sputtering and Au that

prepared by direct current (DC) sputtering laminated with a surface shaped This sample is a fully dielectric based microstructure .

Sample 3: 1D PDMS/MgF_2/ Au/Ni (30)

This sample was from a one-dimensional single grating (PDMS/ MgF2 (10nm))/Au(34)/Ni(30)This sample consists of a periodic one-dimensional square array, basal PDMS, which is a thin layer of MgF2 and Au and Ni that prepared by direct current sputtering(DC) laminated with a surface shaped This sample is a fully dielectric based microstructure.

Group four

- ### Sample 1: 2D PDMS/TiO_2 (34nm)

This sample was from a two-dimensional single grating (PDMS/TiO2(50nm)) This sample consists of a periodic two-dimensional square array, basal PDMS, which is a thin layer of TiO_2 prepared by RF sputtering laminated with a surface shaped This sample is a fully dielectric based microstructure.

Sample 2: 2D PDMS /TiO_2/ Au (34nm)

This sample was from a two-dimensional single grating (PDMS/TiO2(50nm)/Au (34) This sample consists of a periodic two-dimensional square array, basal PDMS, which is a thin layer of TiO_2 and Au laminated with a surface shaped This sample is a fully dielectric based microstructure.

Sample 3: 2D PDMS /Tio_2/ Au /Ni (34nm)

This sample was from a two-dimensional single grating (PDMS/TiO2(50nm)/Au/Ni (34) This sample consists of a periodic two-dimensional square array, basal PDMS, which is a thin layer of TiO_2 and Au and Ni laminated with a surface shaped This sample is a fully dielectric based microstructure.

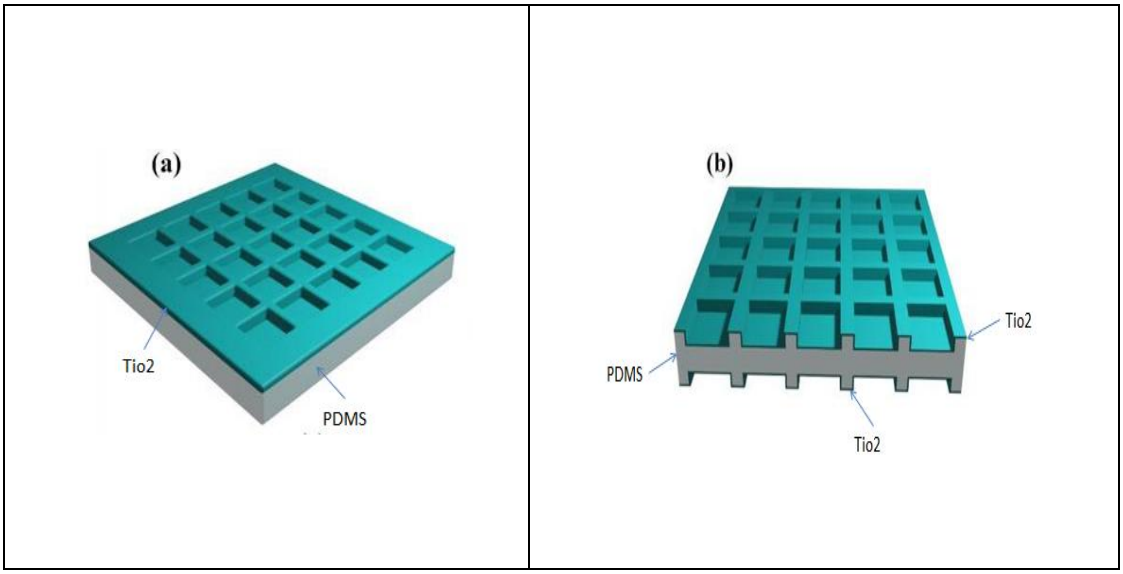

Figure (3-7)Sample(a) one –side 2D grating (PDMS/TiO_2(50nm)) (b) two-side 2D grating (etalon) (TiO_2(50nm)/PDMS/TiO_2(50nm)

A

B

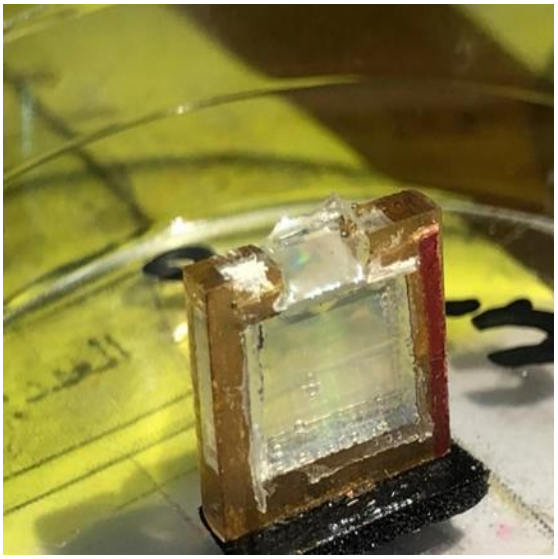

C

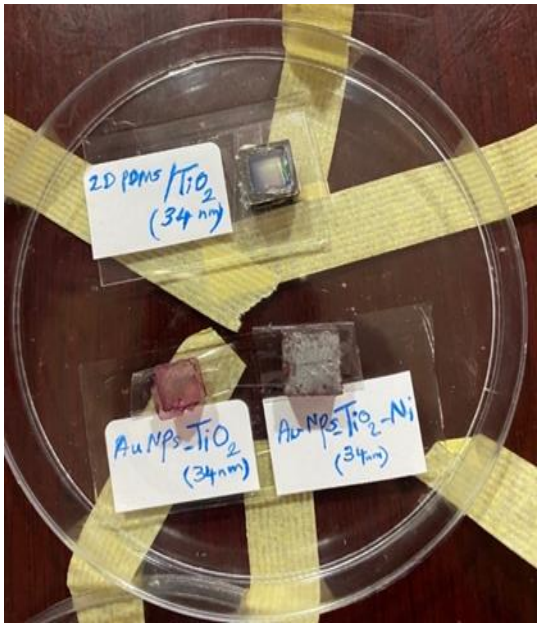

D

Figure (3-8) Sample preparation

3-6 Samples measurement

Three different types of setups are configured

3-6-1 CCD and spectrometer setup

Imaging performed using CCD camera and spectroscopy performed using spectrometer, as shown in Figures (3-9),(3-10) Specialized in optical properties and measuring the negative refractive index of metasurfase According to this setup, the green laser beam is illuminated and CCD imaging is performed as the initial procedure, then the spectral lamp is illuminated and the spectroscopy and then a polarizer is added with an angle change at S(orthogonal polarization) times and at P(Parallel polarization) again and is performed using Focused on the metasurface by the lens. The light beam is then focused and captured by the penetrating surface, and a sample image is created at the objective lens's working distance. The sample picture will then be enlarged by the

Spectrometer's lens and recorded on the CCD. With this setting, transmission spectra of metasurface samples will also be captured. It will be feasible to produce in transmission mode.

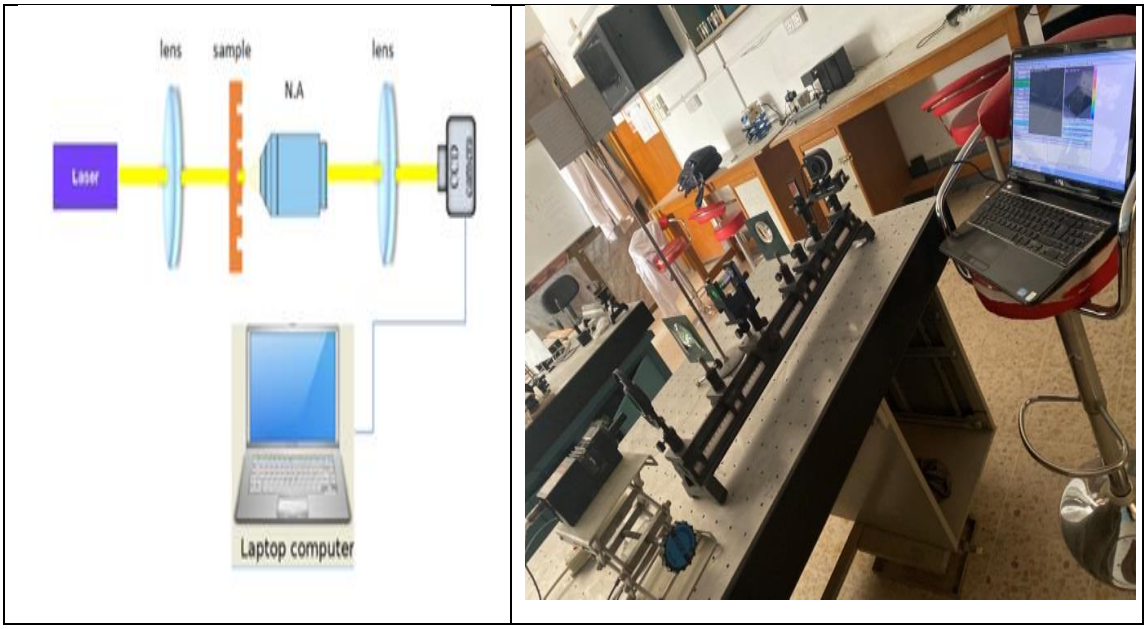

Figure(3-9) Charge-Coupled-Device (CCD camera) setup

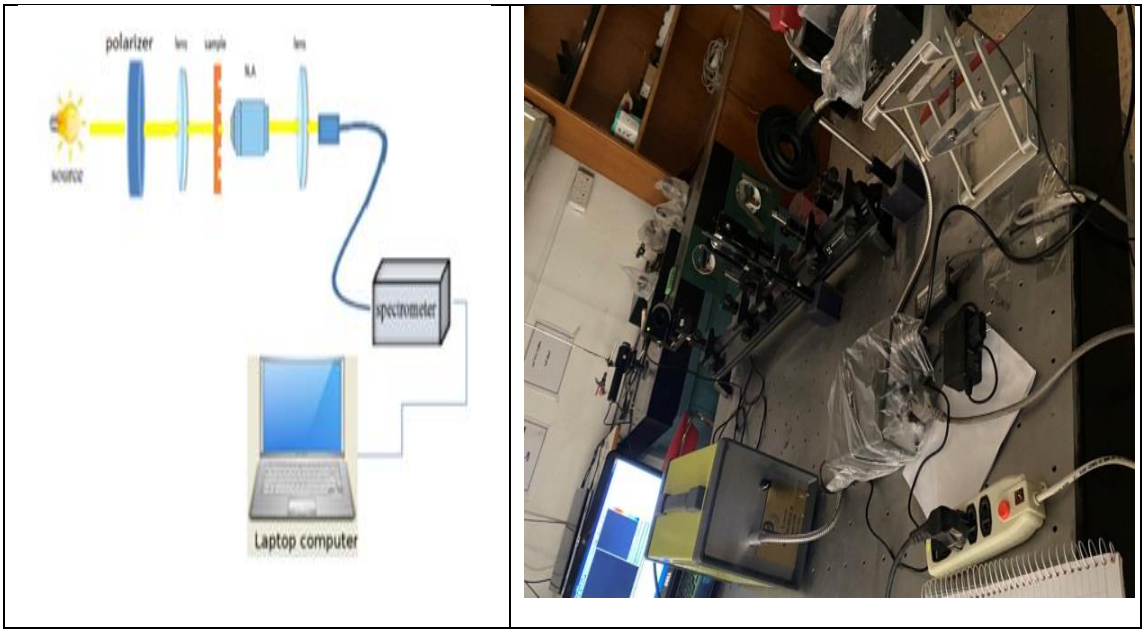

Figure(3-10) Spectrometer setup

3-6-2 The Magneto-Optical Setup

As in the figure (3-11) it is to calculated the magneto-optical properties of the three and four group of models, where it consists of a white light

source, beam splitter, and lens, and they are connected to a magnetic field, and the voltage and current are set at (6V,1.5 A), respectively, and the sample is placed by means of a holder after the lens, where the white light passes through the sample and after it leaves the sample It passes through a lens, then a polarizer, and then it passes to the spectrometer, where it is connected to a computer, and the results are obtained using the tansu program, and then the results are entered into a lap view program to make the last calculations

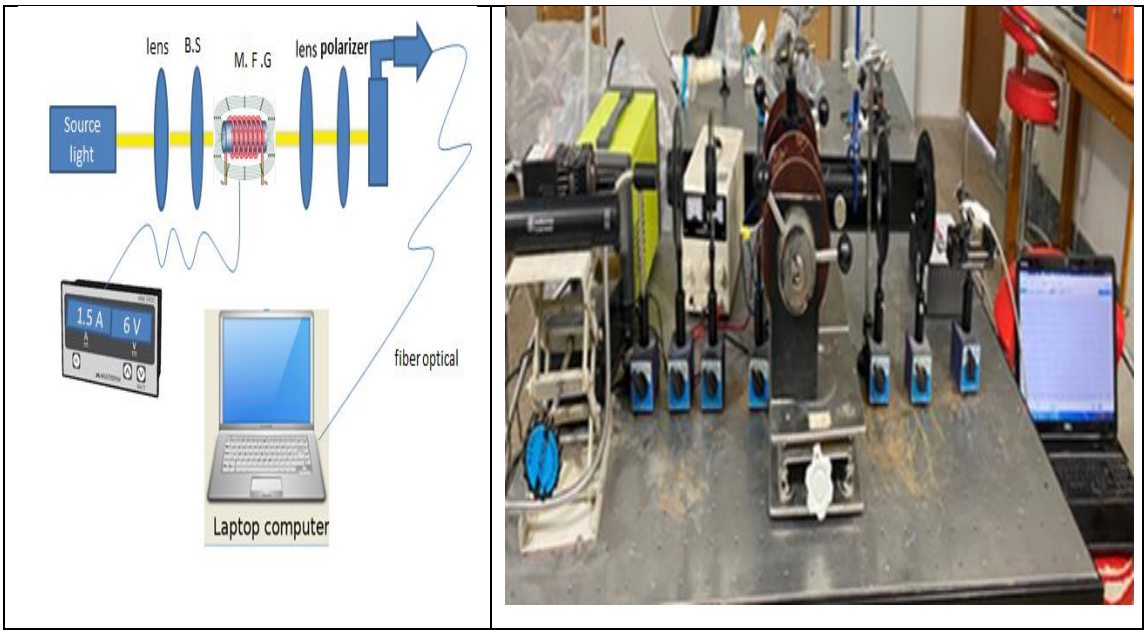

figure (3-11) the magneto-optical setup

The setups (3-9,10,11) It has been prepared in University of Babylon

College of Science for Women Department of Laser Physics

Chapter Four

Results and Discussions

4-1 Introduction

In this chapter, a description of the results obtained during our study, where the results of the XRD that were measured in private laboratories were shown to confirm the identity of the material used, as well as the SEM measurements, where the composition of the sample is given, and the gaps and dimensions of the protrusions are observed . The samples were also examined using the CCD camera to find out the intensity, and then the results of the magneto-optical setup were calculated.

4-2 Metamaterail structures Properties

4-2-1 X-Ray Diffraction (XRD) for group one and two

Figure (4-1a),(4-1b) represented X-ray diffraction patterns of (PDMS/TiO_2(50nm)), (TiO_2(50nm)/PDMS/TiO_2(50nm) as one sided, S_1, S_2 have polycrystalline structure of metastable phase of β- TiO_2 according to the (JCPDS card no. 46-1238). For S_1 film, the notable preferred orientations are along (200), (401), and (020) planes at (2θ= 15.88°, 37.24°, and 48.08°) respectively. In addition, the notable preferred orientations of S_2 are along (201), (002), and (310) planes at (2θ= 23.18°, 28.35°, and 33.68°) respectively .

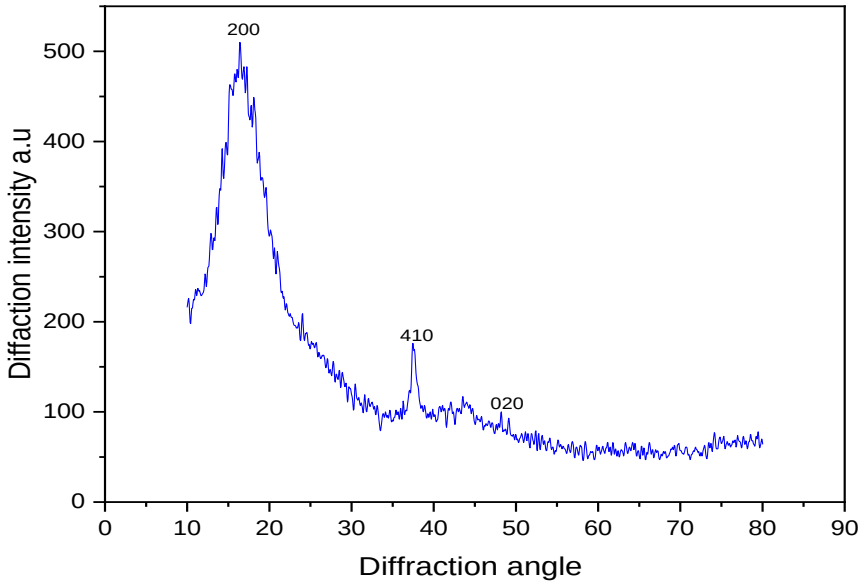

Figure (4-1) (a)XRD for (PDMS/TiO_2(50nm))

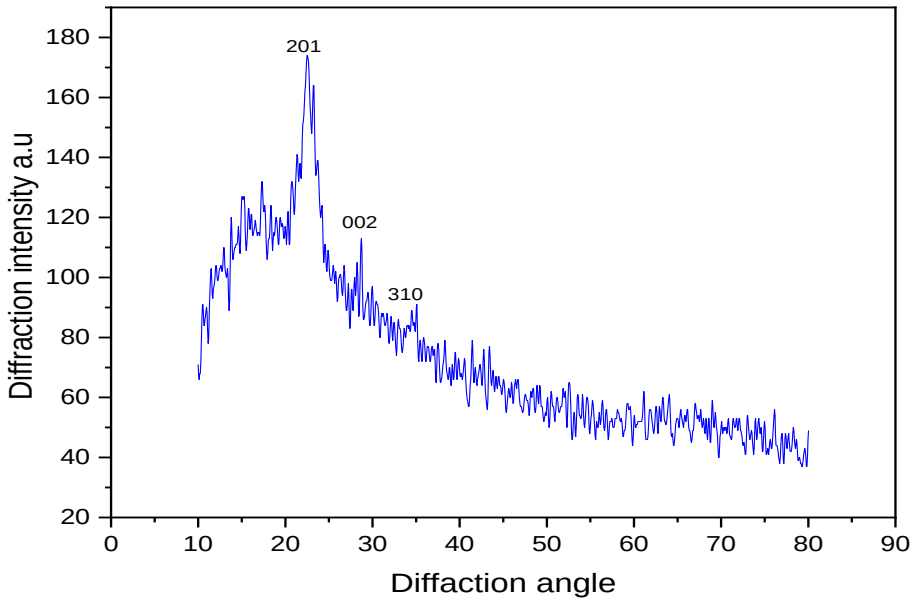

Figure (4-1)(b) XRD for TiO2(50nm)/PDMS/TiO2(50nm)

Figure (4-2) represented X-ray diffraction patterns of for2D(PDMS/MgF_2) different periodic this XRD analysis investigates that the film of polycrystalline structure, in which two diffraction peaks of MgF_2 film can be observed, corresponding to the 37.57° (302) and 70.3° (721) given by (JCPDS, no. 16-0160, and the wide peak at 16.4° is belong to

PDMS **[245]**. These diffraction peaks demonstrate that the MgF_2 nanomaterial had been successfully deposited onto the surface of the PDMS substrates.

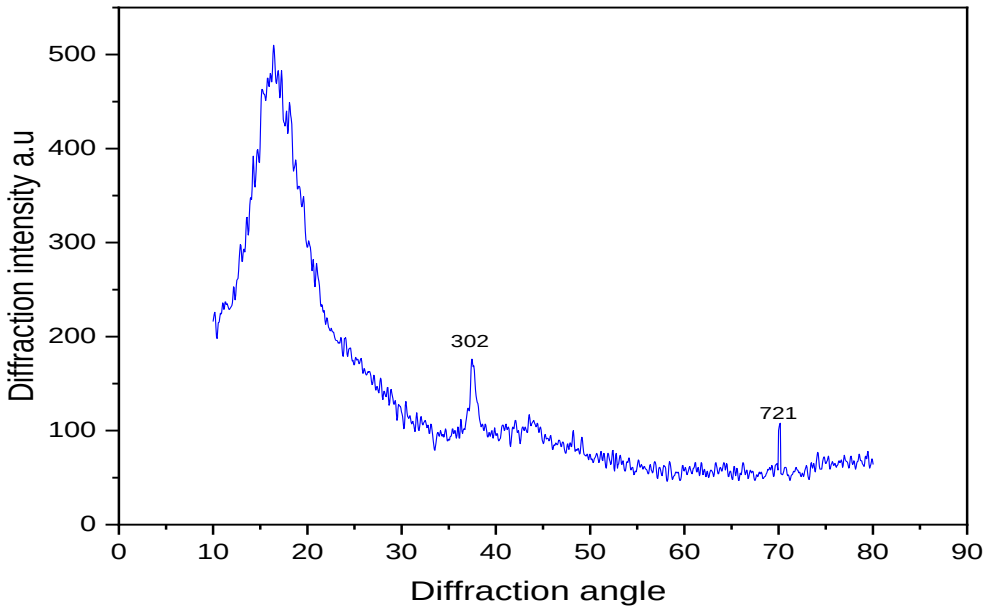

Figure (4-2) XRD for2D(PDMS/MgF2) different periodic

The crystallite sizes values indicate that the sample films of nano crystal structure, as given in Table 1.The crystalline nature of nanostructured films can be determined by dislocations density (δ) using equations (4-1) [16]:

$$\delta=\frac{1}{D^2} \qquad \textbf{(4-1)}$$

Low value of dislocation indicates that the film of high crystalline quality and low deformations in the film structure.

Table(4-1)the confirmed data of XRD pattern of group one and two

No. of samples	2θ (deg)	Θ (deg)	Θ(rad)	cos θ	B(deg)	B(rad)	D (nm)	$\delta \times 10^{-3}$ /nm^2
PDMS/TiO_2	15.88	7.94	0.1385	0.990	3.96	0.069	2.02	0.2450
	37.24	18.62	0.3248	0.947	1.03	0.0179	8.14	0.0150
	48.08	24.04	0.4193	0.913	3.96	0.069	2.19	0.2085
TiO_2/PDMS/TiO_2	23.18	11.59	0.2021	0.979	2.82	0.049	2.87	0.1214
	28.35	14.175	0.2472	0.969	1.6	0.0279	5.12	0.0381
	33.68	16.84	0.2937	0.957	3.37	0.058	2.46	0.1652
PDMS/MgF2	37.57	18.785	0.327	0.997	0.42	0.007	19.98	0.0025
	70.3	35.15	0.613	0.829	0.53	0.009	18.33	0.0029

4-2-2 X-ray diffraction (XRD) for group three and four

Figure (4-3) represented X-ray diffraction patterns of (PDMS/MgF_2) ,(PDMS/Au/MgF_2) , (PDMS/TiO_2)and (PDMS /TiO2/ Au) , The XRD was examined for all the prepared samples. All the calculated results of the XRD analysis are confirmed through Figure 1 for the Au/PDMS films. We note that the angles (16.48 and 37.54) are for the PDMS material, while the angle (43.41) is for the Au material and it is identical to the gold card (JCPDS card no 040784).But when MgF_2 is added as a layer between the PDMS and the Au, in the presence of the two angles belonging to the PDMS, and the angle is symmetrical for the

two cards ((JCPDS card no 040784) for gold and (JCPDS card no 160160) for MgF_2 And when using TiO2 with the PDMS, we notice the same behavior of the PDMS with gold, according to the TiO2 card (JCPDS card no 461238) at an angle of 43.41 and in the direction of (003) and changing it to 43.58 by adding TiO_2 with the PDMS and Au to the angle of 43.58 which corresponds to Au and TiO_2 (003) (200), respectively.

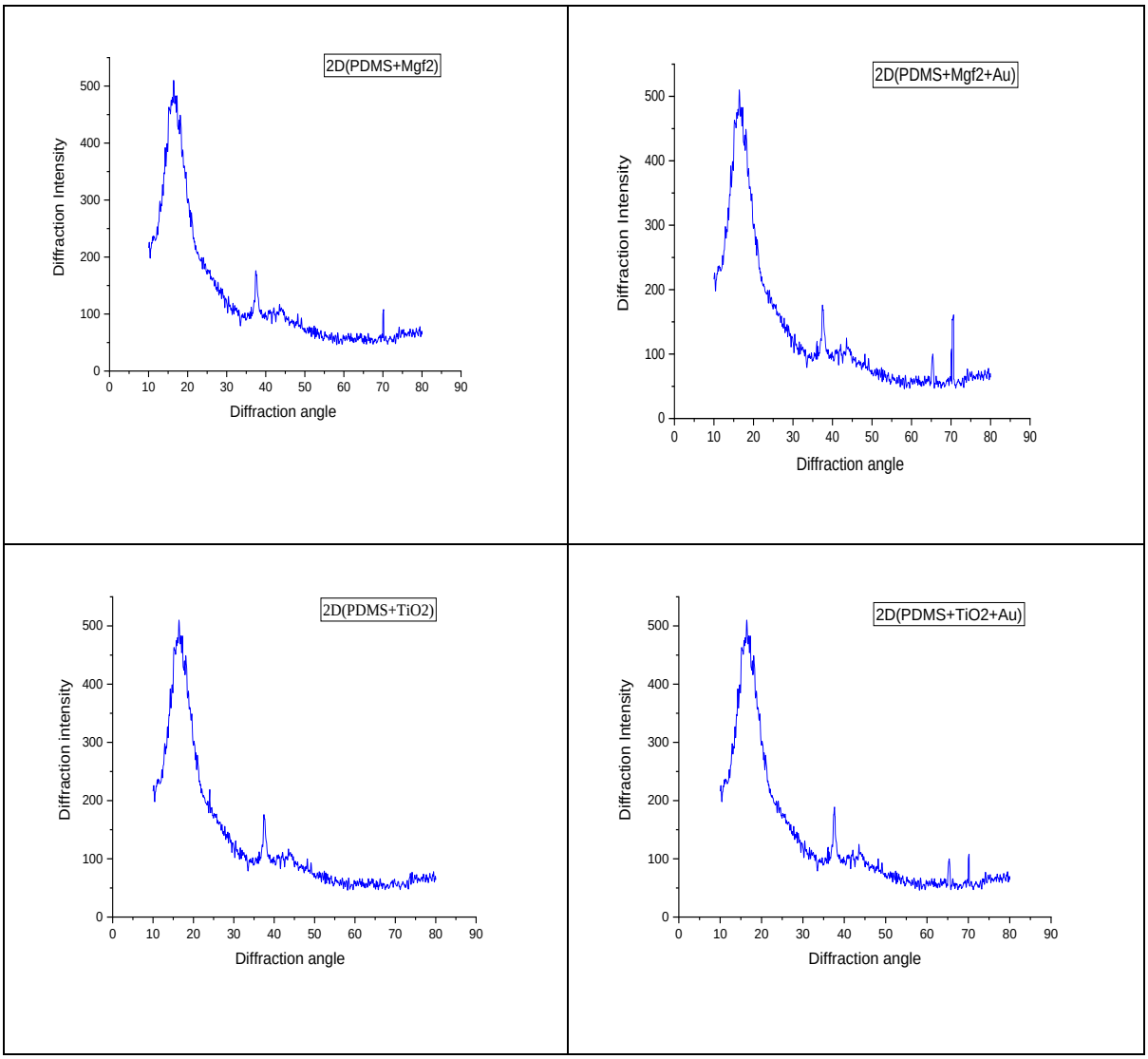

Figure (4-3)X-ray diffraction for group three and four

Table(4-2)the confirmed data of XRD pattern of group three and four

No. of samples	2θ (deg)	Θ (deg)	Θ(rad)	cos θ	B(deg)	B(rad)	D (nm)	δ $\times 10^{-3}$ /nm^2
PDMS/Mgf2	16.48	8.24	0.143742	0.989687	9.747	0.170031	0.834919	1.434536973
	37.54	18.77	0.327432	0.946871	1.58	0.027562	5.150602	0.037695021
	43.41	21.705	0.378632	0.929171	0.16	0.002791	50.8622	0.000386554
2D PDMS/MgF_2/ Au	16.25	8.125	0.141736	0.989972	10.096	0.176119	0.806057	1.539105881
	37.67	18.835	0.328566	0.946506	1.58	0.027562	5.150602	0.037695021
	43.58	21.79	0.380114	0.928622	0.513	0.008949	15.86345	0.003973787
2D PDMS/Tio_2	16.78	8.39	0.146359	0.989309	11.84	0.206542	0.687327	2.116767791
	37.48	18.74	0.326909	0.947039	1.369	0.023881	5.94445	0.028299366
	43.41	21.7	0.378632	0.929171	0.348	0.006071	23.38492	0.00182864
2D PDMS /Tio_2/ Au	16.43	8.215	0.143306	0.989749	11.491	0.200454	0.708202	1.993817774
	37.67	18.835	0.328566	0.946506	1.745	0.030441	4.663582	0.045979122
	43.58	21.79	0.380114	0.928622	0.165	0.002878	49.32092	0.000411091

all the measurements are done in the central laboratory of University ALsheed Bahasty

4-3 Scanning Electron Microscopy (SEM)

Figure (4-4) represented the SEM OF The samples were prepared, In the first sample (PDMS/TiO2(50nm)), we note that the particles have dimensions (2.7-3.04 mm), while the distance between the particles is (227-979nm).As for the second sample(TiO2(50nm)/PDMS/TiO2(50nm), the dimensions of the particles were (2.53-2.89 mm) and the distance between the particles (343-773 nm) from the top. As for the lower part of the sample, the dimensions of the particles were (1.71-2.09mm) and the distance between the particles was (465-272nm) as in figure (4-5).

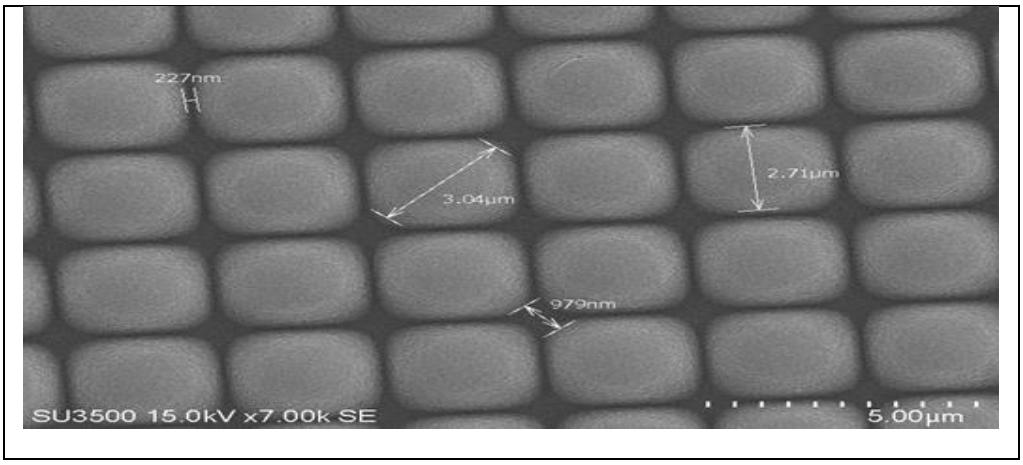

Figure(4-4) SEM of sample(1)one-side 2Dgrating(PDMS/TiO_2(50nm))

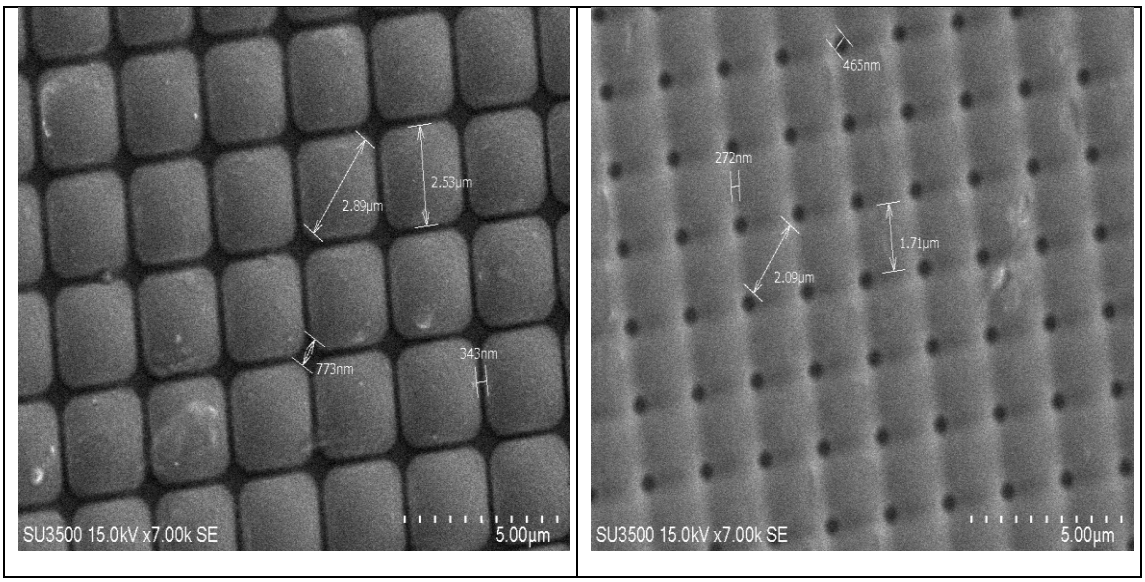

Up **Dawn**

Figure (4-5)SEM of sample (2) two-sided 2D grating (etalon) (TiO_2(50nm)/PDMS/TiO_2(50nm)

The third samples were prepared with different periodicity. In this sample, we note that the bumps in Q1 have dimensions (2.84,3.56,4.09mm). as for the Q2 the bumps is(1.94,1.95.2.08,2.03mm)as the dimensions bumps of the Q3 (4.55,5.62,4.67mm)and the the dimensions bumps of the Q4 is(4.81,4.42,6.30mm) as figure (4-6).

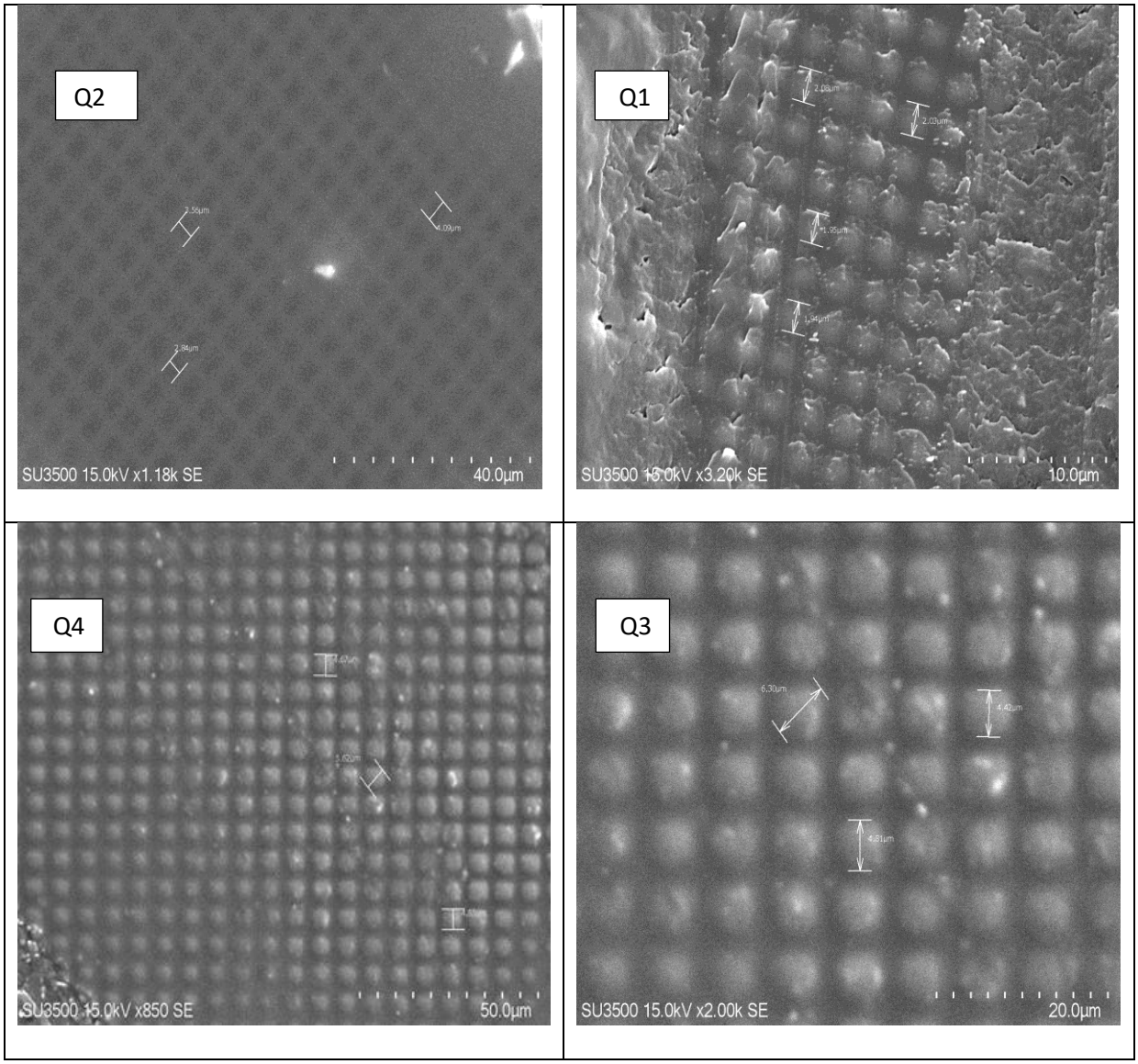

Figure (4-6) SEM of sample (3) 2D (PDMS/MgF2 different periodicity)

Figure (4-7) displays the scanning electron microscopy , with a focus on (2d PDMS+TiO_2+Au+Ni) at particular wavelengths (500,200nm)(10,5µm). Notably, it reveals distinct gold (Au) presence on

the surface The distinctive appearance of gold (Au) in the scanning electron microscopy (SEM) whereas Gold is a noble metal with a unique elemental composition. Thicker layers may appear brighter and more distinct in the images. The particle size has been calculated to be D=31.09 at a wavelength of 200nm

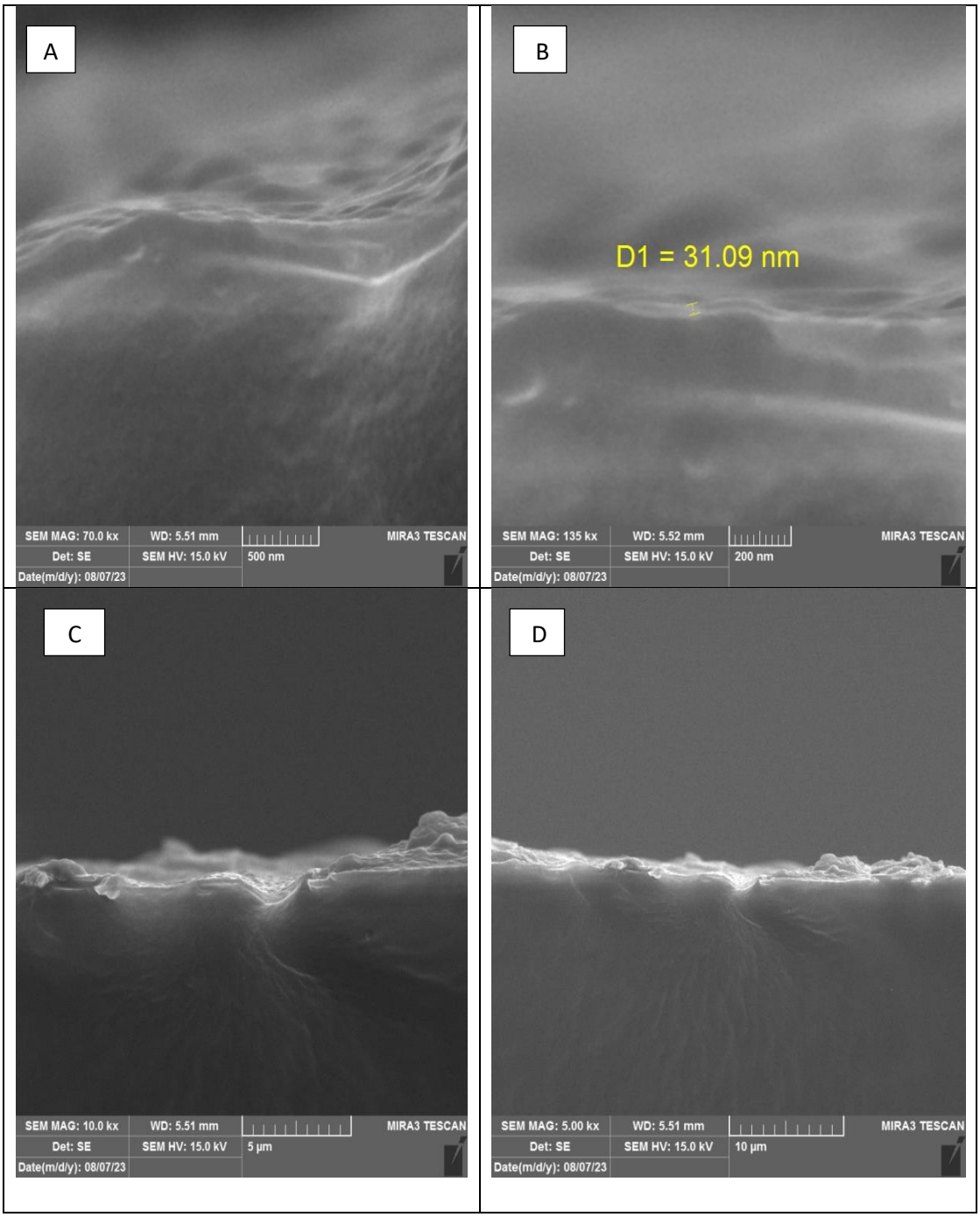

Figure (4-7)SEM of (2d PDMS+TiO_2+Au+Ni)

Figure (4-7)studying the scanning electron microscopy of the compound PDMS+MgF_2+Au+Ni, the Ni component appears clearly, it suggests that the Nickel (Ni) portion of the compound has distinctive surface characteristics that are easily. This clarity could be due to several reason Nickel (Ni) has different material properties compared to the other components (PDMS, MgF_2, Au). It may have a different texture, roughness, or reflectivity that makes it stand out when studied .

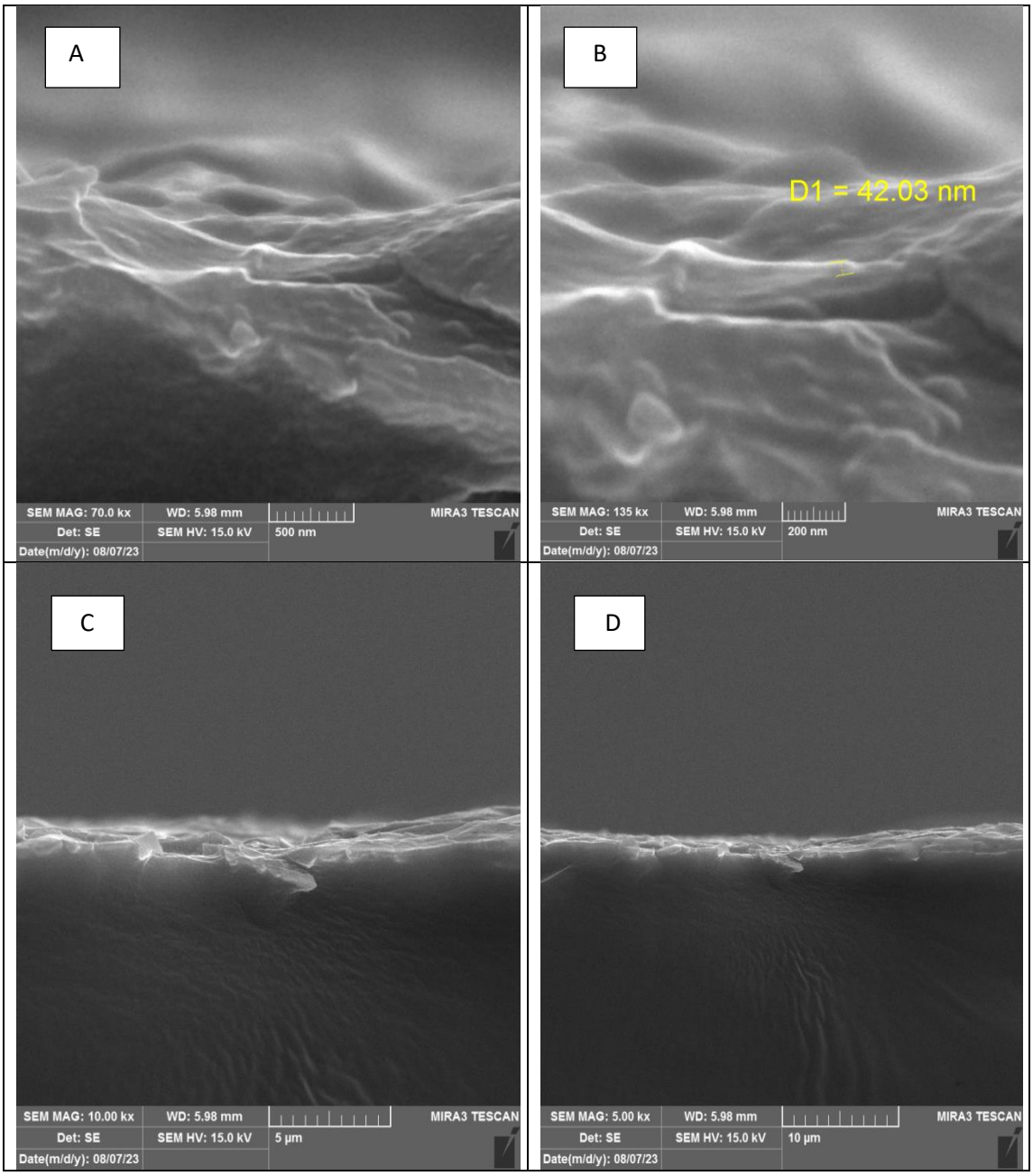

Figure (4-8)SEM of (2d PDMS+MgF_2+Au+Ni)

4-4 Imaging by The Charge-Coupled-Device (CCD camera)

Pictures were taken using the CCD camera for the prepared samples, and the results were as follows

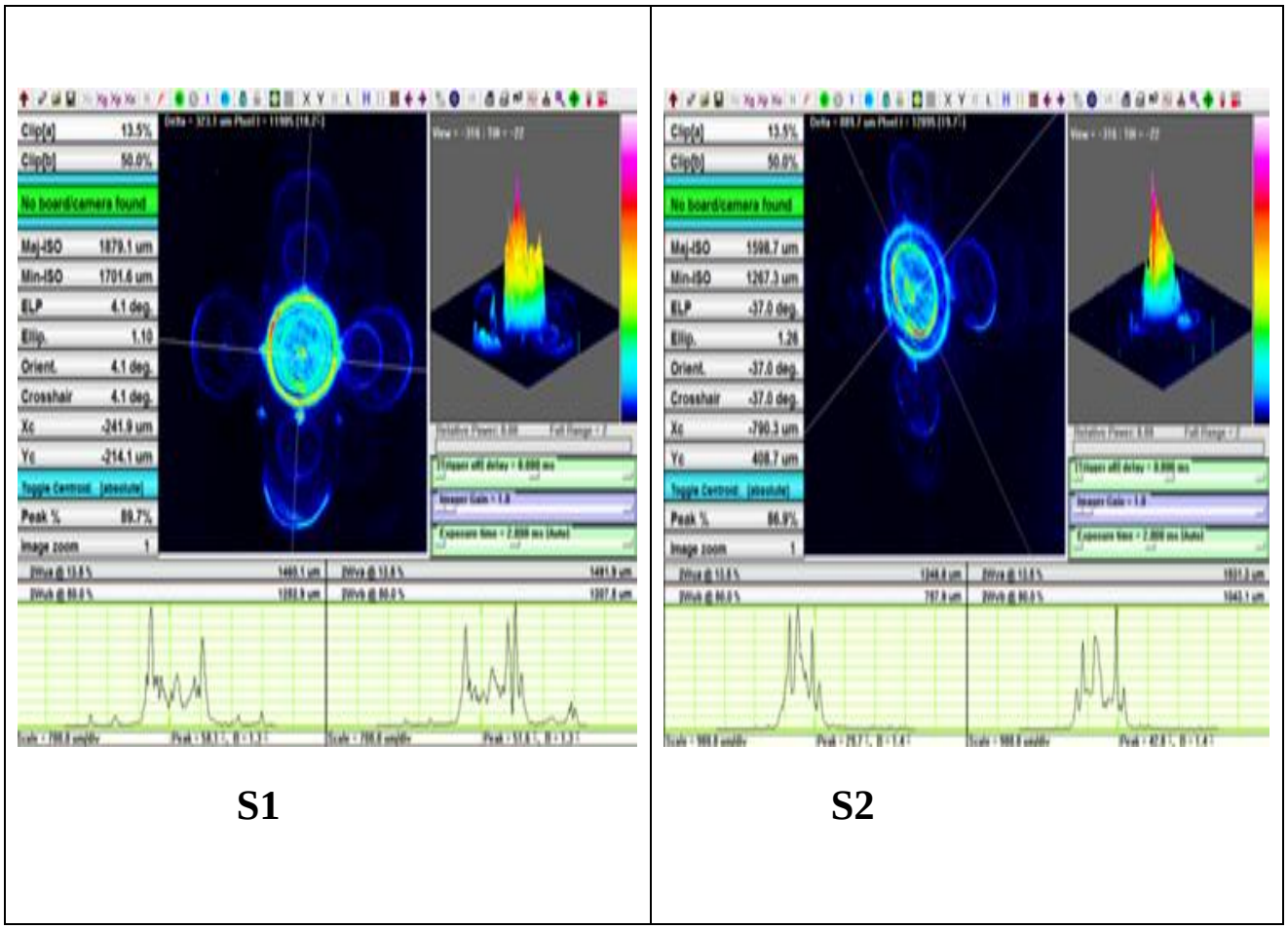

Figure (4-9) ccd camera osample(1) one-side 2Dgrating(PDMS/TiO_2(50nm)) & sample(2) two-sided 2D grating (etalon) (TiO_2(50nm)/PDMS/TiO2(50nm)

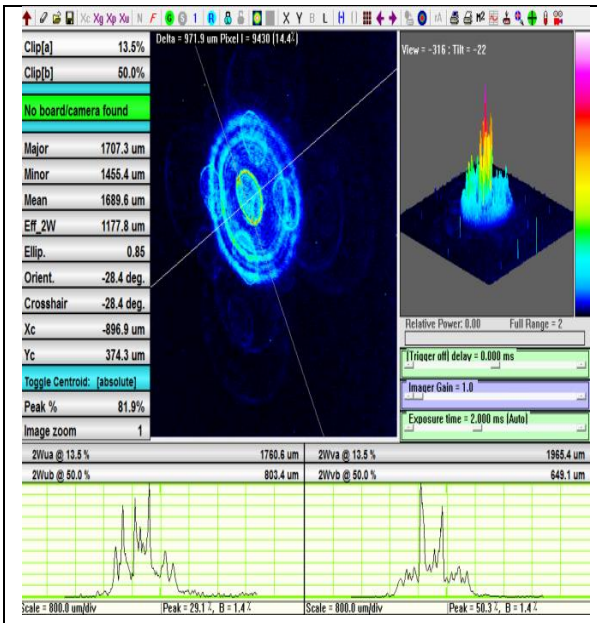

S3 Q1

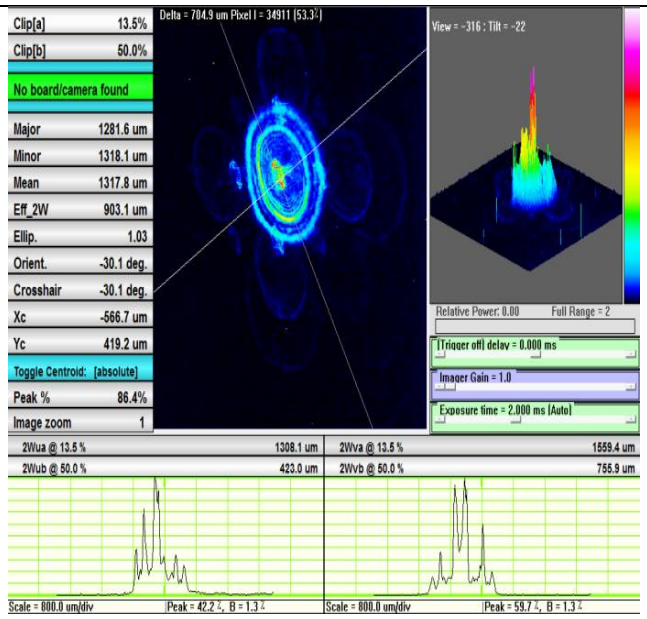

S3 Q2

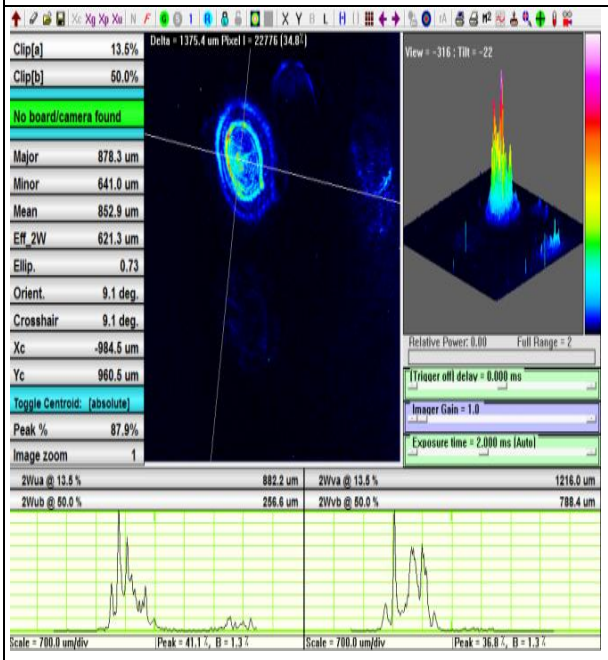

S3 Q3

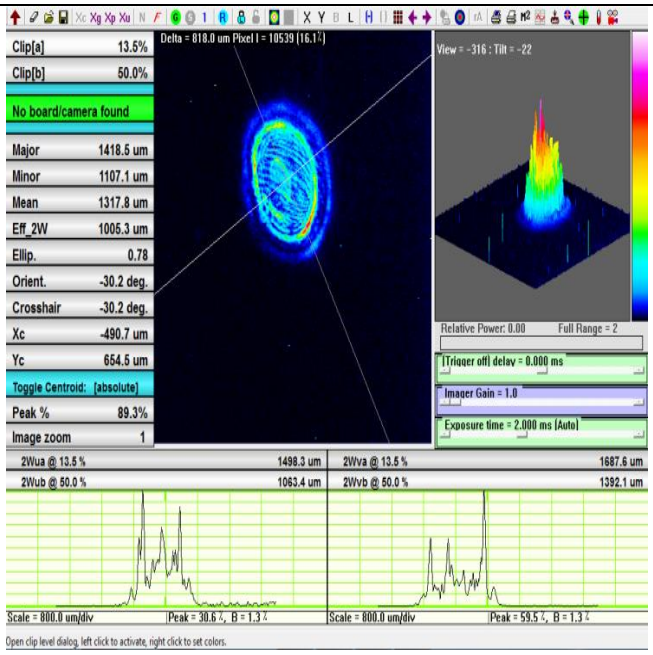

S3Q3

Figure (4-10) CCD camera of sample1 2D(PDMS/MgF_2) different periodic

Table(4- 3) Characteristics of the hotspot of two samples

Samples	Width of hotspot at X direction(µm)		Width of hotspot at Y direction(µm)		Peak value %
	50%	13.5 %	50%	13.5 %	
PDMS/TiO_2(50nm)	1252.9	1460.1	1207.5	1490.9	89.7
TiO_2(50nm)/PDMS/TiO_2(50nm)	528.4	1307.9	1195.2	1685.7	73.5
2D (PDMS/MgF_2) Q1	1558.4	1931.3	805.4	2167.9	89.7
2D (PDMS/MgF_2) Q2	423.6	1308.1	755.9	1559.4	86.4
2D (PDMS/MgF_2) Q3	6.17.5	1490.4	1033.6	1485.4	79.8
2D (PDMS/MgF_2) Q4	1329.6	1852.2	1645.4	1965.4	59.2

It is noticed through the results that the intensity is high in the first sample, because it consists of one layer, and therefore the absorbance is lower. As for the second sample, the intensity is lower because it has two layers, and therefore the absorbance is higher in this sample. As for diffraction, it is noticed that the beam width is greater in the second sample because the exposure is larger considering the presence of two grating . The case of high symmetry that appeared in the previous images, which came from the presence of a supercell of the prohibited samples, and that the first sample (one side) showed a higher symmetry than (two side). as well as for the sample three It is noticed from the table(4-3) and the figure that the intensity is high at Q1, Q2, while the intensity is lower at Q3, Q4. The reason for the difference is that the sample consists of

different periodic sizes. As for the diffraction, it is notice the bandwidth in Q1, Q2 is greater than that of Q3, Q4, due to exposure, and thus the symmetry in Q1, Q2 is clear , due to the supercell.

4-5 Reflection spectra

The reflection spectra was measured for the sample(PDMS/TiO_2(50nm)) and (TiO_2(50nm)/PDMS/TiO_2(50nm)and the results were

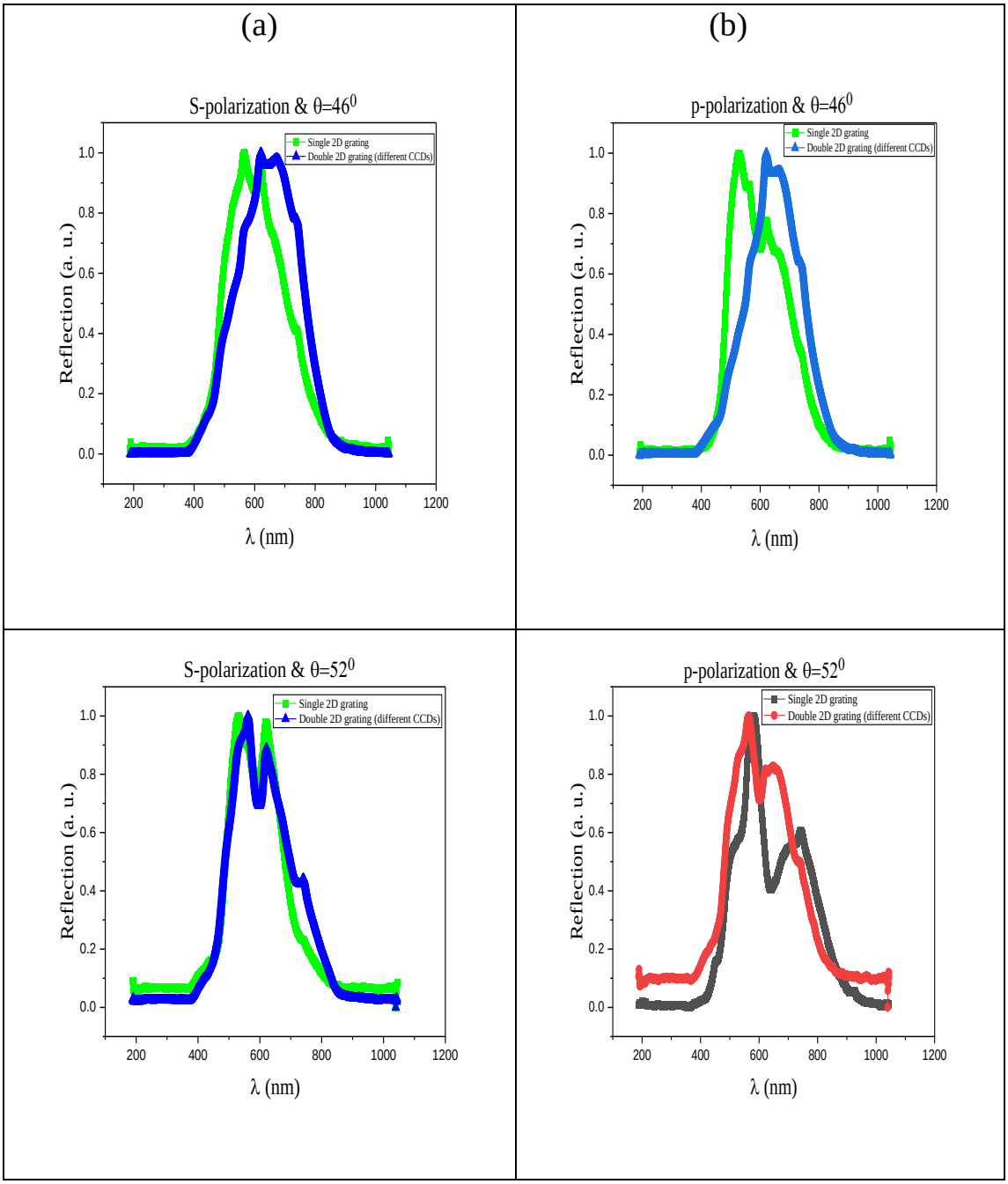

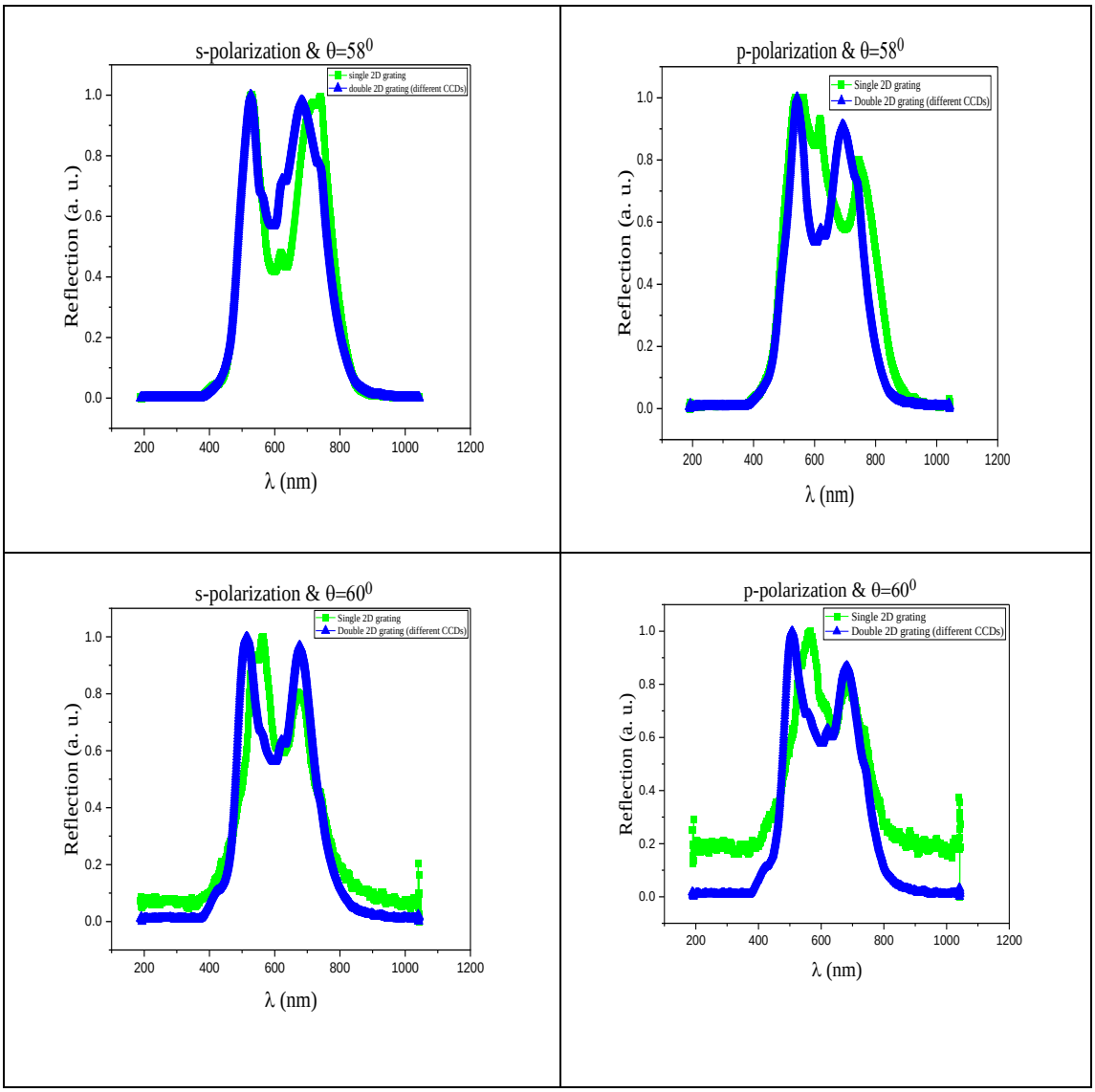

Figure(4-11) reflection spectra for (a) (PDMS/TiO_2(50nm)) (b) (TiO_2(50nm)/PDMS/TiO_2(50nm) with change the angle

It is noticed through the results, the increase in the angle due to the increase the separation in the peak, where the clear separation represents the electric dipole (E.D) on the left and magnetic dipole (M.D) on the right, and it is notice that the gradient of the increase in the angle begins to appear and become more clear, as it is noticed its appearance at the angle (52) and the increase at (58) and the most obvious at the angle (60), and the reason for this separation at these angles may be the fall of the beam by the oblique angle, and it is clear that the fall by the oblique angle leads to the behavior of the metamaterail more clearly.

4-6 Refractive index

the refractive index was measured for the sample(PDMS/TiO_2(50nm)) and (TiO_2(50nm)/PDMS/TiO_2(50nm)and the results were

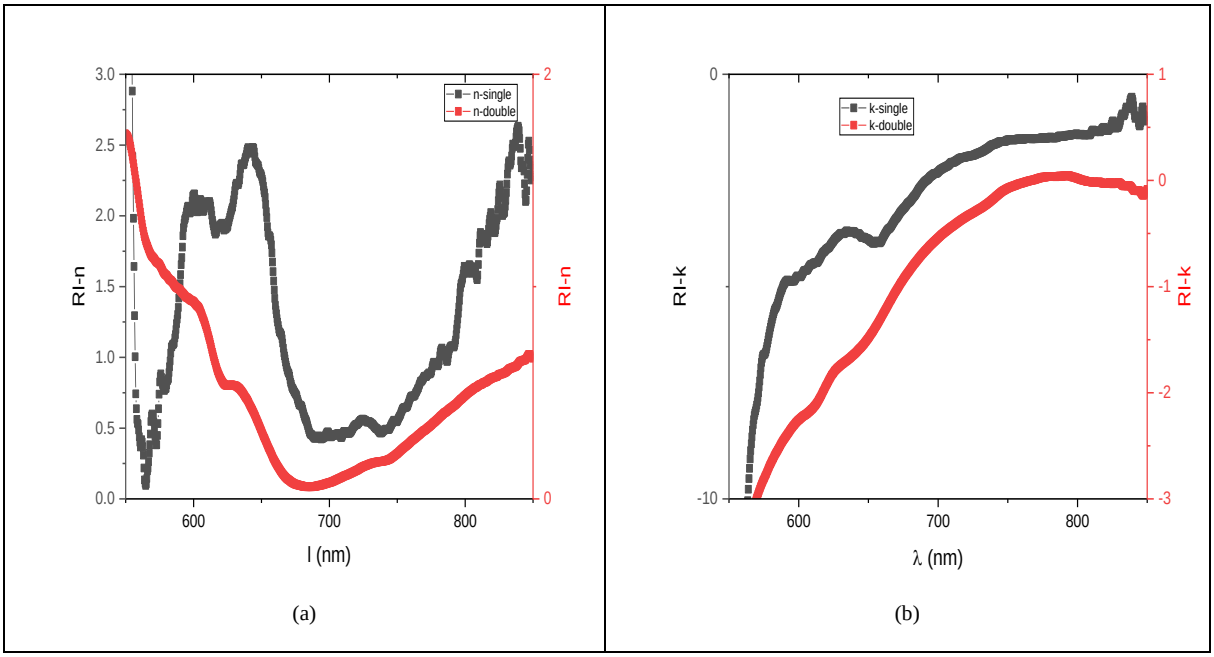

Fig (4-12)the refractive index (a)real and(b) imaginary for the sample(PDMS/TiO_2(50nm)) and (TiO_2(50nm)/PDMS/TiO_2(50nm)

It is noticed from the figure(4-10) the change in the refractive index within the wavelengths, where it is noticed the convergence at the wavelength (700)nm and there are the difference is large at the wavelength (650)nm, where the single is higher and therefore the linear applications of the double are more because it has a greater refractive index and thus decreases speed As for the imaginary refractive index, we note the increase in the single within the wavelengths from (550)nm to the end of the visible spectrum, and after that there is a clear decrease. While the double has a different behavior, as there is a decrease down to the end of the visible spectrum due to the effect of the metamaterail with a note Single has much lower k-values than double.

4-7 Magneto-optics properties

The figure (4-13) is represented to the transmission spectrum when edit magnetic field for the sample in the left and right by using the setup showed in the figure (3-11)

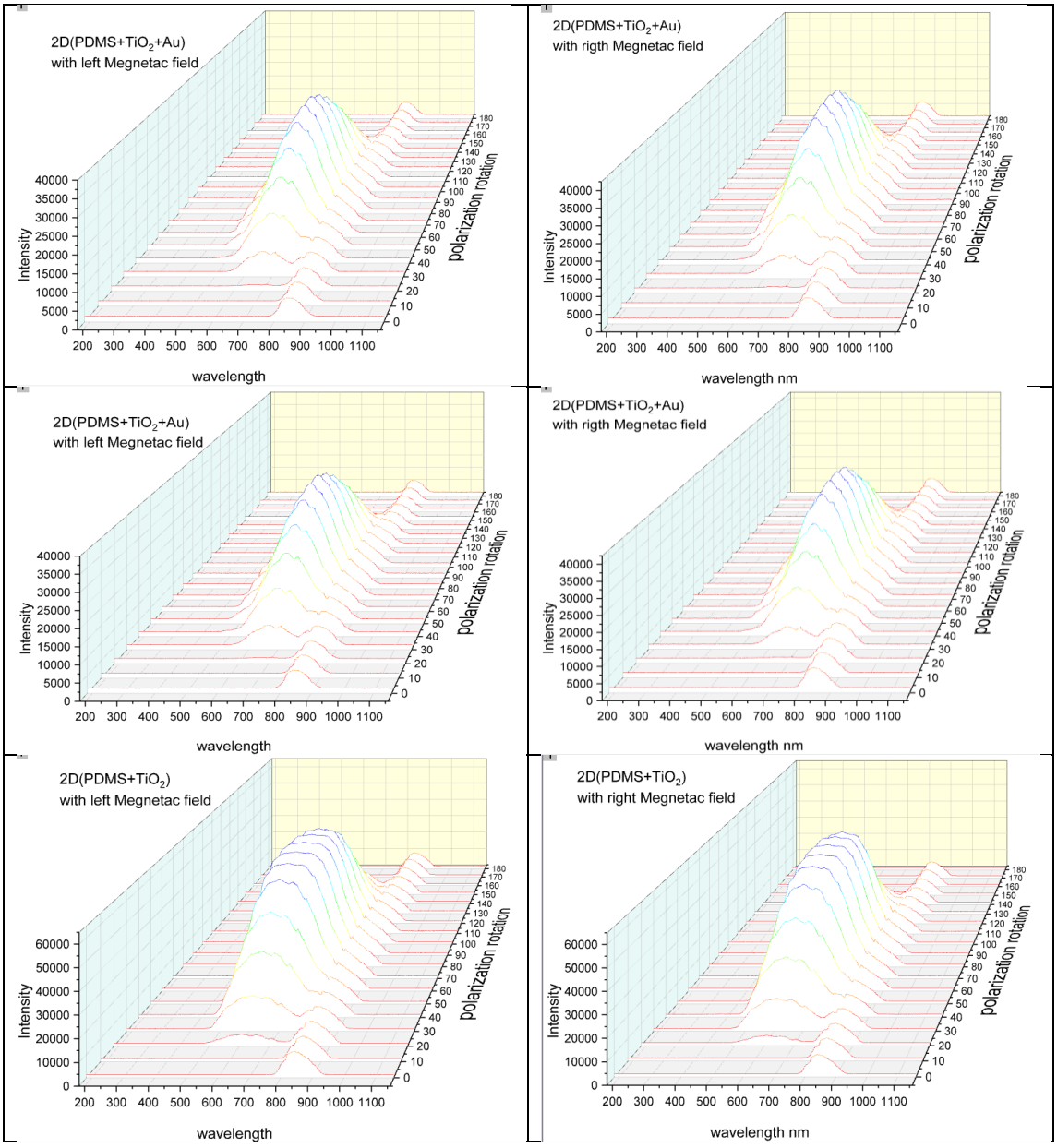

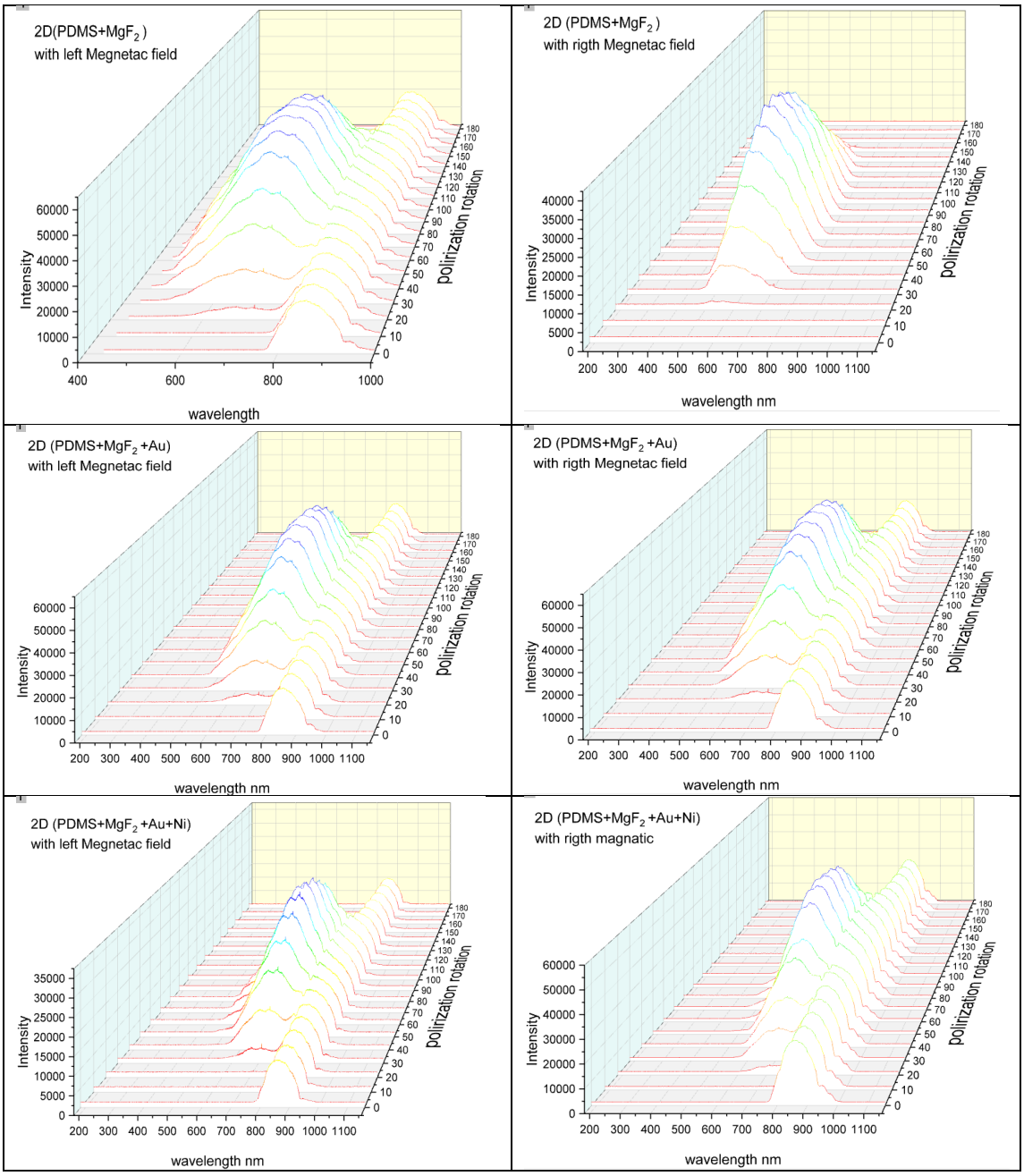

Figure (4-13) Transmission spectrum of the prepared samples

And its obtain the result of the sample (PDMS+TiO_2) with the edit the layers after insert it in program in the figure (4-13)

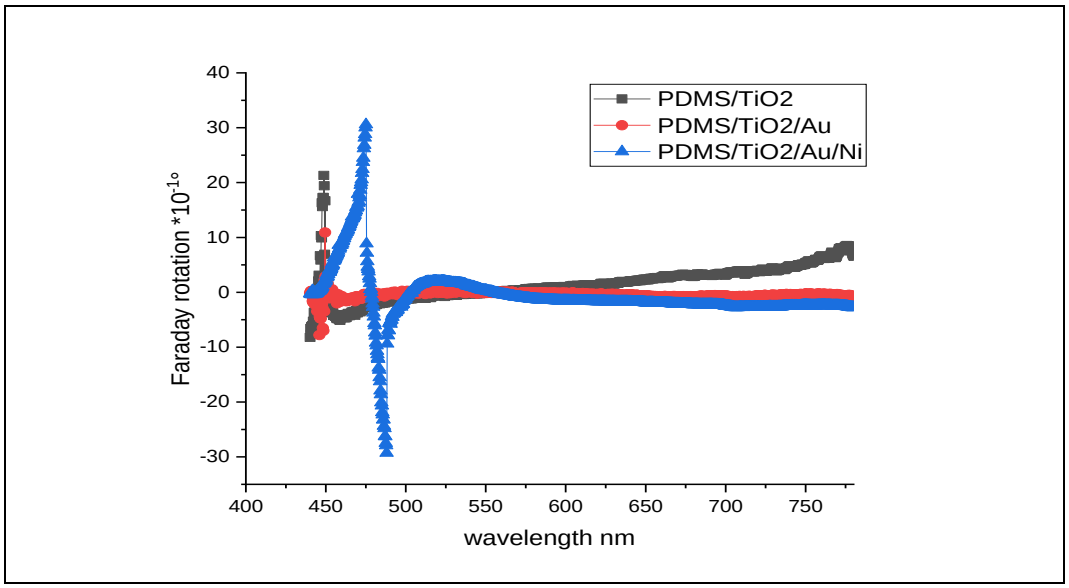

Figure (4-14) experimental result of the group three

From the diagram it is noticed the first sample (2D PDMS + TiO_2) for high rotating that begins to descend to sub-zero (Negative)and then gradually increases to the wavelength at 550nm, becomes the positive peak and then rises at the wavelength of 600nm. As for the second sample(2D PDMS + TiO_2+Au), it is noticed the high rotation in the behavior, as we notice the increase that occurs between the 500nm and 550nm from negative to positive, and the reason is the effect of the plasmon(localizes surface Plasmon resonance).As for the third sample(2D PDMS + TiO_2+Au+Ni), where the influence of the magnetic field is evident here) and the rotation process is very high between the 450nm and 500nm, and we notice at the 525nm the effect of the Plasmon appears on the nickel, where it is noticed the area between the 510 nm and 540 nm under the influence of the magneto Plasmon. And its obtain the result of the sample (PDMS+MgF_2) with the edit the layers after insert it in program in the figure (4-14)

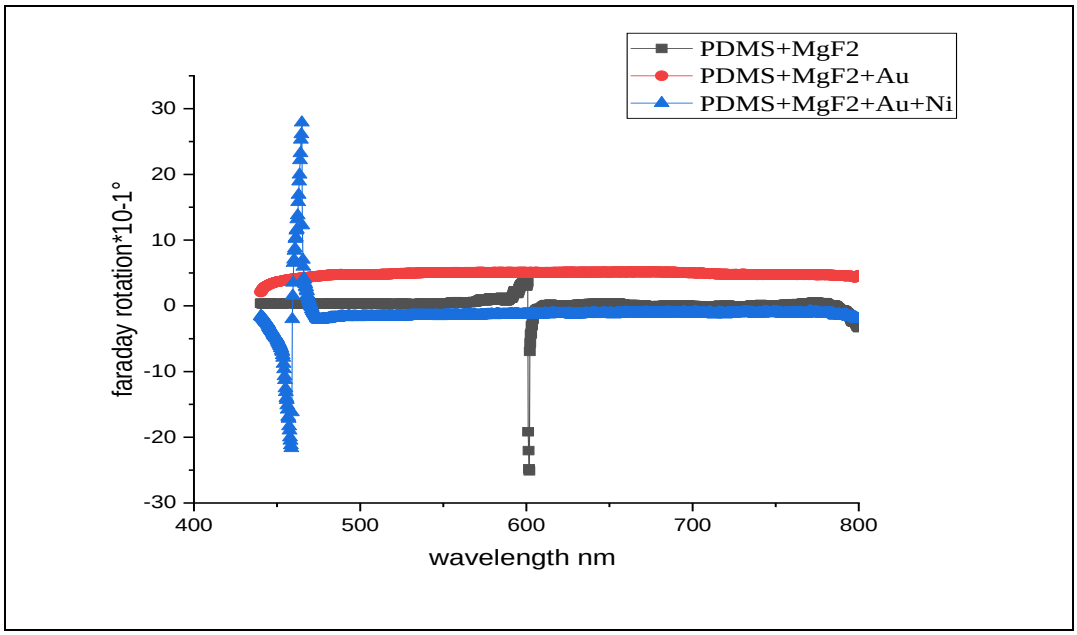

Figure (4-15) experimental result of the group four

From the diagram, we can observe that the initial layer, (1DPDMS+$MgF_{2)}$, remains relatively stable without any significant rotation. There is a minor upward trend, which could be attributed to a potential error or inaccuracies in the device readings. Upon introducing Au, we observe a consistent linear progression, but a noticeable rotation becomes apparent when Ni is introduced. It is plausible that the introduction of Ni may have filled the gaps responsible for Plasmon generation, consequently preventing the formation of the metasurface, as opposed to the TiO_2 model where this does not occur.

4-8 Conclusions

Form the obtained results of present work , it concluded the following :

1- From the CCD measurements findings indicate that in the single-layer sample, intensity increases while absorption decreases, whereas in the two-layer sample, the opposite trend is observed, with absorption increasing and intensity decreasing. and for the sample with different periodic the intensity is high at Q1, Q2, while the intensity is lower at Q3, Q4. The reason for the difference is that the sample consists of different periodic sizes.

2- In terms of diffraction, it's noticeable that the beam width is wider in the single -layer sample due to the larger exposure , considering the presence of two gratings . This contrast is particularly evident when we examine the high symmetry observed in the previous images, which results from the presence of a supercell in the prohibited samples. It's worth noting that the first sample (single-layar) exhibits a higher degree of symmetry compared to the second sample (double-sided), leading to more pronounced diffraction conditions in the first sample . while the different periodic sample , we notice the bandwidth in Q1, Q2 is greater than that of Q3, Q4, due to exposure , and thus the symmetry in Q1, Q2 is visible, due to the supercell.

3- The spectral absorption data reveals that the metamaterial 's behavior becomes more pronounced when the incident beam is directed at an oblique angle.

4- The refractive index measurement reveals that the single-layer model exhibits superior linear applications owing to its elevated refractive index. In terms of the imaginary refractive index, the

single-layer displays a rising trend, whereas the double-layer demonstrates an opposing behavior, characterized by a gradual decline attributed to the impact of the metamaterial.

5- The transmission spectrum measurement reveals The influence of surface plasmon resonance on the rotational behavior of the samples is evident. In the case of the sample (2D PDMS + TiO_2), we observe a significant initial increase in rotation followed by a subsequent drop below zero (negative), and then a gradual rise. Similarly, in the sample (2D PDMS + TiO_2 + Au), we observe a pronounced rotational behavior with a noticeable impact from the magnetic plasmon. This effect is further amplified in the sample (2D PDMS + TiO_2 + Au + Ni), resulting in a substantial increase in rotation.

4-9 Future Work

1- Another material is proposed from which can be made metamaterial , such as Silicon dioxide (SiO_2)

2- The stricture can be changed to shapes other than the square shape that was used in the search.

3- It is possible to generate plasmons using Ag.

4- It is possible to generate magnetons using cobalt instead of nickel.

5- The study can be applied to create a filter to separate colors in the future.

Reference

1. Klinger, R. E. "Thin film deposition technologies, and structure/property relationships applied to solid state ionic conductors." Solid State Ionics 52, no. 1-3 (1992): 249

2. Smith, Donald L., and David W. Hoffman. "Thin-Film Deposition: Principles and Practice." (1996): 60-62.

3. T. Wagner ,"Thin Film Science", Stuttgart, Germany: Max-Planck-Institute for Metalliforchung, **1999**.

4. Siegel, R. W., E. H. Hu, and M. C. Roco. "WTEC panel report on R&D status and trends in nanoparticles." In Nanostructure Materials and Nanodevices, Workshop. 1997.

5. A. Kumar, Y.W. Chung, J. J. Moore and J. E. Smugeresky ,"Surface Engineering Science and Technology" ,Warrendale (PA): The Minerals, Metals &Materials Society, 1999 .

6. Lakhtakia, Akhlesh, and Russell Messier. Sculptured thin films: Nanoengineered morphology and optics. Vol. 143. SPIE press, 2005.

7. Lakhtakia, Akhlesh, and Tom G. Mackay. "Meet the metamaterials." Optics and photonics news 18, no. 1 (2007): 32-39.

8. Mackay, Tom G., and Akhlesh Lakhtakia. "Negative refraction, negative phase velocity, and counterposition in bianisotropic materials and metamaterials." Physical Review B 79, no. 23 (2009): 235121.

9. Weiglhofer, Werner S., and Akhlesh Lakhtakia, eds. Introduction to complex mediums for optics and electromagnetics. Vol. 123. SPIE press, 2003.

10. Ali, Adnan, Anirban Mitra, and Brahim Aïssa. "Metamaterials and metasurfaces: A review from the perspectives of materials, mechanisms and advanced metadevices." *Nanomaterials* 12, no. 6 (2022): 1027.

11. Rodríguez-Oliveros, Rogelio, and José A. Sánchez-Gil. "Gold nanostars as thermoplasmonic nanoparticles for optical heating." Optics express 20, no. 1 (2012): 621-626.

12. Baffou, Guillaume, and Romain Quidant. "Thermo-plasmonics: using metallic nanostructures as nano-sources of heat." Laser & Photonics Reviews 7, no. 2 (2013): 171-187.

13. Baffou, Guillaume, Romain Quidant, and F. Javier García de Abajo. "Nanoscale control of optical heating in complex plasmonic systems." ACS nano 4, no. 2 (2010): 709-716.

14. Han, Gang, Partha Ghosh, Mrinmoy De, and Vincent M. Rotello. "Drug and gene delivery using gold nanoparticles." Nanobiotechnology 3 (2007): 40-45.

15. Boyer, David, Philippe Tamarat, Abdelhamid Maali, Brahim Lounis, and Michel Orrit. "Photothermal imaging of nanometer-sized metal particles among scatterers." Science 297, no. 5584 (2002): 1160-1163.

16. Cao, Linyou, David N. Barsic, Alex R. Guichard, and Mark L. Brongersma. "Plasmon-assisted local temperature control to pattern individual semiconductor nanowires and carbon nanotubes." Nano letters 7, no. 11 (2007): 3523-3527.

17. Palermo, Giovanna, Ugo Cataldi, Luigia Pezzi, Thomas Bürgi, Cesare Umeton, and Antonio De Luca. "Thermo-plasmonic effects on E7 nematic liquid crystal." *Molecular Crystals and Liquid Crystals* 649, no. 1 (2017): 45-49.

18. Pendry, John B., A. J. Holden, W. J. Stewart, and I. Youngs. "Extremely low frequency plasmons in metallic mesostructures." Physical review letters 76, no. 25 (1996): 4773.

19. Pendry, John B., Anthony J. Holden, David J. Robbins, and W. J. Stewart. "Magnetism from conductors and enhanced nonlinear phenomena." *IEEE*

transactions on microwave theory and techniques 47, no. 11 (1999): 2075-2084.

20. Smith, David R., Willie J. Padilla, D. C. Vier, Syrus C. Nemat-Nasser, and Seldon Schultz. "Composite medium with simultaneously negative permeability and permittivity." *Physical review letters* 84, no. 18 (2000): 4184.

21. Shelby, Richard A., David R. Smith, and Seldon Schultz. "Experimental verification of a negative index of refraction." *science* 292, no. 5514 (2001): 77-79.

22. Kojima, N. "Elementary Excitations in Magnetically Ordered Materials." In *Magneto-Optics*, pp. 37-74. Berlin, Heidelberg: Springer Berlin Heidelberg, 2000.

23. Jalas, Dirk, Alexander Petrov, Manfred Eich, Wolfgang Freude, Shanhui Fan, Zongfu Yu, Roel Baets et al. "What is—and what is not—an optical isolator." *Nature Photonics* 7, no. 8 (2013): 579-582.

24. Khanikaev, A. B., and G. Shvets. "Nat. Photonics 11, 763 (2017)."

25. Yu, Zongfu, Georgios Veronis, Zheng Wang, and Shanhui Fan. "One-way electromagnetic waveguide formed at the interface between a plasmonic metal under a static magnetic field and a photonic crystal." Physical review letters 100, no. 2 (2008): 023902.

26. Shridhar E. Mendhe1 & Yogeshwar Prasad Kosta2 " Metameterail properties and applications" International Journal of Information Technology and Knowledge Management January-June, Volume 4, No. 1, pp. 85-89(2011).

27. Rukhlenko, Ivan D., Pavel A. Belov, Natalia M. Litchinitser, and Alexandra Boltasseva. "Modern trends in metamaterial applications." Adv. OptoElectron 2012 (2012): 514270.

28. Filiberto Bilotti, Levent Sevgi " Metamaterials: Definitions, Properties, Applications,and FDTD-Based Modeling and Simulation"No. 21, Acıbadem/Kadıkoy, _Istanbul, Turkey 5 January (2012)

29. Myung-Geun Jeong a, Hyun Ook Seo a, Kwang-Dae Kim a, Young Dok Kim a, Dong Chan Lim b"Enhanced photocatalytic activity of TiO2 by polydimethylsiloxane deposition and subsequent thermal treatment at 800 °C" Thin Solid Films 520 ,4929–4933(2012)

30. R. Yahiaoui; U.-C. Chung; C. Elissalde; M. Maglione; V. Vigneras; P. Mounaix " Towards left-handed metamaterials using single-size dielectric resonators: The case of TiO2-disks at millimeter wavelengths"*Phys. Lett.* 101, 042909 (2012).

31. Němec, H., C. Kadlec, F. Kadlec, P. Kužel, Riad Yahiaoui, U-C. Chung, Catherine Elissalde, Mario Maglione, and Patrick Mounaix. "Resonant magnetic response of TiO2 microspheres at terahertz frequencies." Applied Physics Letters 100, no. 6 (2012).

32. Filiberto Bilotti, Levent Sevgi " Metamaterials: Definitions, Properties, Applications, and FDTD-Based Modeling and Simulation " International Journal of RF and Microwave Computer-Aided Engineering July(2012).

33. S.M. Hamidi · M.M. Tehranchi"Magneto-Optical Faraday Rotation in Ce:YIG Thin Films Incorporating Gold Nanoparticles" Supercond Nov Magn 25:2713–2717, 11 August (2012).

34. Anand Kumar Tripathi a,b, Manish Kumar Singh a,c, Mohan Chandra Mathpal a, Sheo Kumar Mishra d, Arvind Agarwal a"Study of structural transformation in TiO2 nanoparticles and its optical properties" Journal of Alloys and Compounds 549 ,114–120(2013) .

35. Yizhuo He, Junxue Fu, Yiping Zhao1"Oblique angle deposition and its applications in plasmonics"May 29,(2013)

36. M.T.S. Tavares a, A.S.F. Santos b, I.M.G. Santos c, M.R.S. Silva c, M.R.D. Bomio a, E. Longod, C.A. Paskocimas a, F.V. Motta" TiO2/PDMS

nanocomposites for use on self-cleaning surfaces" Surface & Coatings Technology 239 ,16–19(2014).

37. S. M. Hamidi , A. Sobhani, A; Aftabi, and M. Najafi" Optical and magneto-optical properties of aligned Ni nanowires embedded in polydimethylsiloxane" Journal of Magnetism and Magnetic Materials 07.065, 31 July (2014).

38. S. M. Hamidi, H. Goudarzi & S. Sadeghi" Surface Plasmon Resonance Magneto-Optical Kerr Effect in Au/Co/Au Magneto-Plasmonic Multilayer" Journal of Superconductivity and Novel Magnetism Article Original Paper: 14 November (2014).

39. Watts, Claire. "Metamaterials and their applications towards novel imaging technologies." Boston College (2015).

40. Kapridaki, Chrysi, and Noni-Pagona Maravelaki. "TiO2–SiO2–PDMS nanocomposites with self-cleaning properties for stone protection and consolidation." *Geological Society, London, Special Publications* 416, no. 1 (2016): 285-292.

41. Claire Watts" Metamaterials and their applications towards novel imaging technologies" Boston College Electronic Thesis or Dissertation, (2015).

42. Gurwinder, Rajni, Anupma Marwaha " A Review of Metamaterials and its Applications" International Journal of Engineering Trends and Technology (IJETT) – Volume 19 Number 6 – Jan (2015).

43. Irina Khromova,Petr Kužel, Igal Brener, John L. Reno, U-Chan Chung Seu, Catherine Elissalde, Mario Maglione, Patrick Mounaix, Oleg Mitrofanov" Splitting of magnetic dipole modes in anisotropic TiO2 micro-spheres" Volume10, Issue4 July 2016 Pages 681-68.

44. S. M. Hamidi, S. Behjati & F. Sohrabi "Transverse Tunable Magneto-Plasmonic Kerr Effect in Large Area Micro-Patterned Au/Co/Au Structures"Journal of Superconductivity and Novel Magnetism 31, pages1465–1473 22 September(2017).

45. Bo Fan, Mazhar E. Nasir, Luke H. Nicholls, Anatoly V. Zayats, and Viktor A, Podolskiy " Magneto-optical metamaterials: Nonreciprocal transmission and Faraday effect enhancement " (2019),

46. Shan Peng, Weihua Meng, Junxiang Guo, Bo Wang, Zhenguang Wang, Na Xu, Xiaolin Li, Jian Wang, and Jianzhong Xu "Photocatalytically Stable Superhydrophobic and Translucent CoatingsGenerated from PDMS-Grafted-SiO2/TiO2@PDMS with Multiple Application"University of Winnipeg Library24 Jan 2019

47. Syed S. Bukhari , J(Yiannis) Vardaxoglou and William Whittow " A Metasurfaces Review: Definitions and Applications" 5 July(2019)

48. N. S. Shnan, N. Roostaei1 S. M. Hamidi" Tunable and reversible thermo‐plasmonic hot spot imaging for temperature confinement" Journal of Theoretical and Applied Physics 14:367–376(2020).

49. Yixin Chen, Bin Ai and Zi Jing Wong "Soft optical metamaterials"Chen et al. Nano Convergence 7:18 (2020)

50. Tian Gu,Hyun Jung Kim, Clara Rivero-Baleine,and Juejun Hu" Active metasurfaces: lighting the path to commercial success"

51. s.v.tomiln1, a.v.karavayikov,s.d.lyashko ,t.milyukova ,o.a.tomilina ,a.s.yanovsky ,v.i.elotelov , and v.n.berzhansky " Giant enhancement of the Faraday effect in a magnetoplasmonic nanocomposite" Optical Materials Express Vol. 12, No. 4 / 1 Apr (2022).

52. N. S. Shnan ,S. Sadeghi ,M. Farzaneh1 .S. M. Hamidi1 ,V. I. Belotelov, A. I.Chernov" Longitudinal Magneto‐optical Kerr Effect in Insulator/Metal/Insulator Grating Structure" Journal of Superconductivity and Novel Magnetism 35:3397–3401, 23 August (2022).

53. D. A. Djemmah; J.-F. Roux; P.-M. Geffroy; F. Bouamrame; E. Akmansoy; T. Chartier " Characterization of high permittivity and low losses

TiO2 sintered material for THz applications" NSPEC Accession Number: 22092671 26 September 2022

54. N. S. Shnana,b, N. Roostaeia, S. M. Hamidia" Magneto-optical Engineering by Plasmonic and Dielectric Metasurfaces in CoFeB Perforated Microstructure" 2023.

55. Boardman, A.D., and A.V. Zayats. "Nonlinear Plasmonics." Modern Plasmonics, 2014, 329-347.

56. Raether, Heinz. "Surface Plasmons on Smooth and Rough Surfaces and on Gratings." Springer Tracts in Modern Physics, 1988.

57. Myszka, David G. "Survey of the 1998 optical biosensor literature." Journal of Molecular Recognition 12, no. 6 (1999).

58. Otto, Andreas. "Excitation of nonradiative surface plasma waves in silver by the method of frustrated total reflection." Zeitschrift für Physik A Hadrons and nuclei 216, no. 4 (1968): 398-410.

59. Kretschmann, Erwin. "Die Bestimmung optischer Konstanten von Metallen durch Anregung von Oberflächenplasmaschwingungen." Zeitschrift für Physik A Hadrons and nuclei 241, no. 4 (1971),

60. Lee, Byoungho, Il-Min Lee, Seyoon Kim, Dong-Ho Oh, and Lambertus Hesselink. "Review on subwavelength confinement of light with plasmonics." Journal of Modern Optics 57, no. 16 (2010),

61. Li, Ming, Scott K. Cushing, and Nianqiang Wu. "Plasmon-enhanced optical sensors: a review." The Analyst 140, no. 2 (2015).

62. Unser, Sarah, Ian Bruzas, Jie He, and Laura Sagle. "Localized Surface Plasmon Resonance Biosensing: Current Challenges and Approaches." Sensors 15, no. 7 (2015).

63. Caucheteur, Christophe, Tuan Guo, and Jacques Albert. "Review of plasmonic fiber optic biochemical sensors: improving the limit of detection." Analytical and Bioanalytical Chemistry 407, no. 14 (2015),

64. Jain, Prashant K., Xiaohua Huang, Ivan H. El-Sayed, and Mostafa A. El-Sayed. "Review of Some Interesting Surface Plasmon Resonance-enhanced Properties of Noble Metal Nanoparticles and Their Applications to Biosystems." Plasmonics 2, no. 3 (2007), 107-118.

65. Dobson, Peter J. "Introduction to Metal-nanoparticle Plasmonics, by Matthew Pelton and Garnett W. Bryant." Contemporary Physics 55, no. 4 (2014), 352-353.

66. Maier, Stefan A. "Plasmon Waveguides." Plasmonics: Fundamentals and Applications, 2007, 109-139.

67. Amendola, Vincenzo, Roberto Pilot, Marco Frasconi, Onofrio M. Maragò, and Maria A. Iatì. "Surface plasmon resonance in gold nanoparticles: a review." Journal of Physics: Condensed Matter 29, no. 20 (2017), 203002.

68. Homola, Jiri. "ChemInform Abstract: Surface Plasmon Resonance Sensors for Detection of Chemical and Biological Species." ChemInform 39, no. 18 (2008).

69. Ni, Weihai, Xiaoshan Kou, Zhi Yang, and Jianfang Wang. "Tailoring Longitudinal Surface Plasmon Wavelengths, Scattering and Absorption Cross Sections of Gold Nanorods." ACS Nano 2, no. 4 (2008).

70. Lakhtakia, Akhlesh, Werner S. Weiglhofer, and Russell F. Messier. "Complex mediums." Complex Mediums 4097 (2000).

71. Walser, Rodger M. "Electromagnetic metamaterials." In Complex Mediums II: beyond linear isotropic dielectrics, vol. 4467, pp. 1-15. SPIE, 2001.

72. Zouhdi, Saïd, Ari Sihvola, and Mohamed Arsalane, eds. Advances in electromagnetics of complex media and metamaterials. Vol. 89. Springer Science & Business Media, 2012.

73. Fedotov, V. A., M. Rose, S. L. Prosvirnin, N. Papasimakis, and N. I. Zheludev. "Sharp trapped-mode resonances in planar metamaterials with a broken structural symmetry." Physical review letters 99, no. 14 (2007).

74. Sihvola, Ari. "Metamaterials in electromagnetics." Metamaterials 1, no. 1 (2007): 2-11.

75. Canavan, Gerry, and Darko Suvin. "Metamorphoses of science fiction." (2016).

76. Cui, Tie Jun, Lianlin Li, Shuo Liu, Qian Ma, Lei Zhang, Xiang Wan, Wei Xiang Jiang, and Qiang Cheng. "Information metamaterial systems." Iscience 23, no. 8 (2020).

77. Sihvola, Ari. "Metamaterials in electromagnetics." Metamaterials 1, no. 1 (2007): 2-11.

78. Shelby, Richard A., David R. Smith, and Seldon Schultz. "Experimental verification of a negative index of refraction." science 292, no. 5514 (2001): 77-79.

79. Martin, F. "Special issue on Microwave metamaterials: Theory, fabrication and applications." EuMA Proc 2 (2006).

80. Martin, Ferran, and Richard Ziolkowski. "Microwave Metamaterials:: Application to Devices, Circuits and Antennas." IET Microwaves, Antennas & Propagation 4, no. 8 (2010): 975.

81. Sihvola," Electromagnetic Mixing Formulas and Applications, IEEE Electromagnetic Waves Series, London, UK, 47, IEEE Pub., 2000.

82. Tretyakov, Sergei. Analytical modeling in applied electromagnetics. Artech House, 2003.

83. Douglas B. Chrisey and Graham K. Hubler, John "Pulsed Laser Deposition of Thin Films, Wiley & Sons, 1994 ISBN 0-471-59218-8.

84. Oliva-Ramírez, Manuel. "Optofluidic thin-film sensors prepared by Oblique Angle Deposition." (2016).

85. Barranco, Angel, Ana Borras, Agustin R. Gonzalez-Elipe, and Alberto Palmero. "Perspectives on oblique angle deposition of thin films: From fundamentals to devices." Progress in Materials Science 76 (2016): 59-153.

86. Ramírez, Manuel Oliva, A. R. González-Elipe, F. Yubero, and Alfonso Caballero Martínez. Optofluidic thin-film sensors prepared by Oblique Angle Deposition. Universidad, 2016.

87. Dirks, A. G., and H. J. Leamy. "Columnar microstructure in vapor-deposited thin films." Thin solid films 47, no. 3 (1977): 219-233.

88. Van Kranenburg H, Lodder C. Tailoring growth and local composition by oblique-incidence deposition: a review and new experimental data. Mater Sci Eng R 1994;11:295–354.

89. Lakhtakia A, Messier R. Sculptured thin films. Nanoengineered morphology and optics. Bellingham, Washington, USA: SPIE Press; 2005

90. W; Valentine, J. (2014). "Metamaterial Perfect Absorber Based Hot Electron Photodetection". Nano Letters. 14 (6): 3510–14.

91. Yu, Peng, Jiang Wu, Eric Ashalley, Alexander Govorov, and Zhiming Wang. "Dual-band absorber for multispectral plasmon-enhanced infrared photodetection." Journal of Physics D: Applied Physics 49, no. 36 (2016): 365101.

92. Yu, Peng, Lucas V. Besteiro, Yongjun Huang, Jiang Wu, Lan Fu, Hark H. Tan, Chennupati Jagadish, Gary P. Wiederrecht, Alexander O. Govorov, and Zhiming Wang. "Broadband metamaterial absorbers." Advanced Optical Materials 7, no. 3 (2019): 1800995.

93. Kaushal Gangwar1, Dr. Paras2 and Dr. R.P.S. Gangwar3"Metamaterials: Characteristics, Process and Applications"Number 1 (2014).

94. Johnson, R. Colin "Metamaterial cloak could render buildings 'invisible' to earthquakes". EETimes.com. Retrieved 2009-09-09.

95. Barras, Colin. "Invisibility cloak could hide buildings from quakes". New Scientist. Retrieved 2009-10-20.

96. Brun, M.; S. Guenneau; and A.B. Movchan ."Achieving control of in-plane elastic waves". Appl. Phys. Lett. 94 (61903): 061903.

97. Brûlé, S.; Javelaud, E. H.; Enoch, S.; Guenneau, S. "Experiments on Seismic Metamaterials: Molding Surface Waves". Physical Review Letters(. (2014-03-31. 112 (13): 133901.

98. Rudykh, S.; Boyce, "Transforming Wave Propagation in Layered Media via Instability-Induced Interfacial Wrinkling". Physical Review Letters. (2014). 112 (3): 034301.

99. Meng, Yuan; Chen, Yizhen; Lu, Longhui; Ding, Yimin; Cusano, Andrea; Fan, Jonathan A.; Hu, Qiaomu; Wang, Kaiyuan; Xie, Zhenwei; Liu, Zhoutian; Yang, Yuanmu "Optical meta-waveguides for integrated photonics and beyond". Light: Science & Applications(2021-11-22). 10 (1): 235.

100. Halir, Robert; Cheben, Pavel; Luque-González, José Manuel; Sarmiento-Merenguel, Jose Darío; Schmid, Jens H.; Wangüemert-Pérez, Gonzalo; Xu, Dan-Xia; Wang, Shurui; Ortega-Moñux, Alejandro; Molina-Fernández, Íñigo "Ultra-broadband nanophotonic beamsplitter using an anisotropic sub-wavelength metamaterial(November 2016).

101. Meng, Yuan; Hu, Futai; Liu, Zhoutian; Xie, Peng; Shen, Yijie; Xiao, Qirong; Fu, Xing; Bae, Sang-Hoon; Gong, Mali "Chip-integrated metasurface for versatile and multi-wavelength control of light couplings with independent phase and arbitrary polarization"(2019-06-10).

102. Cheben, Pavel; Halir, Robert; Schmid, Jens H.; Atwater, Harry A.; Smith, David R. "Subwavelength integrated photonics". Nature. (August 2018). 560 (7720): 565–572

103. Li, Zhaoyi; Kim, Myoung-Hwan; Wang, Cheng; Han, Zhaohong; Shrestha, Sajan; Overvig, Adam Christopher; Lu, Ming; Stein, Aaron; Agarwal, Anuradha Murthy; Lončar, Marko; Yu, Nanfang "Controlling propagation and coupling of waveguide modes using phase-gradient metasurfaces"(July 2017).

104. Guo, Rui; Decker, Manuel; Setzpfandt, Frank; Gai, Xin; Choi, Duk-Yong; Kiselev, Roman; Chipouline, Arkadi; Staude, Isabelle; Pertsch, Thomas; Neshev,

Dragomir N.; Kivshar, Yuri S. "High–bit rate ultra-compact light routing with mode-selective on-chip nanoantennas"(2017-07-07).

105. He, Tiantian; Meng, Yuan; Liu, Zhoutian; Hu, Futai; Wang, Rui; Li, Dan; Yan, Ping; Liu, Qiang; Gong, Mali; Xiao, Qirong "Guided mode meta-optics: metasurface-dressed waveguides for arbitrary mode couplers and on-chip OAM emitters with a configurable topological charge (2021-11-22).

106. Flueckiger, Jonas; Schmidt, Shon; Donzella, Valentina; Sherwali, Ahmed; Ratner, Daniel M.; Chrostowski, Lukas; Cheung, Karen C. "Sub-wavelength grating for enhanced ring resonator biosensor"(2016-07-11).

107. Morrish, A. H. "The Physical Principles of Magnetism (IEEE, New York, 2001)." an IEEE press classical reissue 30: 344.

108. A. Hubert and R. Schafer, Magnetic Domains: The Analysis of Magnetic Microstructures. Berlin: Springer-Verlag, 2000.

109. K. Sato et al., 'Magnetization suppression in Co/Pd and CoCrPt by nitrogen ion implantation for bit patterned media fabrication,' Journal of Applied Physics, vol.107, pp. 123910–123913, 2010.

110. Kittel, Charles. Introduction to solid state physics. John Wiley & sons, inc, 2005.

111. O'handley, Robert C. Modern magnetic materials: principles and applications. Wiley, 2000.

112. Barnes, W.L.; Dereux, A.; Ebbesen, T.W. Surface plasmon subwavelength optics. Nature 2003,424, 824–830.

113. Stockman, Mark I. "Nanoplasmonics: past, present, and glimpse into future." Optics express 19, no. 22 (2011): 22029-22106.

114. Zayats, Anatoly V., and Stefan Maier, eds. Active plasmonics and tuneable plasmonic metamaterials. John Wiley & Sons, 2013.

115. Krasnok, Aleksandr E., Ivan S. Maksymov, Andrei I. Denisyuk, Pavel Alexandrovich Belov, Andrei E. Miroshnichenko, Constantin R. Simovski, and Yu S. Kivshar. "Optical nanoantennas." Physics-Uspekhi 56, no. 6 (2013): 539.

116. Chiu, K. W., and J. J. Quinn. "Magneto-plasma surface waves in solids." Il Nuovo Cimento B (1971-1996) 10, no. 1 (1972): 1-20.

117. Armelles, Gaspar, Alfonso Cebollada, Antonio García-Martín, and María Ujué González. "Magnetoplasmonics: combining magnetic and plasmonic functionalities." Advanced Optical Materials 1, no. 1 (2013): 10-35.

118. Kovalenko, V. F., and É. L. Nagaev. "Photoinduced magnetism." Soviet Physics Uspekhi 29, no. 4 (1986): 297.

119. Pendry, John B., A. J. Holden, D. J. Robbins, and W. J. Stewart. "Low frequency plasmons in thin-wire structures." Journal of Physics: Condensed Matter 10, no. 22 (1998): 4785.

120. Pendry, J. B., A. J. Holden, D. J. Robbins, and W. J. Stewart. "IEEE Trans. Microwave Theory Tech." IEEE Trans. Microwave Theory Tech 47, no. 2075 (1999).

121. Smith, David R., Willie J. Padilla, D. C. Vier, Syrus C. Nemat-Nasser, and Seldon Schultz. "Composite medium with simultaneously negative permeability and permittivity." Physical review letters 84, no. 18 (2000): 4184.

122. Shelby, Richard A., D. R. Smith, S. C. Nemat-Nasser, and Sheldon Schultz. "Microwave transmission through a two-dimensional, isotropic, left-handed metamaterial." Applied Physics Letters 78, no. 4 (2001): 489-491.

123. Temnov, Vasily V. "Ultrafast acousto-magneto-plasmonics." Nature Photonics 6, no. 11 (2012): 728-736.

124. Aydin, Koray, Kaan Guven, Costas M. Soukoulis, and Ekmel Ozbay. "Observation of negative refraction and negative phase velocity in left-handed metamaterials." Applied Physics Letters 86, no. 12 (2005).

125. Cubukcu, Ertugrul, Koray Aydin, Ekmel Ozbay, Stavroula Foteinopoulou, and Costas M. Soukoulis. "Negative refraction by photonic crystals." Nature 423, no. 6940 (2003): 604-605.

126. Williams, John Michael. "Some problems with negative refraction." Physical Review Letters 87, no. 24 (2001): 249703.

127. Kuzyk, Mark G. "Erratum: Physical Limits on Electronic Nonlinear Molecular Susceptibilities [Phys. Rev. Lett. 85, 001218 (2000)]." Physical Review Letters 90, no. 3 (2003): 039902.

128. Guven, K., and E. Ozbay. "Near field imaging in microwave regime using double layer split-ring resonator based metamaterial." Opto-Electronics Review 14 (2006): 213-216.

129. Grbic, Anthony, and George V. Eleftheriades. "Overcoming the diffraction limit with a planar left-handed transmission-line lens." Physical review letters 92, no. 11 (2004): 117403.

130. Lagarkov, A. N., and V. N. Kissel. "Near-perfect imaging in a focusing system based on a left-handed-material plate." Physical Review Letters 92, no. 7 (2004): 077401.

131. Aydin, Koray, Irfan Bulu, and Ekmel Ozbay. "Electromagnetic wave focusing from sources inside a two-dimensional left-handed material superlens." New Journal of Physics 8, no. 10 (2006): 221.

132. Fang N, Lee H, Sun C and Zhang X 2005 Science 308 534.

133. Taubner, Thomas, Dmitriy Korobkin, Yaroslav Urzhumov, Gennady Shvets, and Rainer Hillenbrand. "Near-field microscopy through a SiC superlens." Science 313, no. 5793 (2006): 1595-1595.

134. Guven, K., and E. Ozbay. "Near field imaging in microwave regime using double layer split-ring resonator based metamaterial." Opto-Electronics Review 14 (2006): 213-216.

135. Pendry, John B., David Schurig, and David R. Smith. "Controlling electromagnetic fields." science 312, no. 5781 (2006): 1780-1782.

136. Schurig, David, Jack J. Mock, 1. BJ Justice, Steven A. Cummer, John B. Pendry, Anthony F. Starr, and David R. Smith. "Metamaterial electromagnetic cloak at microwave frequencies." Science 314, no. 5801 (2006): 977-980.

137. Klein, Matthias W., Christian Enkrich, Martin Wegener, and Stefan Linden. "Second-harmonic generation from magnetic metamaterials." Science 313, no. 5786 (2006): 502-504.

138. Padilla, Willie J., Antoinette J. Taylor, Clark Highstrete, Mark Lee, and Richard D. Averitt. "Dynamical electric and magnetic metamaterial response at terahertz frequencies." Physical review letters 96, no. 10 (2006): 107401.

139. Chen, Hou-Tong, Willie J. Padilla, Joshua MO Zide, Arthur C. Gossard, Antoinette J. Taylor, and Richard D. Averitt. "Active terahertz metamaterial devices." Nature 444, no. 7119 (2006): 597-600.

140. Bayindir, Mehmet, K. Aydin, E. Ozbay, P. Markoš, and C. M. Soukoulis. "Transmission properties of composite metamaterials in free space." Applied Physics Letters 81, no. 1 (2002): 120-122.

141. Guven, Kaan, M. Deniz Caliskan, and Ekmel Ozbay. "Experimental observation of left-handed transmission in a bilayer metamaterial under normal-to-plane propagation." Optics express 14, no. 19 (2006): 8685-8693.

142. Yen, Ta-Jen, W. J. Padilla, Nicholas Fang, D. C. Vier, D. R. Smith, J. B. Pendry, D. N. Basov, and Xiang Zhang. "Terahertz magnetic response from artificial materials." science 303, no. 5663 (2004): 1494-1496.

143. Yen, Ta-Jen, W. J. Padilla, Nicholas Fang, D. C. Vier, D. R. Smith, J. B. Pendry, D. N. Basov, and Xiang Zhang. "Terahertz magnetic response from artificial materials." science 303, no. 5663 (2004): 1494-1496.

144. Tao, Hu, Nathan I. Landy, Christopher M. Bingham, Xin Zhang, Richard D. Averitt, and Willie J. Padilla. "A metamaterial absorber for the terahertz regime: design, fabrication and characterization." Optics express 16, no. 10 (2008): 7181-7188.

145. Chen, Hou-Tong, Jiangfeng Zhou, John F. O'Hara, Frank Chen, Abul K. Azad, and Antoinette J. Taylor. "Antireflection coating using metamaterials and identification of its mechanism." Physical review letters 105, no. 7 (2010): 073901.

146. N. K. Grady, J. E. Heyes, D. R. Chowdhury, Y. Zeng, M. T. Reiten, A. K. Azad, A. J. Taylor, D. A. R. Dalvit, and H.-T. Chen, “Terahertz metamaterials for linear polarization conversion and anomalous refraction,” Science 340(6138), 1304–1307 (2013).

147. N. I. Zheludev and Y. S. Kivshar, “From metamaterials to metadevices,” Nat. Mater. 11(11), 917–924 (2012)

148. Padilla, Willie J., Antoinette J. Taylor, Clark Highstrete, Mark Lee, and Richard D. Averitt. "Dynamical electric and magnetic metamaterial response at terahertz frequencies." Physical review letters 96, no. 10 (2006): 107401.

149. . J. Gu, R. Singh, X. Liu, X. Zhang, Y. Ma, S. Zhang, S. A. Maier, Z. Tian, A. K. Azad, H.-T. Chen, A. J. Taylor, J. Han, and W. Zhang, “Active control of electromagnetically induced transparency analogue in terahertz metamaterials,” Nat. Commun. 3(1151), 1151 (2012).

150. H.-T. Chen, W. J. Padilla, J. M. O. Zide, A. C. Gossard, A. J. Taylor, and R. D. Averitt, “Active terahertz metamaterial devices,” Nature 444(7119), 597–600 (2006).

151. H.-T. Chen, W. J. Padilla, M. J. Cich, A. K. Azad, R. D. Averitt, and A. J. Taylor, “A metamaterial solid-state terahertz phase modulator,” Nat. Photonics 3(3), 148–151 (2009).

152. . H. Tao, A. C. Strikwerda, K. Fan, W. J. Padilla, X. Zhang, and R. D. Averitt, “Reconfigurable TerahertzMetamaterials,” Phys. Rev. Lett. 103(14), 147401 (2009).

153. . T. Kan, A. Isozaki, N. Kanda, N. Nemoto, K. Konishi, H. Takahashi, M. K. -Gonokami, K. Matsumoto, and I. Shimoyama, “Enantiomeric switching of chiral metamaterial for terahertz polarization modulation employing vertically deformable MEMS spirals,” Nat. Commun. 6(8422), 1–7 (2015).

154. Pendry, John Brian. "Negative refraction makes a perfect lens." Physical review letters 85, no. 18 (2000): 3966.

155. X. Zhang and Z. Liu, “Superlenses to overcome the diffraction limit,” Nat. Mater. 7(6), 435–441 (2008).

156. D. R. Smith, W. J. Padilla, D. C. Vier, S. C. Nemat-Nasser, and S. Schultz, “Composite medium with simultaneously negative permeability and permittivity,” Phys. Rev. Lett. 84(18), 4184–4187 (2000).

157. R. A. Shelby, D. R. Smith, and S. Schultz, “Experimental verification of a negative index of refraction,” Science 292(5514), 77–79 (2001).

158. A. N. Lagarkov and V. N. Kissel, “Near-perfect imaging in a focusing system based on a left-handed-material plate,” Phys. Rev. Lett. 92(7), 077401 (2004).

159. M. Awad, M. Nagel, and H. Kurz, “Negative-index metamaterial with polymer-embedded wire-pair structures atterahertz frequencies,” Opt. Lett. 33(22), 2683–2685 (2008).

160. O. Paul, C. Imhof, B. Reinhard, R. Zengerle, and R. Beigang, “Negative index bulk metamaterial at terahertz frequencies,” Opt. Express 16(9), 6736–6744 (2008).

161. P. Weis, O. Paul, C. Imhof, R. Beigang, and M. Rahm, “Strongly birefringent metamaterials as negative index terahertz wave plates,” Appl. Phys. Lett. 95(17), 171104 (2009).

162. Kuester, E.; Mohamed, M.; Piket-May, M.; Holloway, C. Averaged transition conditions for electromagnetic fields at a metafilm. IEEE Trans. Antennas Propag. 2003, 51, 2641–2651.

163. Cai, Wenshan, and Vladimir M. Shalaev. Optical metamaterials. Vol. 10, no. 6011. New York: Springer, 2010.

164. Yu, Nanfang, and Federico Capasso. "Flat optics with designer metasurfaces." Nature materials 13, no. 2 (2014): 139-150.

165. Holloway, Christopher L., Edward F. Kuester, Joshua A. Gordon, John O'Hara, Jim Booth, and David R. Smith. "An overview of the theory and applications of metasurfaces: The two-dimensional equivalents of

metamaterials." IEEE antennas and propagation magazine 54, no. 2 (2012): 10-35.

166. Yoon, Gwanho, Inki Kim, and Junsuk Rho. "Challenges in fabrication towards realization of practical metamaterials." Microelectronic Engineering 163 (2016): 7-20.

167. Soukoulis, Costas M., and Martin Wegener. "Past achievements and future challenges in the development of three-dimensional photonic metamaterials." Nature photonics 5, no. 9 (2011): 523-530.

168. Meinzer, Nina, William L. Barnes, and Ian R. Hooper. "Plasmonic meta-atoms and metasurfaces." Nature photonics 8, no. 12 (2014): 889-898.

169. Kildishev, Alexander V., Alexandra Boltasseva, and Vladimir M. Shalaev. "Planar photonics with metasurfaces." Science 339, no. 6125 (2013): 1232009.

170. Jiang, Zhi Hao, Seokho Yun, Lan Lin, Jeremy A. Bossard, Douglas H. Werner, and Theresa S. Mayer. "Tailoring dispersion for broadband low-loss optical metamaterials using deep-subwavelength inclusions." Scientific reports 3, no. 1 (2013): 1571.

171. McGrath, D. "Planar three-dimensional constrained lenses." IEEE Transactions on Antennas and Propagation 34, no. 1 (1986): 46-50.

172. Pozar, David M., Stephen D. Targonski, and H. D. Syrigos. "Design of millimeter wave microstrip reflectarrays." IEEE transactions on antennas and propagation 45, no. 2 (1997): 287-296.

173. Yu, A., F. Yang, A. Z. Elsherbeni, and J. Huang. "Experimental demonstration of a single layer tri-band circularly polarized reflectarray." In 2010 IEEE Antennas and Propagation Society International Symposium, pp. 1-4. IEEE, 2010.

174. Pozar, D. M. "Flat lens antenna concept using aperture coupled microstrip patches." Electronics Letters 32, no. 23 (1996): 2109-2111.

175. Tretyakov, S. A., S. B. Glybovski, P. A. Belov, Y. S. Kivshar, and C. R. Simovski. "Metasurfaces: From microwaves to visible." Phys. Rep 634 (2016): 1-72.

176. De Vita, P., A. Freni, G. L. Dassano, P. Pirinoli, and R. E. Zich. "Broadband element for high-gain single-layer printed reflectarray antenna." Electronics Letters 43, no. 23 (2007): 1.

177. Yu, Nanfang, and Federico Capasso. "Flat optics with designer metasurfaces." Nature materials 13, no. 2 (2014): 139-150.

178. Monticone, Francesco, Nasim Mohammadi Estakhri, and Andrea Alu. "Full control of nanoscale optical transmission with a composite metascreen." Physical review letters 110, no. 20 (2013): 203903.

179. Niemi, Teemu, Antti O. Karilainen, and Sergei A. Tretyakov. "Synthesis of polarization transformers." IEEE Transactions on Antennas and Propagation 61, no. 6 (2013): 3102-3111.

180. Pfeiffer, Carl, and Anthony Grbic. "Metamaterial Huygens' surfaces: tailoring wave fronts with reflectionless sheets." Physical review letters 110, no. 19 (2013): 197401.

181. Ginn, James, Brian Lail, Javier Alda, and Glenn Boreman. "Planar infrared binary phase reflectarray." Optics letters 33, no. 8 (2008): 779-781.

182. Farmahini-Farahani, Mohsen, and Hossein Mosallaei. "Birefringent reflectarray metasurface for beam engineering in infrared." Optics letters 38, no. 4 (2013): 462-464.

183. . Niu, Tiaoming, Withawat Withayachumnankul, Aditi Upadhyay, Philipp Gutruf, Derek Abbott, Madhu Bhaskaran, Sharath Sriram, and Christophe Fumeaux. "Terahertz reflectarray as a polarizing beam splitter." Optics express 22, no. 13 (2014): 16148-16160.

184. Micheli, Davide, Roberto Pastore, Antonio Vricella, and Mario Marchetti. "Matter's electromagnetic signature reproduction by graded-dielectric multilayer

assembly." IEEE Transactions on Microwave Theory and Techniques 65, no. 8 (2017): 2801-2809.

185. Bellucci, S., I. Bolesta, M. Cestelli Guidi, I. Karbovnyk, V. Lesivciv, F. Micciulla, R. Pastore, A. I. Popov, and S. Velgosh. "Cadmium clusters in CdI2 layered crystals: The influence on the optical properties." Journal of Physics: Condensed Matter 19, no. 39 (2007): 395015.

186. Aieta, Francesco, Patrice Genevet, Mikhail A. Kats, Nanfang Yu, Romain Blanchard, Zeno Gaburro, and Federico Capasso. "Aberration-free ultrathin flat lenses and axicons at telecom wavelengths based on plasmonic metasurfaces." Nano letters 12, no. 9 (2012): 4932-4936.

187. Yu, Nanfang, and Federico Capasso. "Flat optics with designer metasurfaces." Nature materials 13, no. 2 (2014): 139-150.

188. Pors, Anders, Michael G. Nielsen, René Lynge Eriksen, and Sergey I. Bozhevolnyi. "Broadband focusing flat mirrors based on plasmonic gradient metasurfaces." Nano letters 13, no. 2 (2013): 829-834.

189. Aieta, Francesco, Mikhail A. Kats, Patrice Genevet, and Federico Capasso. "Multiwavelength achromatic metasurfaces by dispersive phase compensation." Science 347, no. 6228 (2015): 1342-1345.

190. Engheta, Nader. "An idea for thin subwavelength cavity resonators using metamaterials with negative permittivity and permeability." IEEE Antennas and wireless propagation letters 1 (2002): 10-13.

191. Lapine, Mikhail, Ilya V. Shadrivov, and Yuri S. Kivshar. "Colloquium: nonlinear metamaterials." Reviews of Modern Physics 86, no. 3 (2014): 1093.

192. Wang, Zhengbin, Jinchang Chen, Zhaozhi Wu, and Yuan Zhu. "Wave propagation in two-dimensional left-handed non-linear transmission line metamaterials." IET Microwaves, Antennas & Propagation 10, no. 2 (2016): 202-207.

193. Kim, Evgenia, Feng Wang, Wei Wu, Zhaoning Yu, and Y. Ron Shen. "Nonlinear optical spectroscopy of photonic metamaterials." Physical Review B 78, no. 11 (2008): 113102.

194. Vardaxoglou, John C. "Frequency selective surfaces: analysis and design." (No Title) (1997).

195. S M Shahrokhvand,ASHRozatian, M Mozaffari, S M HamidiandM M Tehranchi" Preparation and investigation of Ce : YIGthin films with a high magneto-opticalfigure of merit" J. Phys. D: Appl. Phys. 45 (2012).

196. . Sugano, Satoru, and Norimichi Kojima, eds. Magneto-optics. Vol. 128. Springer Science & Business Media, 2013.

197. Jalas, Dirk, Alexander Petrov, Manfred Eich, Wolfgang Freude, Shanhui Fan, Zongfu Yu, Roel Baets et al. "What is—and what is not—an optical isolator." Nature Photonics 7, no. 8 (2013): 579-582.

198. Khanikaev, A. B., and G. Shvets. "Nat. Photonics 11, 763 (2017).

199. Yu, Zongfu, Georgios Veronis, Zheng Wang, and Shanhui Fan. "One-way electromagnetic waveguide formed at the interface between a plasmonic metal under a static magnetic field and a photonic crystal." Physical review letters 100, no. 2 (2008): 023902.

200. Sadatgol, Mehdi, Mahfuzur Rahman, Ebrahim Forati, Miguel Levy, and Durdu Ö. Güney. "Enhanced Faraday rotation in hybrid magneto-optical metamaterial structure of bismuth-substituted-iron-garnet with embedded-gold-wires." Journal of Applied Physics 119, no. 10 (2016).

201. . Ginzburg, Pavel, FJ Rodríguez Fortuño, G. A. Wurtz, W. Dickson, Antony Murphy, F. Morgan, R. J. Pollard et al. "Manipulating polarization of light with ultrathin epsilon-near-zero metamaterials." Optics Express 21, no. 12 (2013): 14907-14917.

202. Vestler, D., I. Shishkin, E. A. Gurvitz, M. E. Nasir, A. Ben-Moshe, A. P. Slobozhanyuk, Alexey V. Krasavin et al. "Circular dichroism enhancement in

plasmonic nanorod metamaterials." Optics express 26, no. 14 (2018): 17841-17848.

203. Nasir, Mazhar E., Wayne Dickson, Gregory A. Wurtz, William P. Wardley, and Anatoly V. Zayats. "Hydrogen detected by the naked eye: optical hydrogen gas sensors based on core/shell plasmonic nanorod metamaterials." Advanced Materials 26, no. 21 (2014): 3532-3537.

204. Rodrigues, Raquel O., Diana Pinho, David Bento, Rui Lima, and João Ribeiro. "Wall expansion assessment of an intracranial aneurysm model by a 3D Digital Image Correlation System." Measurement 88 (2016): 262-270.

205. Aigueperse, Jean, Paul Mollard, Didier Devilliers, Marius Chemla, Robert Faron, René Romano, and Jean Pierre Cuer. "Fluorine compounds, inorganic." Ullmann's encyclopedia of industrial chemistry (2000).

206. Nowotny, Janusz. Oxide semiconductors for solar energy conversion: titanium dioxide. CRC press, 2011.

207. Hall, Edwin Herbert. "XVIII. On the “Rotational Coefficient” in nickel and cobalt." The London, Edinburgh, and Dublin Philosophical Magazine and Journal of Science 12, no. 74 (1881): 157-172.

208. Sagdoldina, Zhuldyz, Konstantin Shestakov, Michael Yermolenko, Manarbek Kylyshkanov, Mikhail Podoinikov, Bauyrzhan Rakhadilov, and Yedilzhan Kambarov. "Magnesium Oxide Production by Plasma Chemical Conversion from Fluorine-Containing Industrial Waste." Coatings 12, no. 11 (2022): 1658.

209. Heinzerling, P., and M. Oetken. "Nanochemistry-A Split between 18th Century and Modern Times." World J. Chem. Educ 6, no. 1 (2018): 1-7.

210. Emsley, John. Nature's building blocks: an AZ guide to the elements. Oxford University Press, USA, 2011.

211. Edwards, Peter P., and John Meurig Thomas. "Gold in a metallic divided state—from faraday to present-day nanoscience." Angewandte Chemie International Edition 46, no. 29 (2007): 5480-5486.

212. Hutchings, Graham J., Mathias Brust, and Hubert Schmidbaur. "Gold—an introductory perspective." Chemical Society Reviews 37, no. 9 (2008): 1759-1765.

213. Louis, Catherine, and Olivier Pluchery, eds. Gold nanoparticles for physics, chemistry and biology. World Scientific, 2017.

214. Cai, Weibo, Ting Gao, Hao Hong, and Jiangtao Sun. "Applications of gold nanoparticles in cancer nanotechnology." Nanotechnology, science and applications (2008): 17-32.

215. . Teranishi, Tet, M. Hosoe, T. Tanaka, and M. Miyake. "Size control of monodispersed Pt nanoparticles and their 2D organization by electrophoretic deposition." The Journal of Physical Chemistry B 103, no. 19 (1999): 3818-3827.

216. Turkevich, John, Peter Cooper Stevenson, and James Hillier. "A study of the nucleation and growth processes in the synthesis of colloidal gold." Discussions of the Faraday Society 11 (1951): 55-75.

217. Turkevich, John, and James Hillier. "Electron microscopy of colloidal systems." Analytical chemistry 21, no. 4 (1949): 475-485.

218. Scott, Robert WJ, Orla M. Wilson, and Richard M. Crooks. "Synthesis, characterization, and applications of dendrimer-encapsulated nanoparticles." The Journal of Physical Chemistry B 109, no. 2 (2005): 692-704.

219. Cai, Weibo, Ting Gao, Hao Hong, and Jiangtao Sun. "Applications of gold nanoparticles in cancer nanotechnology." Nanotechnology, science and applications (2008): 17-32.

220. Das, Minakshi, Kyu Hwan Shim, Seong Soo A. An, and Dong Kee Yi. "Review on gold nanoparticles and their applications." Toxicology and Environmental Health Sciences 3 (2011): 193-205.

221. Martin, Charles R. "Nanomaterials: a membrane-based synthetic approach." Science 266, no. 5193 (1994): 1961-1966.

222. Kuo, W. S., Chang, C. N., Chang, Y. T., Yang, M. H., Chien, Y. H., Chen, S. J., & Yeh, C. S. (2010). Gold nanorods in photodynamic therapy, as hyperthermia agents, and in near-infrared optical imaging. Angewandte Chemie, 122(15), 2771-2775.

223. Kumar, V. Ganesh, S. Dinesh Gokavarapu, A. Rajeswari, T. Stalin Dhas, V. Karthick, Zainab Kapadia, Tripti Shrestha, I. A. Barathy, Anindita Roy, and Sweta Sinha. "Facile green synthesis of gold nanoparticles using leaf extract of antidiabetic potent Cassia auriculata." Colloids and Surfaces B: Biointerfaces 87, no. 1 (2011): 159-163.

224. Busbee, Brantley D., Sherine O. Obare, and Catherine J. Murphy. "An improved synthesis of high-aspect-ratio gold nanorods." Advanced Materials 15, no. 5 (2003): 414-416.

225. Narang, Jagriti, Nitesh Malhotra, Gajendra Singh, and C. S. Pundir. "Electrochemical impediometric detection of anti-HIV drug taking gold nanorods as a sensing interface." Biosensors and Bioelectronics 66 (2015): 332-337.

226. Loo, Christopher, Alex Lin, Leon Hirsch, Min-Ho Lee, Jennifer Barton, Naomi Halas, Jennifer West, and Rebekah Drezek. "Nanoshell-enabled photonics-based imaging and therapy of cancer." Technology in cancer research & treatment 3, no. 1 (2004): 33-40.

227. Cai, Weibo, Ting Gao, Hao Hong, and Jiangtao Sun. "Applications of gold nanoparticles in cancer nanotechnology." Nanotechnology, science and applications (2008): 17-32.

228. Chen, Jingyi, Joseph M. McLellan, Andrew Siekkinen, Yujie Xiong, Zhi-Yuan Li, and Younan Xia. "Facile synthesis of gold− silver nanocages with controllable pores on the surface." Journal of the American Chemical Society 128, no. 46 (2006): 14776-14777.

229. Rodrigues, Raquel O., Diana Pinho, David Bento, Rui Lima, and João Ribeiro. "Wall expansion assessment of an intracranial aneurysm model by a 3D Digital Image Correlation System." Measurement 88 (2016): 262-270.

230. Schneider, Fellner, T. Fellner, J. Wilde, and U. Wallrabe. "Mechanical properties of silicones for MEMS." Journal of Micromechanics and Microengineering 18, no. 6 (2008): 065008.

231. Lima, R., M. Nakamura, T. Omori, Takuji Ishikawa, Shigeo Wada, and Takami Yamaguchi. "Microscale flow dynamics of red blood cells in microchannels: an experimental and numerical analysis." Advances in computational vision and medical image processing: methods and applications (2009): 203-220.

232. Hemmilä, Samu, Juan V. Cauich-Rodríguez, Joose Kreutzer, and Pasi Kallio. "Rapid, simple, and cost-effective treatments to achieve long-term hydrophilic PDMS surfaces." Applied Surface Science 258, no. 24 (2012): 9864-9875.

233. Zhao, Jiheng, Debra A. Sheadel, and Wei Xue. "Surface treatment of polymers for the fabrication of all-polymer MEMS devices." Sensors and Actuators A: Physical 187 (2012): 43-49.

234. Martin, Samuel, and Bharat Bhushan. "Transparent, wear-resistant, superhydrophobic and superoleophobic poly (dimethylsiloxane)(PDMS) surfaces." Journal of colloid and interface science 488 (2017): 118-126.

235. Cherney, E. A. "Silicone rubber dielectrics modified by inorganic fillers for outdoor high voltage insulation applications. InElectrical Insulation and Dielectric Phenomena, 2005. CEIDP'05." In 2005 Annual Report Conference on, pp. 1-9. 2005.

236. Kuncova-Kallio J, Kallio PJ. PDMS and its suitability for analytical microfluidic devices. InEngineering in Medicine and Biology Society, 2006. EMBS'06. 28th Annual International Conference of the IEEE 2006 Aug 30 (pp. 2486-2489). IEEE.

237. Qin, Yubo, Poying Yeh, Xingkai Hao, and Xudong Cao. "Developing an ultra non-fouling SU-8 and PDMS hybrid microfluidic device by poly (amidoamine) engraftment." Colloids and Surfaces B: Biointerfaces 127 (2015): 247-255.

238. Yang, Chengxin, and Yong J. Yuan. "Investigation on the mechanism of nitrogen plasma modified PDMS bonding with SU-8." Applied Surface Science 364 (2016): 815-821.

239. Keane TJ, Badylak SF. Biomaterials for tissue engineering applications. InSeminars in pediatric surgery 2014 Jun 1 (Vol. 23, No. 3, pp. 112-118). Elsevier.

240. Habubi, Nadir F., Ramiz A. Al-Anssari, and Jinan A. Abd. "Structural, optical and electrical properties of indium doped cadmium oxide thin films." Nano Science and Nano Technology An Indian Journal 7, no. 5 (2013): 172-178.

241. Fleischman, Dagny. Nanophotonic structures: fundamentals and applications in narrowband transmission color filtering. California Institute of Technology, 2019.

242. Liedberg, Bo, Claes Nylander, and Ingemar Lunström. "Surface plasmon resonance for gas detection and biosensing." Sensors and actuators 4 (1983): 299-304.

243. Peterlinz, K. A., and R. Georgiadis. "Two-color approach for determination of thickness and dielectric constant of thin films using surface plasmon resonance spectroscopy." Optics Communications 130, no. 4-6 (1996): 260-266.

244. Cullen, D. C., R. G. W. Brown, and C. R. Lowe. "Detection of immuno-complex formation via surface plasmon resonance on gold-coated diffraction gratings." Biosensors 3, no. 4 (1987): 211-225.

245. Chen-Hsin Lu 1, Ming-Ren Cheng 1, Sheng Chen 1, Wei-Lin Syu 2, Ming-Yen Chien 2, Kuan-Syun Wang 3,Jeng-Shiung Chen 4, Po-Han Lee 1,* and Ting-Yu Liu 2,5,6"Flexible PDMS-Based SERS Substrates Replicated from BeetleWings for Water Pollutant Detection"30 December 2022.

الخلاصة

يتضمن هذا العمل إعداد أربع مجموعات من العينات المختلفة ذات التراكيب المختلفة. أجريت االفحوصات لجميع العينات المحضرة، وكانت المجموعات

المجموعة الأولى(العينة الأولى:(One-side 2D grating (PDMS/TiO2(50nm))

العينة الثانية: Two-sides 2D grating (etalon) (TiO2 (50nm) /PDMS/ TiO2 (50nm))

المجموعة الثانية(العينة الأولى:1: 2D (PDMS/MgF2) different periodic)

المجموعة الثالثة(العينة الأولى:1D PDMS/MgF2(10nm)), العينة الثانية: 1D PDMS /MgF2/ Au (34n) , العينة الثالثة:(1D PDMS/MgF2/ Au/Ni (30nm)

المجموعة الرابعة (العينة الأولى: 2D PDMS/TiO2 (34nm) , العينة الثانية :2D PDM /TiO2/ Au (34nm) , العينة الثالثة:(2D PDMS /Tio2/ Au /Ni (34nm)

حيث تم إجراء اختبارات حيود الأشعة السينة (XRD) للمواد الداخلة في تحضير الهياكل للتأكد من هوية المادة المحضرة، وتم الحصول على نتائج متطابقة من خلال مقارنتها بالقيم المذكورة في البطاقات الدولية الخاصة بكل مادة. تم إجراء فحص SEM لنفس المواد لتحديد نانوية المادة، وأثبتت النتائج ذلك. تم إجراء الاختبارات. كاميرا CCDللمجموعات (1، 2، 3) وجد من خلالها أن الشدة لـ للمجموعة الأولى عالية في العينة الأولى وللعينة الثانية الشدة أقل، أما الحيود فيلاحظ أن الشعاع يكون العرض أكبر في العينة الثانية، بينما تكون الشدة عالية في في الربع الأول والثاني Q_2Q_1، بينما تكون الشدة أقل في الربع الثالث والرابع Q3، Q4 في المجموعة الثانية

كما تم إجراء اختبارات الانعكاس للمجموعة الاولى ويلاحظ من خلال النتائج زيادة الزاوية بسبب زيادة الانفصال في القمة يلاحظ أن تدرج الزيادة في الزاوية يبدأ في الظهور ويصبح أكثر وضوحا، كما هو لوحظ ظهوره عند الزاوية (52) والزيادة عند (58) والأكثر وضوحاً عند الزاوية (60) لوحظ التقارب عند الطول الموجي (700) نانومتر وهناك فرق كبير عند الطول الموجي (650))nm حيث يكون المفرد أعلى وبالتالي التطبيقات الخطية للثنائي أكثر لأنه يحتوي على معامل انكسار أكبر وبالتالي تقل السرعة أما بالنسبة لمؤشر الانكسار التخيلي فنلاحظ زيادة المفرد ضمن الأطوال الموجية من (550) نانومتر حتى نهاية الطيف المرئي الذي يشير إلى معامل الانكسار المختبر للمجموعة الأولى .

في الجزء الثاني من العمل تمت دراسة الخواص الضوئية المغناطيسية للعينات في المجموعات 3،4 لتحديد التغير الذي يحدث باستخدام الترصيف الذي تم أعداده وبوجود مجال مغناطيسي وملاحظة تأثير البلازمون (يحدد رنين البلازمون السطحي) بسبب العينة الأولى والثانية في المجموعة الثالثة يلاحظ التدوير في العينة الأولى عالي حيث يبدأ في النزول إلى ما دون الصفر (سلبي) ثم يزداد تدريجياً إلى الطول الموجي عند 550 نانومتر، ويصبح الذروة الإيجابية ثم يرتفع عند الطول الموجي 600 نانومتر ويلاحظ التدوير العالي في السلوك كما نلاحظ الزيادة

التي تحدث بين 500 نانومتر و 550 نانومتر من السالب إلى الموجب ويظهر البلازمون على النيكل عند S3 وتكون عملية التدوير عالية جداً بين 450 نانومتر و 500 نانومتر ، ونلاحظ عند 525 نانومتر تأثير البلازمون يظهر على النيكل، بينما أشارت تلك النتيجة في المجموعة الرابعة إلى أن إدخال Ni ربما يكون قد ملأ الفجوات المسؤولة عن توليد البلازمون، وبالتالي منع تكوين السطح الخارق.

وزارة التعليم العالي والبحث العلمي
جامعة بابل
كلية العلوم للبنات
قسم الفيزياء الليزر وتطبيقاتها

الخصائص المغناطيسية ـ البصرية لمواد الميتا مع مختلف التراكيب النانوية

أطروحة
مقدمة الى مجلس كلية العلوم للبنات في جامعة بابل
كجزء من متطلبات نيل درجة الدكتوراه فلسفة في العلوم /فيزياء الليزر وتطبيقاته
من قبل

نــوره عزيــز عليــوي عبيـــد

بكالوريوس علوم فيزياء 2013
ماجستير علوم فيزياء الليزر وتطبيقاته 2017

بأشراف

أ.د جنان علي عبد/جامعة بابل /كلية العلوم للبنات

أ.م.د نزار سالم شنان/جامعة بابل/كلية العلوم للبنات

2023 م 1444 هـ